

Published in final edited form as:

*Prog Polym Sci.* 2007 August ; 32(8-9): 1083–1122.

# Smart Polymeric Gels: Redefining the Limits of Biomedical Devices

Somali Chaterji<sup>1</sup>, Il Keun Kwon<sup>2</sup>, and Kinam Park<sup>1,2</sup>

<sup>1</sup> Weldon School of Biomedical Engineering Purdue University, 206 S. Intramural Drive, West Lafayette, IN 47907

<sup>2</sup> Department of Pharmaceutics Purdue University, 206 S. Intramural Drive, West Lafayette, IN 47907

## Abstract

This review describes recent progresses in the development and applications of smart polymeric gels, especially in the context of biomedical devices. The review has been organized into three separate sections: defining the basis of smart properties in polymeric gels; describing representative stimuli to which these gels respond; and illustrating a sample application area, namely, microfluidics. One of the major limitations in the use of hydrogels in stimuli-responsive applications is the diffusion rate limited transduction of signals. This can be obviated by engineering interconnected pores in the polymer structure to form capillary networks in the matrix and by downscaling the size of hydrogels to significantly decrease diffusion paths. Reducing the lag time in the induction of smart responses can be highly useful in biomedical devices, such as sensors and actuators. This review also describes molecular imprinting techniques to fabricate hydrogels for specific molecular recognition of target analytes. Additionally, it describes the significant advances in bottom-up nanofabrication strategies, involving supramolecular chemistry. Learning to assemble supramolecular structures from nature has led to the rapid prototyping of functional supramolecular devices. In essence, the barriers in the current performance potential of biomedical devices can be lowered or removed by the rapid convergence of interdisciplinary technologies.

## Keywords

Stimuli-Responsive; Reversible Volume Transitions; Polyelectrolytes; Molecular Imprinting; Microfluidics; Supramolecular Chemistry; Bottom-Up Design

## 1 INTRODUCTION

Smart polymeric gels constitute a new generation of biomaterials that are now being developed at a prolific pace for use in a range of applications including templates for nanoscale and other biomedical devices, scaffolds for tissue engineered prostheses, and biosensors and actuators. In tissue engineering, the last few years have witnessed a significant paradigm shift in the design of new biomaterials—from inert biomaterials to extracellular matrix (ECM)-mimetic biomaterials [1-4]. Two main classes of macromolecules make up the ECM: (1) fibrous proteins, including collagen, elastin, fibronectin, and laminin and (2) glycosaminoglycans

Correspondence should be addressed to: Kinam Park, Ph. D. Purdue University Department of Biomedical Engineering 206 S. Intramural Drive West Lafayette, IN 47907 Tel: 765-494-7759 Fax: 765- 496-1912 E-mail: kpark@purdue.edu.

**Publisher's Disclaimer:** This is a PDF file of an unedited manuscript that has been accepted for publication. As a service to our customers we are providing this early version of the manuscript. The manuscript will undergo copyediting, typesetting, and review of the resulting proof before it is published in its final citable form. Please note that during the production process errors may be discovered which could affect the content, and all legal disclaimers that apply to the journal pertain.

(GAGs) covalently linked to proteins—proteoglycans (PGs) [5]. The highly hydrated, hydrogel-like properties of PG molecules of the ECM have made synthetic and semi-synthetic counterparts of these native hydrogels versatile candidates for tissue engineering.

The history of synthetic hydrogels dates back to the late 1950s when Wichterle and Lim synthesized the first hydrogels for biomedical applications, specifically the first contact lenses based on poly(hydroxyethyl methacrylate) crosslinked with ethylene dimethacrylate [6]. Although contact lens materials constitute a microcosm in the large domain of biomaterials, the pioneering use of soft hydrogels by Wichterle and Lim ignited a whole new wave of investigations in the quest for novel biomaterials with greater and “smarter” capabilities. Hydrogels are three-dimensional polymeric “swell gels” [7]; they swell in aqueous solutions without dissolving in them. When a hydrogel is in a dehydrated state, the polymer chains are in a collapsed state, allowing little room for molecular diffusion. As the hydrogel swells and attains an equilibrium swelling value, the swelling pressure on the chains is counteracted by the force holding the chains together, namely, the force of crosslinking. At this equilibrium value, the network mesh size ( $\xi$ ) is the greatest and molecular diffusion reaches its peak values [Figure 1] [8,9].

In the realm of nanotechnology, advances in nanofabrication strategies require a wide range of smart biomaterials. It is now known that biological tissue interfaces have nanoscale roughness [10-15], making the advances in nanotechnology all the more important for fabricating smart biomedical devices. Progresses in nanotechnology have attracted considerable interest in the self-assembling property of various molecules, which is a critical prerequisite for the burgeoning bottom-up design of nanoscale structures. When these molecules undergo molecular self-assembly, the resulting structural components, such as nanotubes or vesicles, can be further modified to confer specific properties to the components. Nanotubes, for example, can be coated with metals or semi-conducting materials to make nanowires [16]

Recent advances in the development of novel biomaterials to supplant cellular damages include the formation of nanofibrillar networks by self-assembling associative blocks, synthesis of artificial polymer networks from protein polymers, or the generation of polymer-peptide bioconjugates that present bioactive ligands on the surface. As an example, polymer-peptide bioconjugates are amenable to proteolytic degradation in response to secreted proteases, such as matrix metalloproteases (MMPs) from cells [17-19]. Such “smart” ECM-mimetics have already found applications in differentiating stem cells into neurons [20,21], repairing orthopedic defects [22,23], and inducing vascular angiogenesis [24,25]. Thus far, synthetic ECMs are proving to be viable substitutes for tissue transplants and in many cases more effective scaffolds to transplant tissue progenitor cells and induce guided tissue morphogenesis. However, the temporal and the spatial complexity of natural tissue microenvironments demand greater synergy between materials engineering concepts and core biochemical principles [2]. The complexity also affords ECM-mimetics a large space of possibilities to explore, in the quest for novel biomaterials

Importantly, in the area of biomaterials research, stimuli-sensitive hydrogels or smart hydrogels has been gaining greater momentum. Response to stimuli is a basic phenomenon in living systems. Mimicking this property of living systems can offer a ready solution to many of the current day biomedical problems. Smart hydrogels respond to diverse stimuli, which can be in the form of pH, temperature, light, pressure, electric field, chemicals, or ionic strength, or a combination thereof. These hydrogels have the ability to respond to minute changes in ambient stimuli and exhibit dramatic property changes. For a biomaterial to be truly smart, the alterations in hydrogel microstructures should be fast and reversible. However, the first challenge with conventional stimuli-responsive hydrogels is the slow response time to stimuli

and the hysteresis associated with the on and off states. One way to eliminate this drawback is to have thinner and smaller hydrogels without significantly deteriorating their mechanical properties. The second challenge is to engineer hydrogels that degrade in response to appropriate ambient stimuli in the body. This is in contrast to the current technology where hydrogels degrade at a predetermined rate when implanted in the body. For example, proteolytic stimuli, that is, biochemical signals from cells in the vicinity of an implanted biomaterial scaffold can dynamically transduce signaling cues if the scaffold can degrade and remodel its infrastructure in a stimuli responsive manner. Here, the stimulus is the cascade of biochemical signals from the cells in the vicinity of the biomaterial. The third challenge in the fabrication of smart hydrogels is to make hydrogels biocompatible such that the immune system does not set off immunogenic reactions in the body. In fact, ECM-mimetic hydrogels that evade attacks from the immune system can also be viewed upon as smart hydrogels, responding dynamically to signals from the host tissue. The structure of such ECM-mimetics aims to emulate the ECM, albeit in a much simpler form, capturing the essence of the structural and functional parameters of the ECM.

Russell in his interesting article on “Surface-Responsive Materials” has presented a brilliant analogy between cell adhesion on a receptor-mediated surface and stimuli-responsive materials [26]. The spreading of the cell on the surface is governed by a delicate interplay of surface forces, which include attractive van der Waals forces, electrostatic forces, cell membrane elasticity, steric interactions, and receptor-ligand binding interactions. The cell responds to this set of forces and smartly makes the decision whether to recoil (i.e., not adhere) or to spread on the surface (i.e., adhere). In spite of the enormous progress in engineering smart materials, development of the level of intricacy encoded in living cells is a task of tremendous challenge. One of the main objectives of this review article is to gauge the gap between this daunting challenge and the existing state of the art, and in light of that, describe the directions current biomaterial scientists are pursuing to bridge the gap.

Sections 2, 3, and 4 describe some of the properties and applications of stimuli-sensitive gels, with an emphasis on smart polymeric hydrogels based on the ECM-mimicking property. The stimuli to which polymeric gels respond are discussed in Section 3, and those include pH, temperature, and biochemical analytes, as representative examples of a wide range of possible stimuli. Molecularly imprinted polymers (MIPs) have also been discussed in this section in the context of “imprinting” analyte recognition in the polymer networks using this powerful technology. In Section 4, microfluidics has been selected as a model application to elucidate the potential of polymeric gels as well as hybrid polymeric structures, in actuating microfluidics-based biomedical devices. Also in Section 4, certain applications of the versatile aminopolysaccharide, chitosan, have been discussed in the light of its unique device-biology interfacing potential.

A gel is formed by the use of a crosslinker (physical or chemical) or by supramolecular association to create tie-points or entanglements in the polymeric matrix, resulting in hydrogels or organogels. In fact, self-assembling organogels are evolving as new functional materials based on supramolecular chemistry [27], and they are discussed in the light of self assembling nanofabrication strategies in Sections 4 and 5. Without such crosslinking-based or supramolecular assembling-based entanglements, polymers would react to stimuli by cycling between the sol and the gel states, rather than oscillating between the swollen and the collapsed states. For both kinds of oscillations, there are discrete and (ideally) reversible on and off states triggered by ambient stimuli. This is enough to actuate a device under different system requirements and operating conditions. Further, in hybridizing a polymeric gel with inorganic fillers or protein motifs, one can facilitate the combination of the best of multiple worlds—the polymeric gel world and the inorganic world or the protein world. The polymeric gel world often imparts the smartness (smart polymeric gels) while the inorganic or the protein world

often imparts properties such as enhanced mechanical strength (e.g., by the incorporation of carbon nanotubes) or self-assembling potential (e.g., by utilizing variants of coiled-coil motifs). In essence, it is noted that the barriers in the current performance potential of biomedical devices are artificial; produced by the limits of current technology. The power generated by the fabrication of smart polymeric devices as well as their conjugates can elegantly transcend these synthetic barriers by the rapid convergence of interdisciplinary technologies.

## 2 CLASSIFICATION OF SMART POLYMERIC GELS ON THE BASIS OF STRUCTURAL PROPERTIES

This section is divided into three sub-sections and aims to highlight various material properties that confer “smartness” to polymeric gel networks. For one, superporous hydrogels (SPHs) have been used to increase the responsiveness of hydrogels. In the case of SPHs, the increase in stimuli responsiveness is achieved by engineering interconnected porous networks, as discussed below in Section 2.1. Shape-memory polymers constitute another class of smart biomaterials and function by a ubiquitous mechanism found in our day-to-day lives. Consider the analogy of the intrinsic memorizing ability of an elastic rubber band that is stretched and then allowed to relax; if the entropic energy associated with the stretched rubber band can be stored for use on demand, that itself would be a shape-memory based application. Finally, protein hydrogels unfurl a whole new class of biomaterials by emulating and integrating the self-assembling codes from nature in smart hybrids, as further elaborated in Section 5.

### 2.1 Superporous Hydrogels

Superporous hydrogels (SPHs) represent a fast-swelling class of hydrogels with pore sizes much larger than the typical mesh size of a conventional hydrogel. They were originally developed as novel gastric retention devices increasing the residence time of drugs in the stomach [28,29]. Typical mesh size of a conventional hydrogel is below 100 nm [30,31] compared to the pore size of SPHs which ranges from less than 1  $\mu\text{m}$  to more than 1,000  $\mu\text{m}$  [Figure 2]. The swelling kinetics of SPHs is much faster than that of conventional hydrogels [Figure 3]. This difference can be appreciated in the light of the difference in morphology of the two classes of hydrogels. Since the mesh size of conventional hydrogels is small, the swelling in such relatively closed systems is limited by diffusion of water through the glassy polymer matrix. On the other hand, SPHs have large interconnected pores resulting in the capillary intake of water.

The same monomer or the same mix of co-monomers can produce different types of water-absorbing networks, depending upon the presence of a foaming agent, a foam stabilizer, and the modulation of foaming and polymerization kinetics. The main challenge in achieving a homogeneous, interconnected SPH matrix by the gas-blowing technique is to uniformly trap the *in situ* generated gas, when escaping from the polymer matrix [30,32-35]. Interestingly, the escaping gas confers a distinct directionality to the pore structure, as it escapes from the bottom of the reaction vessel to the top. Compressing SPHs can further enhance their swelling ratio; the swelling property of compressed SPHs was shown to be dependent on the orientation of the SPHs during compression further attesting to the pore structure directionality [34].

Over the years, SPHs have evolved from mechanically weak, first generation SPHs (conventional SPHs), to the mechanically strengthened second generation SPHs (SPH composites), and finally to the third generation SPHs (SPH hybrids) with elastic and rubbery properties in the swollen state [35,36]. Vinyl monomers, including highly hydrophilic acrylamide, salts of acrylic acid, and sulfopropyl acrylate, have been commonly used for the synthesis of first generation SPHs. The first generation SPHs had compromised mechanical properties due to the small volume fraction of the polymer content. They were subsequently

modified to strengthen their mechanical property by including a composite agent, such as the internally crosslinked form of sodium carboxymethylcellulose (NaCMC), *Ac-Di-Sol*<sup>®</sup>. *Ac-Di-Sol* fibers mechanically strengthened the polymer matrix by physically entangling with the polymer chains. This resulted in a polymer matrix with higher mechanical moduli but susceptible to failure due to brittle cleavage fracture. Further modification of SPH composites to form SPH hybrids involved the formation of semi-interpenetrating or fully interpenetrating networks (IPNs) using a hybrid agent. In contrary to the pre-crosslinked composite agent used in SPH composites, the hybrid agent was crosslinked *in situ* during SPH fabrication. Water-soluble or water-dispersible polymers such as polysaccharides (e.g., sodium alginate), proteins (e.g., chitosan, gelatin), or synthetic hydrophilic polymers (e.g., poly(vinyl alcohol)) have been used as hybrid agents [32,37]. Along these lines, elastic SPH hybrids exhibiting mechanical resilience and a rubbery property in its fully water-swollen state have been recently reported by Park *et al.* [36]. These hydrogel hybrids of acrylamide and alginate could be stretched to about two to three times of their original lengths and could be loaded and unloaded cyclically at least 20 times. Further the hybrids could resist a static mechanical pressure of at least 10 N. Also, it was found that an increase in calcium concentration resulted in stronger and smaller IPNs. This was due to the intimate entanglement of the ionotropically crosslinked alginate chains with the synthetic acrylamide chains. Thus, metal complexation of the polysaccharide or protein contents of SPHs affords an innovative modality for the fabrication of elastic and mechanically resilient third generation SPH hybrids with promising potentials in tissue engineering.

Interestingly, Baek *et al.* coated the surface of poly(acrylamide-*co*-acrylic acid) SPHs with an amphiphilic block copolymer, namely, poly(ethylene glycol-*b*-tetramethylene oxide) (PEGTMO) in order to control the swelling kinetics of the fabricated SPHs in aqueous solutions [38]. PEGTMO was dissolved in ethanol for use as the surface coating agent. The SPHs were coated by dipping and equilibrium soaking them in PEGTMO solutions. The delay in swelling of PEGTMO-coated SPHs in aqueous solutions was found to be dependent on the PEGTMO concentrations used. The delay mechanism was postulated to be stemming from the reduced surface hydrophilicity as well as the reduced surface porosity of the SPHs with increasing PEGTMO concentrations. The lowered hydrophilicity of PEGTMO-coated SPHs was recorded via contact angle measurements; scanning electron micrographs revealed a decrease in the surface pores. Thus, the coating of SPHs with the block copolymer of PEG and PTMO was shown to be a promising technique for modulating the SPH swelling kinetics without significantly deteriorating the mechanical properties or the equilibrium swelling value of the SPHs [39,40]. SPHs exhibiting delayed swelling kinetics could be especially valuable in tissue expansion systems where a lag time in swelling would be beneficial in healing the traumatized damaged tissue.

Further, SPHs with environmentally sensitive swelling characteristics have also been synthesized [33]. Poly(acrylamide-*co*-acrylic acid) (p(AM-AA)) SPHs have been found to exhibit pH-sensitivity as well as fast swelling properties. Repeated swelling and de-swelling was observed when these SPHs were exposed to alkaline and acidic conditions respectively, due to alternating ionization and deionization of the carboxyl functionalities. Temperature-sensitive swelling was observed in poly(*N*-isopropylacrylamide-*co*-acrylamide) (poly(NIPAM-AM)) SPHs. The lower critical solution temperature (LCST) of the poly(NIPAM-AM) SPHs can be hydrophobically modulated by altering the polymer composition, as explained in Section 3.2.

## 2.2 Shape-Memory Gels

Responses actuated by shape-memory and stimuli-responsiveness are interrelated. In fact, stimuli-responsiveness can be considered to be an archetypal example of the shape-memory



property in materials. Materials are said to exhibit a shape-memory effect if they can be deformed and fixed into a temporary shape, and have the ability to recover the original, permanent shape only on exposure to an external stimulus. The first shape-memory materials to be discovered were shape-memory alloys (SMAs). The concept of a “metal with a memory” was first discovered in the shape-retaining alloy Nitinol (**N**ickel **T**itanium **N**aval **O**rdnance **L**aboratory), discovered in 1959 by William J. Buehler of the U.S. Naval Ordnance Laboratory, and was subsequently developed by Buehler and Frederick E. Wang. This discovery paved the way to its diverse set of applications, ranging from “shrink-to-fit” pipe couplers for aircrafts, solid state heat engines and toys, to biomedical applications in orthopedics, orthodontics, and cardiovascular surgery. Raychem Corporation's Cryofit “shrink-to-fit” pipe couplers, introduced in 1969, was the first successful Nitinol product on the market [41]. Today SMAs, such as Nitinol®, have been instrumental in significantly improving the quality of diagnostics, treatments, and surgeries [42]. However, the mechanical properties of SMAs can only be varied to a limited extent. The deformation between the temporary and permanent shape is limited to a maximum of 8%. Further, SMAs are non-degradable and the programming of these materials is time-consuming and demands temperatures of several hundred degrees Celsius. Therefore, degradable polymer implant materials with shape-memory have been developed for biomedical applications [43-45]. Though the specific mechanism and applications of shape-memory in metals is outside the scope of this review, the recapitulation of this discovery in metals highlights the far-reaching effects of the shape-memory property in a materials' world.

Shape-memory polymers show stimuli-responsive alterations in structure. Upon exposure to external stimuli, such as an increase in temperature, these materials have the ability of changing their shape. The shape-memory effect is not a specific material property of single polymers. The effect results from the structure and morphology of the polymer coupled with the processing and programming technology. The deformation, and thus, strain energy, is captured in the shape-memory material by a reversible morphology change induced by the deformation, e.g., martensitic transformation for SMAs and thermal or strain-induced crystallization for SMPs. The higher the shape fixity imparted by strain-induced crystallization, the greater the potential of the shape-memory material to exert a force and enable mechanical work on demand. An example of this would be the deployment of a shape-memory stent after proper placement in the vascular graft. In fact, the main applications of SMPs revolve around the ability to use the entropically stored energy to exert force, enabling the transduction of the stored latent energy to mechanical work [46].

Alteration in the shape of a shape-memory material by a thermal stimulus will result in what is termed “thermally induced shape-memory effect.” By exceeding the switching temperature,  $T_{\text{trans}}$ , the polymer switches from its temporary shape to its memorized, permanent shape. The netpoints, that can be chemical or physical in nature, determine the permanent shape. The net chains show a thermal transition either at a glass transition point ( $T_g$ ) or a melting point ( $T_m$ ) in the temperature range in which the shape-memory effect is supposed to be triggered. For biomedical applications a thermal transition of the switching segments from the room temperature to the body temperature range is of great interest [43,47].

Osada and Matsuda demonstrated the shape-memory effect in poly(*N,N'*-methylenebisacrylamide) [48] in 1995. Since then, biodegradable SMPs have been synthesized, including network polymers formed by crosslinking oligo( $\epsilon$ -caprolactone) dimethacrylate and *N*-butylacrylate [45], a multiblock copolymer of oligo( $\epsilon$ -caprolactone) and 2,2(4),4-trimethylhexanediisocyanate [44], a composite of poly(D,L-lactide) and hydroxyapatite [49], and polyurethane derivatives containing polyesters [50,51]. In addition to biodegradability, other criteria attractive for SMP-based biomedical implants include reversibility in the on-off signal transition with minimal hysteresis and reinforced mechanical properties to act as mechanical actuators without buckling under stress. Dramatic improvement

in the stiffness and recovery force of SMPs can be achieved by the synthesis of fiber-reinforced SMP composites. Liu *et al.* studied the thermomechanics of a shape-memory polymer and its composites made by adding nanoscale SiC reinforcements [52]. SMP nanocomposites were demonstrated to have a higher elastic modulus and were capable of generating higher recovery forces as compared to SMP alone. Constitutive models are critical for predicting the deformation and recovery of SMPs under varying thermomechanical conditions. In view of this, Liu *et al.* constitutively modeled SMPs, quantifying the storage and release of entropic deformation during thermomechanical processing. Modeling of strain and stress recovery responses under various flexible external constraints in SMPs can prove to be valuable for engineering SMP-based actuators and other biomedical devices [53].

Vaia *et al.* tested the thermomechanical behavior of shape-memory nanocomposites incorporating anisotropic carbon nanotubes in traditionally monolithic SMPs. These polymer carbon nanotube nanocomposites (PCNs) demonstrated enhanced mechanical characteristics and novel actuation properties. Non-radiative decay of infrared photons absorbed by nanotubes raises the internal temperature; melting strain-induced polymer crystallites and remotely actuating the release of the entropic strain energy [46]. In fact, carbon nanotubes impart unique electrical, optical, and thermal properties to polymer matrices at very low concentrations, in addition to substantial mechanical enhancements [54].

Many new robotic and teleoperated applications require a high degree of mobility or dexterity that is difficult to achieve with current actuator technology. Reinforcement of SMPs can in fact play a major role in their use in novel actuators. Natural muscle is an actuator that has many features, including high energy density, fast speed of response, and large stroke, that are desirable for such applications. Gall *et al.* have characterized the shape-memory mechanics of electrostrictive polymer artificial muscle (EPAM) actuators that can produce strains of up to 30% and pressures of up to 1.9 MPa. A rotary motor using EPAM actuator elements has been shown to produce a specific torque of 19 mNm/g and a specific power of 0.1 W/g, demonstrating the potential toward greater specific power and specific torque than conventional electric motors [55].

Fast-responsive shape-memory hydrogels have been largely useful in the fabrication of microfluidic devices. Several microvalves utilizing shape-memory hydrogels have been developed [56-59]. In-channel polymerization of hydrogel-based flow modulators greatly simplifies device construction, assembly, and operation. Hydrogel-based microvalves have a number of advantages over conventional microvalves, including relatively simple fabrication, no external power requirement, no integrated electronics, and large displacement force generation. However, electronically controllable hydrogel microvalves, based on temperature sensitive hydrogels, offer greater precision in flow modulation and signal actuation, stemming from the integrated electronic circuitry. Richter *et al.* devised smart microvalves with short switching times in the range of 0.3 sec to 10 sec [58]. Microfluidic applications of polymeric gels have been described in greater detail in Section 4 of this article.

Smart, biodegradable implant materials also demonstrate promising potentials toward minimally invasive surgery. For example, the mechanical characteristics and degradability of shape-memory, multiblock copolymers can be used for the preparation of smart surgical sutures. By increasing the temperature higher than the  $T_{trans}$ , shape-memory fibers, programmed to apply the optimum force, shrink and tighten suture knots [43]. Other relatively bulky biodegradable implants can be inserted into the body in a compressed, temporary shape through a small incision via laparoscopy. Their shape-memory ability enables such implants to perform complex mechanical deformations automatically. The additional advantage of designing biodegradable SMPs would be to prevent the discomfort of a follow-on surgery. New polymers have been synthesized with this concept in mind, including phase segregated

multiblock copolymers whose starting materials are proven biocompatible monomers, such as  $\epsilon$ -caprolactone and *p*-dioxanone [44,45,60]. Generally, these materials have at least two separated phases, each with thermal transition (glass or melting) temperatures. The phase with the higher transition temperature is responsible for the permanent shape, whereas the second phase acts as a molecular switch, enabling the fixation of the temporary shape.

Another, opportunity afforded by SMPs is the ability to inject drug loaded SMPs into the body through a laparoscopic hole and retaining the ability to form an implant via thermally induced shape alterations. Interestingly, a thermally induced shape-memory effect that can be activated by an increase in temperature can potentially be induced by heating on exposure to an electrical current or by photoinduction. For one, significant advances have recently been made in the development of SMPs that “move in response to light” [61]. The main challenge in the development of such polymer systems is the conversion of photoinduced effects at the molecular level to macroscopic scales of movement. Examples include the contraction and bending of azobenzene-containing liquid-crystal elastomers and volume alterations in gels. Using light as a trigger for the shape-memory effect will extend the applications of shape-memory polymers, especially in the field of medical devices where triggers other than heat are highly desirable [62].

The concept underlying the responsiveness of shape-memory materials has been very deftly described by Russell, exemplifying the responsive energy stored in a stretched rubber band [26]. If this latent energy of recoil, or the generated elastic retractive force, can be stored in the rubber band for a finite time period, the stored force can be utilized to do useful “work”. In semi-crystalline or glassy polymers, in which crystals act as crosslinking points, a frozen-in strain can produce a similar response. The melting of the strain-induced polymer crystallites (which are responsible for temporarily securing the deformed shape) remotely triggers the release of the stored energy. In fact, shape-memory polymers possess the capacity to recover large strains of the order of 50–400% by the application of heat. This ability of shape-memory polymers to spontaneously recover inelastic strain energy in restricted environments span diverse applications, including heat-shrink tubing, deployable aerospace structures, microsystems, and biomedical devices. Further, the stiffness and stress recovery parameters of shape-memory polymers can be enhanced manifold by the inclusion of ceramic fillers or, more recently investigated, inclusion of anisotropic carbon nanotubes. This unique optimization of properties unfolds promising potentials for developing shape-memory systems as a powerful class of stimuli responsive materials [46,63-66].

### 2.3 Artificial protein hydrogels

Limitations of hydrogels fabricated by traditional methods, such as crosslinking copolymerization, include the absence of precise control of structural morphology and the hysteresis associated with “on” and “off” transitions. Protein engineering [Figure 4] offers powerful solutions to overcome these limitations via the formation of well-defined, supramolecular structures. For example, self-assembling structural domains found in native proteins, e.g.,  $\beta$ -sheets and  $\alpha$ -helices, can be outfitted with integrin binding domains (e.g., Arginine-Glycine-Aspartic Acid or, RGD) or with enzymatic domains [67]. Further, the possibility of going beyond the domain of the natural amino acids and incorporating unnatural amino acids in protein or peptide structures instill greater versatility in genetically engineered motifs [68-76]. Prompted by protein engineering as well as self-assembling strategies for nanofabrication, two new models for engineering smart hydrogels are evolving—first, the synthesis of hydrogels or their associative building blocks by genetic engineering methods, and second, the approach of spontaneous association of the building blocks by molecular self-assembly. The combination of these two techniques affords a promising strategy for the design of hydrogels with a rapid on-off transition [26].



Molecular self-assembly is a powerful approach for creating novel supramolecular architectures. Formation of such supramolecular structures is ubiquitous in the natural world, ranging from the formation of lipid domain structures in plasma membranes, the spontaneous self-assembly of two  $\alpha$  and  $\beta$  chains in hemoglobin forming a quaternary structure, or even the very basic example of formation of oil globules in water. The unique three-dimensional shape of proteins, culminating in protein folding, arises from non-covalent interactions between regions in the linear sequence of amino acids. In fact, only when a protein is in its correct three-dimensional structure, or conformation, is it able to function efficiently [77].

Along the lines of self-assembly of associative blocks, Deming *et al.* have fabricated novel copolypeptide hydrogels with smart, tunable properties [78-80]. Specifically, the properties of these copolypeptide-based hydrogels can be tuned by varying the secondary structure and the charge character of the associative blocks via alteration of the incorporated amino acid building blocks. The facile assembly of hydrogels using amino acid building blocks closely mimics the supramolecular assembly of living matter and affords the advantage of tuning the secondary conformation of the constituting blocks, akin to the self-assembly of proteins in living systems. Thus, gelation depends not only on the overall amphiphilic nature of the fabricated polypeptides, but also on the secondary structure of the individual amino acid monomers ( $\alpha$ -helix,  $\beta$ -strand, or random coil). Further, contrary to most protein gels, which generally dissolve at temperatures greater than 60 °C, transition-metal mediated polypeptide gels, fabricated by Deming *et al.*, did not demonstrate visible thinning up to temperatures as high as 90 °C. Also, the dynamics of the gelation process were investigated by subjecting the polymer gels to large amplitude oscillations and observing the recovery process as a function of time. The hydrogels recovered 80–90 % of their strength within relatively short time intervals, followed by a slower recovery to finally attain the initial storage modulus. Such bottom-up, supramolecular approaches toward fabricating smart materials for various biomedical and pharmaceutical applications are discussed in greater detail in Section 5 of this article.

Recombinant DNA methods have also been used to create artificial proteins that undergo reversible gelation in response to alterations in pH or temperature. The architecture of such proteins emulates those of naturally occurring protein multimeric structures, mostly based on a class of protein motifs called coiled-coil motifs. Kopecek *et al.* have synthesized hybrid hydrogel systems using coiled-coil domains to drive the self-assembly of polymer chains [81-83]. Coiled-coil induced self-assembly has been shown to be strongly dependent on environmental stimuli such as concentration, temperature, pH, and properties of the solvent. To understand the marvels of innovative research, emulating the self-assembling potential of such coiled-coil motifs, it is important to understand the architecture of such motifs. A coiled coil is comprised of a bundle of  $\alpha$ -helices wound into a superhelix [84]. It is a common and important structural motif that mediates protein-protein interactions, and is formed by approximately 3–5% of all amino acids in native proteins. It was first described in 1953 by Crick [85] and Pauling and Corey [86,87] as the main structural element of a large class of fibrous proteins, including keratin, myosin, and fibrinogen. The most commonly observed coiled-coil motif is left-handed; here each helix has a periodicity of seven (a heptad repeat), usually denoted as (a-b-c-d-e-f-g)<sub>n</sub> in one helix and (a'-b'-c'-d'-e'-f'-g')<sub>n</sub> in the other. In this model, a and d are typically non-polar core residues found at the interface of the two helices, juxtaposed in such a manner that they can hydrophobically interact; whereas e and g are solvent-exposed polar residues that confer specificity to the interaction between the two helices via electrostatic interactions. Consequently, two  $\alpha$  helices with these hydrophobic “stripes” spanning the surface can wrap around each other with the non-polar side chains of one  $\alpha$  helix interacting with the non-polar side chains of the other. Typically, in gene regulation the portion of the protein responsible for dimerization is distinct from the portion that is responsible for DNA binding; gene regulatory proteins normally being homodimeric. Notably,

however, leucine zipper motifs efficiently combine these two discrete functions into one. These motifs are so named because of the way the two  $\alpha$  helices, one from each helical monomer, dimerize to form a short coiled-coil. The hydrophobic force of interaction mostly arises from leucine residues interacting with one another. Just beyond the dimerization interface the two  $\alpha$  helices separate from each other to form a Y-shaped structure, allowing their side chains to bind to the major groove of DNA [5,88-91].

Many native and *de novo* designed coiled-coils undergo conformational transitions, such as folding or oligomerization, in response to temperature, pH, ionic strength, and other stimuli. In fact, dramatic alterations in coiled-coil stability, conformation, and responsiveness can result from minor alterations in the primary structure. By incorporating coiled coil motifs as crosslinks in polymeric hydrogels, Kopecek *et al.* conferred predetermined sensitivity to the fabricated hybrid hydrogels [92]. Specifically, they prepared a linear hydrophilic copolymer of *N*-(2-hydroxypropyl)-methacrylamide (HPMA), and a metal-chelating monomer *N*-(*N*',*N*'-dicarboxymethylaminopropyl)-methacrylamide (DAMA). Complex formation between iminodiacetate (IDA)-Ni<sup>2+</sup> pendant chains and the terminal histidine tags of the coiled coil motifs anchored the peptide motifs to the primary hydrogels chains [Figure 5]. Temperature induced collapse of the coiled-coil conformation resulted from the transition from the elongated coiled-coil conformation to random-coiled conformation. This occurred at a temperature close to the melting temperature of the native coiled-coil protein ( $T_m = 35^\circ\text{C}$ ) and structurally altered the gels. Further, with the same copolymer precursor and similarly charged, two different coiled-coil motifs, different swelling profiles were obtained. This difference was possibly due to considerable difference in the size of the motifs, resulting in different crosslinking densities and/or difference in the polymer-solvent interaction parameter,  $\chi$ . Also, increase in the swelling of the gels was observed when imidazole was added to the system, since imidazole, in moderate concentrations, competes with the histidine-tagged coiled-coils to bind to Ni<sup>2+</sup>. In effect, this method of crosslinking brilliantly combines the features of the synthetic polymer and peptide world and indicates huge promise in the tailoring of coiled-coil domains and obtaining different structural transition temperatures. Other transition metal ions, such as Zn<sup>2+</sup> and Ga<sup>2+</sup>, can replace Ni<sup>2+</sup> in order to stabilize tagged proteins or to track hydrogels *in vivo* using magnetic resonance imaging (MRI).

Further, coiled-coil stem loop (CCSL) peptides, immobilized on a solid substrate, were also demonstrated to enable biorecognition by forming a rigid brush-like structure with the loop regions exposed to the environment [Figure 6]. Specifically, the designed epitope-display model system consisted of two main components: epitope-containing histidine-tagged peptide, and a synthetic polymer with two types of functionalities, one for covalent attachment to the substrate and the other for peptide immobilization [82].

In a recent article, Kopecek *et al.* documented the synthesis of coiled-coil grafted HPMA hydrogels, where, in contrast to metal-induced complexation, grafting of coiled-coil motifs to the HPMA backbone was done. The coiled-coil motifs flanked with cysteine residues (at the C terminus) were attached to the HPMA backbone via thioether linkages with side chain maleimide groups. It was found that at least four coiled-coil heptads were needed to enable the association of graft copolymers into hybrid hydrogels. The properties and environmental sensitivity of these advanced hydrogels were largely modulated by the structure of the coiled-coil domain [81].

Another interesting example of an artificially engineered motif, inspired by the natural coiled-coil architecture, has been reported by Tirrell *et al.* [93]. In their report they discuss the formation of a multidomain ("triblock") artificial protein in which the two apparently contradictory properties of hydrogels, namely, polymer chain crosslinking and solvent retention have been captured in a discrete modular manner. Specifically, the topology of the

protein is comprised of relatively short “leucine zipper” end blocks flanking a central, hydrophilic, polyelectrolyte domain, namely (PEG)<sub>x</sub>; (PEG = polyethylene glycol). The hydrogel formed by the coiled–coil interaction of the terminal leucine zipper domains gradually turned into a viscous solution with increasing temperature and when the pH was increased above 8.0. The mild conditions under which gel formation can be tuned (near–neutral pH and near–ambient temperature) and the reversible gel–sol transformation demonstrate promising potential in bioengineering applications. Further, aggregation number and kinetics, dimerization specificity, and aggregate structure can be manipulated broadly by simply changing the number and type of amino acid residues constituting the modules. Thus, the architecture of protein motifs employed in gene regulation have been deftly mimicked to confer switchable “on–off” transition abilities to these “smart” hydrogels. The elegant modular design allows independent regulation of the structure of the polyelectrolyte domain and the flanking, hydrophobic end blocks; thereby fine–tuning the properties of the hydrogel to perform specific functions.

In a recently reported attribute of protein hydrogels, Harden *et al.* indicated the promise of ECM–mimetic protein hydrogels with modular integrin binding domains in tissue engineering applications [94]. The integrin–binding activity of natural adhesion proteins can be partially mimicked by oligopeptide sequences [95,96], such as the ubiquitous RGD (i.e., arginine–glycine–aspartic acid) [97–100], RGD and PHSRN (i.e., proline–histidine–serine– arginine–asparagine) (in synergy) [101,102], IKVAV (i.e., isoleucine–lysine–valine–alanine–valine) [103–105], YIGSR (tyrosine–isoleucine–glycine–serine–arginine) [106,107], PHSRN, and so on. Harden *et al.* went a step further from the triblock architecture initially proposed by Tirrell *et al.* by conjugating RGD to the central block of the modular triblock protein architecture. So, the modified architecture now contained three distributed repeats of the RGD sequence. The terminal leucine repeats of the original telechelic triblock motif engineered by Tirrell *et al.* [93], is retained in this modular structure with the addition of three RGD sequences.

Responsive gels have also been formed by the molecular self–assembly of  $\beta$  strands to form polymeric  $\beta$ –sheet tapes [108,109]. Aggeli *et al.* designed long, semi–flexible  $\beta$ –sheet tapes that became entangled even at low volume fractions to form gels [108]. The viscoelastic properties of this gel system can be modulated by chemical (pH) or physical (shear) influences. The rheological properties of this  $\beta$ –aggregated system indicated characteristics such as response to small–strain oscillatory shear, reminiscent of highly entangled polymer gels. Interestingly, this follows the same type of molecular self–assembling dynamics as in the fibrillization of the amyloid  $\beta$  peptides—A $\beta$ 40 and A $\beta$ 42, a defining pathological feature of the Alzheimer's disease [110].

On a slightly different note, the far–reaching potentials of molecular self–assembly help us appreciate the huge promise in this emerging field. Recent research in the field of nanometer–scale electronics is probing into the “bottom–up” approach for fabricating nanostructured materials. This is in contrast to the conventionally adopted miniaturization strategies, i.e., the established “top–down” fabrication techniques. Biological macromolecules, especially proteins, provide many valuable properties, but poor physical stability and poor electrical characteristics have prevented their direct use in electrical circuits. Linquist *et al.* have described the use of self–assembling amyloid protein fibers to construct nanowire elements [111]. These fibers were placed across gold electrodes, and additional metal was deposited by highly specific chemical enhancement of the colloidal gold by reductive deposition of metallic silver and gold from salts. The resulting silver and gold wires were 100 nm wide and demonstrated the conductive properties of a solid metal wire, such as low resistance and ohmic behavior. Thus, exploiting the far–reaching potentials of molecular self–assembly, it is possible to harness the extraordinary diversity and specificity of protein functions for nanoscale fabrication.

### 3 CLASSIFICATION OF SMART POLYMERIC GELS ON THE BASIS OF STIMULI

This section describes pH, temperature, and an array of biochemical analytes as representative stimuli modulating volume transitions in smart polymeric gels. In the context of analyte sensitivity, the applications of the molecular imprinting technology in enabling molecular recognition in smart gels are also described. The analyte to be “sensed” by such “imprinted gels” is used as the template to actuate selective recognition behavior in the gels. For example, for molecularly imprinted glucose sensitive gels, where glucose serves as the analyte; glucose would be used as the template to enable the smart polymer to memorize glucose's three dimensional structure. Further, it may be appropriate to reiterate here that there is a host of other stimuli that can actuate smart responses in gels; a small subset of these have been alluded to in Section 2.2, on shape–memory polymers, and in Section 4, illustrating microfluidic applications.

#### 3.1 pH–sensitive gels

Polymers containing acidic or alkaline functional groups that respond to changes in pH are called pH–sensitive polymers. A pH change around the  $pK_a$  value of the functional groups results in the ionization of the groups and the generated electrostatic repulsive force leads to an increase in the hydrodynamic volume of the polymeric hydrogel (i.e., swelling). For pH–sensitive hydrogels, the difference in concentration of mobile ions in the hydrogel interior relative to external solution (osmotic pressure), with changes in solvent pH, drives the volume change [112]. The volume change, and hence the degree of swelling of these hydrogels, with acidic or alkaline functionalities would depend on the degree of ionization of the functional groups. Poly(acrylic acid) [113,114], poly(methacrylic acid) [115–117], poly(ethylene imine) [118], poly(propylene imine) [119], chitosan [120–123], poly(L–lysine) [124,125], and poly(L–histidine) [126–129] are typical examples of pH sensitive polymeric hydrogels.

Since ionization (protonation or deprotonation) mostly governs the swelling of pH–sensitive gels, it is important to understand the factors affecting the swelling equilibriums in ionic gels. These factors include: (i) free energy of mixing of the network chains with the solvent; (ii) ion osmotic pressure; and (iii) elastic retractile response of the expanding gel network. The volume transition in stimuli–sensitive ionic gels based on vinyl polymers with side–chain dissociative groups (e.g., poly(acrylic acid)) is driven by the persistence length transition. The concept of electrostatic persistence length was first suggested and elaborated by Odijk [130–132]. Konak and Bansil extended the idea of electrostatic persistence length to conformational changes of polymer chains and derived equations for the swelling equilibriums of polyelectrolyte gels. The swelling behavior of ionized poly(methacrylic acid) hydrogels in the absence of salts was described reasonably well by these persistence length relations [133]. At the swelling equilibrium, the osmotic pressure is balanced by the elastic pressure generated by the stretching of the polymer network [134].

Several methods have been used to develop pH–sensitive polymers with a  $pK_a$  in the range of 5–8. By incorporating hydrophobic moieties, such as side chain alkyl groups, into poly(acrylic acid), the pH at which there is a conformational change in the polymer increases. This is because hydrophobic modification of the polymeric structure would translate to greater values of electrostatic repulsion to separate the increasing force of hydrophobic polymer–polymer interaction [135]. Khokklov *et al.* were able to demonstrate this phenomenon by hydrophobically modifying poly(acrylic acid), forming alkyl acrylates. It was shown that the swelling transition shifts to alkaline pH values with increasing hydrophobicity of the gel. The higher pH required for the behavioral transitions in these pH–sensitive anionic gels was due to the stabilization of the collapsed state of the gel by the increasing extent of hydrophobic

aggregation with greater side chain alkylation [136]. Along similar lines, Tirrell *et al.* extended the versatility of the polyelectrolyte poly(2-ethylacrylic acid) (PEAA) system by modifying the critical pH for the onset of the targeted membrane solubilization. This was achieved by copolymerizing 2-ethyl acrylic acid (EM) with methacrylic acid (MAA) to obtain copolymers of varying composition. Increasing MAA mole fractions led to progressive reduction in the critical pH for membrane solubilization, which was observed turbidometrically. This method of hydrophobically modifying the polymeric structure thus affords the ability to “tune” the critical pH of a pH sensitive system; specifically in this case, hydrophobic modification altered the critical pH value from 5.7 to 6.5. This kind of modulation is especially useful in biological applications that require targeting to different intracellular destinations, which may typically maintain different degrees of acidity or alkalinity [137]. Notably, the pH variation in the gastrointestinal tract (GIT) is pronounced. The stomach has an acidic environment with a pH of 1–2 in a fasting condition and a pH of 4 during digestion. The intestine has an alkaline pH with a pH of 5.5 at the duodenum, this being the pH at which the acidic chyme mixes with the bicarbonate secreted from the pancreatic juices. Also, the extracellular or intracellular pH values in most cancers are more acidic than in normal tissues or cells [138,139].

Cancer drug targeting is a challenging area, especially due to problems like multi-drug resistance (MDR). MDR confers on cancer cells the ability to pump out toxic anticancer agents before they can kill the cells. There are two general classes of resistance to anticancer drugs: those that impair delivery of anticancer drugs to tumor cells, and those that arise in the cancer cell itself due to genetic and epigenetic alterations that affect drug sensitivity. Impaired drug delivery can result from poor absorption of orally administered drugs, increased drug metabolism or increased excretion, resulting in lower levels of drug in the blood and reduced diffusion of drugs from the blood into the tumor mass [140]. Further, the metabolic profile of cancer cells is different due to poor oxygen perfusion, resulting in elevated levels of lactic acid production and a reduction in pH from 7.4 to about 6.0 [141,142]. This property has been exploited by drug researchers by employing pH-sensitive polymers to target actively metastizing cancer cells. For one, Haag *et al.* generated dendritic core-shell nanocarriers based on hyperbranched poly(ethylene imine) cores and different shells containing aliphatic chains and poly(ethylene glycol) chains, respectively [143]. pH-triggered release of polar drugs was studied. Fast pH-sensitive cleavage of the imine bond occurred at pH 5–7 while relatively high stability of the imine bond was observed at a pH of 8. This pH shift corresponds to the pH shift observed in malignant tissues from that of normal tissues and hence is a valuable trigger for releasing encapsulated drugs at the target site. Further, the effect of enhanced permeability and retention (EPR) and the mechanism of receptor-mediated endocytosis (RME) are thought to be useful mechanisms for targeting macromolecular drugs specifically to tumor tissues on a vasculolymphatic level [144].

Another important application of pH sensitive controlled delivery is in the realm of gene delivery. Polyelectrolyte complexes (PECs) formed between DNA and cationic pH sensitive polymers are attracting increasing attention as novel synthetic vectors for delivery of genes [118,126,145]. Transport of naked DNA is difficult because of the large size and the negatively charged phosphate backbone of DNA. Cationic polymers, such as poly(L-lysine) (PLL), poly(ethylene imine), amine containing dendrimers, and amine containing fractured dendrimers have been investigated for this purpose. Schacht *et al.* went a step further from the formation of pristine DNA-cationic polymer complexes. They successfully grafted the cationic polymer, PLL, with a range of hydrophilic polymer blocks, including poly(ethylene glycol) (PEG), dextran and poly(*N*-(2-hydroxypropyl)methacrylamide) (PHPMA) to form cationic-hydrophilic block copolymers. Discrete complexes were formed, typically about 100 nm in diameter, and with surface charges slightly shielded by the presence of the hydrophilic polymer. The complexes generally show decreased cytotoxicity compared with simple PLL/DNA



complexes. Further, PEG-containing complexes showed increased transfection activity using cells *in vitro* [125].

In fact, pH-sensitive ionization of constituting macromers is a ubiquitous property of several PECs. For example, the stability of a PEC formed using chitosan and alginate would depend on the ionization of the carboxylate groups of the alginate macromer and of the amino groups of the chitosan macromer, forming the PEC [146-150]. Since alginate–chitosan matrices exhibit pH-dependent swelling, the reversible ionization/deionization of the amino groups in chitosan and the carboxylate groups of alginate would essentially determine the stability of the PEC structure. Chitosan, a biopolymer widely used in nature, is also known to be complexed by citrate in the range of 4.3–7.6 [151]. Thus, chitosan, being a pH-sensitive natural polymer can be used to deliver drugs in a controlled manner by exploiting the pH-sensitive formation and disintegration of chitosan containing PECs.

Research efforts along the direction of cellular membrane mimicking strategies have drawn increasing attention toward the self-assembling properties of phospholipid-like molecules. These naturally occurring compounds usually comprise of double hydrophobic tails and a polar head group [5], which in many cases contains the phosphorylcholine (PC) motif. This has led to a class of biomaterials synthesized by either grafting PC-based macromolecules of clinically proven biocompatibility or by polymerizing PC-containing vinyl monomers [152]. One of the most fascinating properties of amphiphilic block copolymers is the micellization tendency of the block polymer when dissolved in a selective solvent, i.e., a solvent that would selectively solubilize one of the blocks but not the other and hence thermodynamically favor the formation of micelles. Giacomelli *et al.* synthesized biocompatible block copolymers consisting of a poly(2-methacryloyloxyethyl phosphorylcholine) (PMPC) corona-forming block and a pH-sensitive poly(2-(diisopropylamino)ethyl methacrylate) (PDPA) core-forming block (PMPC-*b*-PDPA) [152]. When PMPC-*b*-PDPA copolymers were molecularly dissolved in dilute acid solution, the DPA block was protonated and hydrophilic. However, when the pH was elevated to 6–7, the DPA block got deprotonated. This triggered hydrophobicity led to the micellization of the block copolymer, with the dehydrated PDPA forming the core and the hydrated PMPC forming the corona. There are several advantages of block copolymer micelles for drug delivery applications. First, the block copolymer micelles can be designed biocompatible and/or biodegradable by the proper selection of blocks. Second, they are nanosized and have a narrow size distribution, which allows intravenous injection. Third, they are able to encapsulate and release (in response to appropriate stimuli) their contents, which could be relatively insoluble or highly toxic compounds for delivery at specific sites (e.g., site of metastases). Fifth, they increase the bioavailability of the drug by minimizing drug degradation and loss.

Exploring the wide diversity in the behavior of polymer gels, Nagasaki *et al.* stumbled upon an interesting property in silicone-based polysilamine gels. The chemistry of this novel class of hydrogels comprises of alternating diamine and organosilyl units. These gels, surprisingly, hardened on swelling based on a reversible rod-globule transition [153]. This is in contrast to most hydrogels in which modulus decreases with increasing swelling degree at comparatively low values of solvent content. Further, in aqueous media, polysilamine hydrogels exhibit reproducible swelling/syneresis behavior in response to the protonation degree ( $\alpha$ ) of the network. The gel network chains expand and rigidify their conformation on protonation and anion binding, which induce the gel swelling consistently. Since a drawback in the use of most conventional hydrogels as biomedical devices is the decrease in mechanical properties on swelling, the unique property of this class of silicone based hydrogels makes them attractive for use in controlled drug delivery, especially as pump systems in pulsatile drug delivery.

### 3.2 Temperature-sensitive or thermo-responsive gels

The study of thermo-responsive gels started in 1978. Tanaka reported the thermodynamics underlying the collapse of the polymer network in polyacrylamide gels [154]. Poly(*N*-isopropylacrylamide) (poly(NIPAM)) in water demonstrated remarkable hydration–dehydration changes in response to changes in temperature, resulting in a lower critical solution temperature (LCST). Temperature is a commonly used triggering signal for modulating drug release [155,156]. Thermal stimuli are physiologically very relevant, a common example being elevation of body temperature under the influence of pyrogens in fever. This is mediated by elevated concentrations of prostaglandin E<sub>2</sub> (PGE<sub>2</sub>) within certain areas of the brain altering the firing rate of neurons that control thermoregulation in the hypothalamus [157].

In general, the solubility of most polymers increases with increase in temperature. However, in the case of polymers exhibiting LCST, increase in temperature decreases the polymer's water solubility due to predominating hydrophobic interactions. Thus, LCST is a characteristic facet of “inversely” thermo-responsive polymers. It is defined as the temperature at which the polymer solution undergoes a phase transition from a soluble state (i.e., random coil form) to an insoluble state (i.e., collapsed or globule form) on elevating the temperature. In fact this coil-to-globule transition of poly(NIPAM) has been clearly seen on a nanometer scale using atomic force microscopy (AFM) [158]. Using laser scanning confocal microscopy (LSCM), the mesoscopic internal structures of network polymers, including those of poly(NIPAM), were shown to be composed of continuous two-domain structures with dense and sparse regions in the polymer network demonstrating “fixed concentration fluctuations” [159].

A wide range of poly(*N*-substituted acrylamide)s, such as poly(*N*-isopropylacrylamide) and poly(*N,N'*-diethylacrylamide) [Figure 7], have been investigated. Intermolecular forces originating from the hydrophobic groups in the polymer result in changes in the orientation of the polymer in its solvent. Such interactive forces primarily include hydrogen bonding resulting in association/dissociation and hydrophobic interactions resulting in gel shrinkage in crosslinked polymers [160]. In general, the temperature sensitivity of swelling can be attributed to the delicate hydrophilic–lipophilic balance (HLB) of polymer chains and is affected by the size, configuration, and mobility of alkyl side groups. A sharp swelling transition occurs at LCST, when an optimum HLB value is attained in networks demonstrating sharp thermo-responsive properties; such as poly(NIPAM) networks [161,162].

Increasing the temperature increases the hydrophobic interaction, causing association of hydrophobic polymer chains. Moreover, the hydrogen bonding between polymer and water becomes unstable with increase in temperature, further favoring hydrophobic association. Due to the positive or negative dependence of polymer chain relaxation with temperature alteration, diffusion kinetics modulated by the polymer matrix also varies with alterations in temperature [163]. This unique property of thermally responsive polymers, demonstrating reversible phase transitions with thermal alterations, has made them especially attractive in the realm of modulated drug delivery.

Poly(NIPAM), like other LCST polymers, is fully hydrated with an extended chain conformation below 32 °C and gets extremely dehydrated and compact above 32 °C. The huge promise in the thermo-responsive property of poly(NIPAM), however, lies in the fact that its LCST phase transition occurs close to the body temperature [164]. In general, the LCST of thermo-responsive polymers can also be tuned to such useful values, by simply adjusting the ratio of hydrophilic and hydrophobic segment of the polymer [165–168]. Modification of LCST polymers (e.g., poly(NIPAM)) with more hydrophilic monomers (e.g., acrylic acid) will favor hydrogen bonding in preference to hydrophobic interactions and will increase the LCST of the copolymer [169–171]. Interestingly, co-polymerizing poly(NIPAM) with more hydrophobic monomers (e.g., *N*-butyl methacrylate) resulted in the formation of a dense skin during the

de-swelling process (i.e., when the temperature was raised above LCST) [172-174]. This dense skin formed at high temperatures blocked release of drugs loaded in the matrix, resulting in the abrupt tapering off of drug release, modulated by temperature.

Further, engineering dual stimuli-responsive polymers, such as poly(NIPAM-co-methacrylic acid), has resulted in the pulsatile delivery of drugs by simultaneous pH and temperature alterations. The pulsatile delivery of the thrombolytic agent, streptokinase, by such a mechanism was found to be useful in its application at the site of blood clotting [175]. This kind of alternating on-off drug release pattern was obtained via interpenetrating polymer networks (IPN) of poly(acrylamide-co-butylmethacrylate) and poly(acrylic acid) [176] and poly(*N,N*-dimethylacrylamide) and poly(acrylic acid) [177], among others. Thermo-responsive polymers also afford a smart strategy to combat restenosis in vascular myopathies. Kavanagh *et al.* studied the release of colchicine from copolymer films such as *N*-isopropylacrylamide and *N*-tert-butylacrylamide (NIPAM/NtBAM). The copolymer collapsed above LCST, releasing colchicine, an anti proliferative agent to prevent restenosis [178].

Interestingly, the temperature-dependent switching characteristic of LCST polymers can afford a smart strategy to control the affinity of an enzyme for its ligand. Hoffman *et al.* used genetically engineered streptavidin (mutant form) to control the affinity kinetics of the mutated protein with immobilized biotin [179]. Cassette mutagenesis was carried out to introduce a cysteine residue in streptavidin and allow conjugation of the protein to poly(NIPAM). The conjugation of poly(NIPAM) to streptavidin resulted in the temperature modulated molecular “gating” of streptavidin's active site [Figure 8].

Thus, the site-specific conjugation of such phase reversible polymers to genetically modified protein affords an attractive tool to control biomolecular recognition processes, allowing “gating” of on-off rates as well as “switching” of on-off signals. Combinatorial libraries of thermo-responsive polymers, both compositionally and on the basis of molecular mass, can be created and utilized for the fine-tuning of such recognition processes. Further, triggered release of bound ligands can also be actuated using phase transition of polymers, this strategy being useful both in controlled drug delivery modalities and in size exclusion chromatographic methods.

Another widely researched area of exploring the potentials of thermo-responsive polymers is in the realm of cell manipulation techniques. The temperature dependent switching characteristic of poly(NIPAM) surface coatings, or more specifically, the switch from being hydrophilic at low temperature to hydrophobic at high temperature has been useful in both *in vitro* cell culturing and in fabricating layered constructs for engineering novel tissues. Thermo-responsive artificial extracellular matrices (ECMs), such as poly(NIPAM)-grafted gelatin (poly(NIPAM)-gelatin) have been researched to investigate the phenomenon of thermo-responsive adhesion and detachment of cells from the polymer surface [180]. The methods currently used to detach cells by enzymes, such as trypsin-induced cell peeling from the surface, have the potential to damage cells [181,182]. For example, a decrease in cell culture temperature below LCST resulted in the release of cardiac myocyte sheets without the aid of enzymes [183]. Recovered cell sheets can potentially be transferred to other surfaces; this strategy represents a novel method for fabricating organ-mimicking layered constructs in tissue engineering [165]. Along similar lines, Okano *et al.* detached neonatal rat cardiomyocyte sheets from NIPAM-grafted surfaces and overlaid the cell sheets to construct cardiac grafts [184]. Layered cell sheets began to pulse simultaneously and morphological communication via connexin 43 was established between the sheets. Promising results were achieved with electrically communicative pulsatile 3-D cardiac layered constructs both *in vitro* and *in vivo*.

This strategy of layering cell sheets thus appears to afford a sizeable step jump toward engineering cardiac tissue and thus enabling cardiovascular tissue repair.

Several researchers have investigated the thermal switching phenomenon using different compositions of NIPA-grafted polymers and have attempted to characterize and control the properties of these temperature sensitive coatings [185-190]. Matsuda *et al.* determined the adhesive strength of cell monolayers on thermo-responsive poly(NIPAM)-grafted gelatin [191]. The adhesive strength of monolayered tissue on a non-coated dish was reported to be approximately 560 Pa or 230 nN/cell at 37 °C. For dishes coated with thermo-responsive gelatin, the adhesive strength was reported to be 1050 Pa or 584 nN/cell at 37 °C, and 26 Pa or 14 nN/cell at room temperature. This technique affords a promising tool for determining the adhesive strength of interaction between a tissue monolayer and its substrate. Determination of tissue-substrate adhesive strength can potentially provide critical indications toward the performance of implant devices. Proteolytically sensitive thermoresponsive hydrogels have also been engineered and may well be considered doubly intelligent. Specifically, MMP-13 (collagenase-3)-sensitive peptide crosslinkers have been used to fabricate semi-interpenetrating networks (SIPN), as a synthetic equivalent of the ECM [192]. The idea of a modular EC-mimetic hydrogel with cell-adhesive signals and proteolytically sensitive peptides offers a robust rationale toward parametric modeling. This would enable analysis of the effects of individual, modular properties of the hydrogel on cell adhesion, proliferation, and differentiation.

Another area of extensive research has been in the use of thermally responsive polymers in anti-tumor treatment modalities, specifically targeting polymer-drug conjugates to solid tumors while limiting systemic exposure [193-196]. Elastin-like polypeptides (ELP), which are biopolymers of the pentapeptide repeat (VPGXG; i.e., valine-proline-glycine-X-glycine), where the “guest residue” X can be any of the natural amino acids except proline. ELPs exhibit LCST or inverse temperature transition and have been researched in novel tumor treatment modalities [197,198]. Thermal targeting, resulting in the collapse of the ELP structure with phase transition, synergistically combines the benefits of polymer carriers (e.g., increased plasma half-life, high loading capacity) with the thermally induced actuation of a favorable response at the target site [198]. Recently, a thermally responsive ELP-based intra-articular drug delivery system was devised that could spontaneously aggregate upon injection into the knee joint, forming a drug-depot [199]. Biodistribution studies of these radiolabeled ELP aggregates revealed a 25-fold longer half-life in the locally injected form than in non-aggregating (soluble) similar molecular weight proteins. This strategy points toward the potential use of ELP-based fusion proteins in therapeutic modalities to treat osteoarthritis and other arthritides. Further, the conformational phase transition demonstrated by these responsive polymers can potentially be harnessed for force generation in actuation devices on nano and micro-scales. Chilkoti *et al.* probed the force-extension and conformational behavior of ELPs, below and above their transition temperature [200]. The results indicated a collapsed, potentially entangled, hydrophobic state of ELP with large, unspecific adhesion forces, above LCST. However, the extension behavior below the phase transition temperature closely followed conformational changes in the random polymer coil, without any significant unspecific adhesion forces. The excellent fit of a simple extended freely jointed chain model to the data at intermediate and large extension suggested that the ELP below LCST was in a random conformational state without significant secondary structure. Forces associated with polymer phase transition associated with a hydrophobic collapse can potentially be harnessed for reproducible recognition and actuation.

A large number of poly(ethylene oxide) (PEO) and poly(propylene oxide) (PPO) block copolymers have been found to possess an inverse temperature-sensitive micellization and gelation potential, and are commercially available under the names of Pluronics® (or,

Poloxamers®) and Tetronics® [201]. Specifically, Pluronics (e.g., commercially available PF127 which is a PEO-*b*-PPO-*b*-PEO triblock copolymer) have distinct amphiphilic properties and the ability to form thermally reversible non-crosslinked gels. At appropriate concentration levels and thermal conditions, aqueous Pluronic solutions form micellar systems consisting of dehydrated, hydrophobic, PPO cores and solvated, hydrophilic, PEO coronas. Recently, Kabanov *et al.* synthesized nano-sized block ionomer complexes (BICs) composed of graft-comb copolymers of Pluronic and polyacrylic acid (Pluronic-PAA) and a model cationic surfactant hexadecyltrimethylammonium bromide (HTAB) [202]. The fabricated BICs were of a spherical morphology and responded to changes in environmental parameters such as ionic strength, pH, and temperature. The stability of the BICs was found to be dependent on the structure of Pluronic (the lengths of the PEO and PPO chains) and the charge ratio of polyacrylic acid and the cationic surfactant, HTAB. These environmentally sensitive BICs can thus be used as nano-containers for *in vivo* drug delivery. By using cationic surfactants such as Lipofectamine™, they can potentially be evaluated as DNA delivery vehicles. The hydrophobic PPO group of Pluronics, can be replaced with other hydrophobic groups, such as poly(1,2-butylene oxide) (PBO) [203,204], poly(L-lactic acid) (PLLA), and poly(DL-lactic acid-co-glycolic acid) (PLGA) [203-207]. Further, Cohn *et al.* have developed new family of “reverse thermoresponsive gels” (RTGs) consisting of alternating [A-B]<sub>n</sub> block copolymers, with PEO and PPO as the blocks, using phosgene as a novel coupling agent [208]. The gels exhibited superior rheological properties, when compared with existing RTG displaying PEO-PPO-PEO triblocks. In fact, the relatively low viscosity of conventionally crosslinked RTG polymers, such as PEO-PPO-PEO triblocks, on phase transition, has been a disabling factor in their applications, especially due to the limited stability and short residence times.

Degradable composite Pluronic hydrogels, conjugated with hyaluronic acid (HA) have also been synthesized to combine the thermo-responsive property of Pluronic, specifically, PF127, with the biocompatibility and biodegradability of HA [209].

Further, multiblock copolymers based on Pluronic, that combine amphiphilic, thermo-responsive Pluronic triblocks, with associative blocks responsive to other stimuli have also been researched. The ability to tune the stimuli responsive properties of block copolymers by modifying the architecture of the individual blocks as well as by incorporating blocks supplementing the properties of the parent block(s), have made the evolution process of novel block copolymers increasingly exciting. Along these lines, Mallapragada *et al.* have conferred pH-sensitivity to Pluronic-based triblock copolymers by flanking on either side of the PF127 triblock, cationic moieties consisting of poly(diethylaminoethyl methacrylate) (PDEAM), a methyl ether of poly(ethylene glycol) with pendant amines [210]. At physiological temperature and pH values, aqueous solutions of this novel block copolymer coalesced to form phase-separated hydrogels, stemming from the increasing hydrophobicity of the cationic PDEAM blocks at higher pH values ( $pK_a$  value of the pendant amines of PDEAM = 7.6). The continual increase in the size of the spherical micelles with further increase in pH finally resulted in macroscopic phase separation, above pH values of 11, with the formation of a turbid solution. This occurred due to the precipitation of the copolymer micelles with increasing hydrophobicity of the cationic PDEAM blocks. Further heating of the precipitate above 70 °C resulted in the spontaneous formation of an elastic hydrogel with only 25–35 wt % water. Interestingly, this novel material exhibited reversible pH sensitive phase transitions, while retaining the thermo-reversible property inherent of Pluronic-based gels. In effect, even the structures of the phase-separated hydrogels could be reversibly tuned from nanoscale to microscale dimensions, via stimuli sensitive alterations in micellar morphology [211]. In addition, when these block polymers were complexed with reporter genes, the resultant polyplexes appeared to be promising candidates for controlled, localized, non-viral gene delivery [212]. Deming *et al.* also fabricated novel diblock copolymers consisting of a PEG block conjugated with a polycationic block. The polycationic block comprised of polylysine



or, alternately, an amine substituted methacrylate ester, and demonstrated similar pH sensitivity [202]. The effects of total cationic charge, type of cationic anchor for the PEG block, and the PEG molecular weight were investigated in relation to pH-sensitivity.

Some natural polymers including proteins [213], polysaccharides [214,215] or hybrids of protein and polysaccharides [216-218] have been found to demonstrate thermo-responsive behavior. Among them, cellulose derivatives, such as methylcellulose (MC) and hydroxypropyl methylcellulose (HPMC), have shown thermo-responsive behavior with phase transition temperatures between 40 °C and 50 °C for MC and between 75 °C and 90 °C for HPMC [219]. Kawasaki *et al.* studied a naturally occurring thermo-responsive polysaccharide xyloglucan, derived from tamarind seeds, as a vehicle for oral delivery. Degradation of xyloglucan derived from tamarind seeds by  $\beta$ -galactosidase results in the formation of a product that undergoes sol-gel transition. This property is not found in native xyloglucan [220]. Further, Grinberg *et al.* developed temperature-sensitive chitosan-poly(NIPAM) based interpenetrating networks (IPNs) with enhanced drug loading capacity and exhibiting controlled drug release kinetics [221]. The IPNs were formed by free-radical polymerization using bisacrylamide as crosslinker, followed by subsequent crosslinking of chitosan with glutaraldehyde solutions, to form fully interpenetrated networks. In this delivery system, pH sensitivity and improved drug loading capacity, assessed using the model drug diclofenac, was due to the incorporation of chitosan; temperature sensitivity stemmed from the inclusion of poly(NIPAM). Further, due to the polycationic nature of chitosan, this delivery system can potentially be used for modulating the release kinetics of an array of anionic drugs and therapeutics. Thus the formation of IPNs is an effective way of combining two partially compatible or incompatible polymers. This facilitates the incorporation of the properties of the constituting polymers, thereby modulating the network mesh size in the case of conventional hydrogels; and the capillary radius in the case of fast-swelling superporous hydrogels.

### 3.3 Analyte-sensitive gels

Most physiological processes are carried out in the form of closed feedback loops to maintain body homeostasis. For example, in a normal subject, the release of insulin from  $\beta$ -cells of the pancreas is governed by the physiological levels of blood glucose. In an endeavor to mimic such physiological processes, researchers are trying to fabricate such closed loop platforms. These are expected to deliver therapeutics to patients at a rate regulated by feedback modulation, rather than following the hitherto targeted zero order rate kinetics. Due to the promising potentials of ionic hydrogels to respond to environmental stimuli, the latter have been a far more interesting avenue of research than non-ionic hydrogels that do not typically respond to ambient stimuli.

Further, many biodegradable synthetic biomaterials have been designed to degrade at a pre-determined rate, by the cleavage of hydrolyzable functionalities such as esters. However, such non-enzymatic degradation processes are uncommon *in vivo*. In fact, the degradation of extracellular matrix (ECM) components by cell-secreted and cell-activated proteases, primarily by matrix metalloproteases (MMPs) and serine proteases, result in ECM remodeling and release of essential bioactive components [2,19,222].

Biomolecule-sensitive hydrogels that undergo swelling changes in response to specific biomolecules can be modified to design smart hydrogels that could degrade in response to increase in concentration of specific biomolecules [223]. For example, the widely researched glucose-sensitive hydrogels have the ability to sense the levels of blood glucose and release insulin in accordance with the glucose levels. In general, since glucose sensitive hydrogels are in the limelight in area of analyte-sensitive hydrogels, this section will concentrate on glucose-sensitive hydrogels and then discuss other types of analytes that are being targeted, including calcium, proteins (antigens, enzymes), nucleotides, and enantiomer-sensitive hydrogels. In

addition, novel methods, specifically molecular imprinting techniques, to fabricate analyte-sensitive hydrogels for specific molecular recognition are described.

**3.3.1 Glucose-sensitive gels**—The measurement of glucose is extremely important in the treatment of diabetes and is also of value in monitoring cell growth, since glucose is the primary carbon source in most fermentation processes [224]. Therefore, precisely engineered glucose-sensitive gels have huge potential in the quest to generate self regulated modes of insulin delivery and to facilitate the construction of an artificial pancreas which would function in a manner similar to the  $\beta$ -cells of the pancreas.

Among glucose sensitive gels, immobilized enzymes, specifically gels with glucose oxidase conjugated to them have been extensively investigated [225–227]. The underlying rationale in using glucose oxidase (GOx) basically exploits the pH sensitivity of the polymer used to immobilize the enzyme. Glucose acts as a substrate for GOx and the pH sensitive gel demonstrates a volume transition in response to the lowered ambient pH, precipitated by the formation of gluconic acid. Thus, the swelling ratio of the pH-sensitive gel is modulated by the ambient glucose level. For example, Ghanem and Ghaly ionotropically conjugated the carboxyl groups of glucose oxidase to the biopolymer amino groups of chitosan using carbodiimide chemistry [225]. Further, poly(acrylic acid) (PAA)–“gates” have been used in conjunction with GOx, to regulate solute diffusion permeability of porous poly(vinylidene fluoride) (PVDF) membranes [228]. The glucose-responsiveness of the PVDF membranes was found to be strongly influenced by the functional PAA-gating. In fact, for an ideal gating response a proper grafting yield of PAA is critical. In addition, glucose-sensitive microcapsules, with covalently bound GOx and constituted of PAA-gated porous polyamide membranes have been prepared [229]. The proposed microcapsules show promise as self-regulated injectable drug delivery systems having the ability of adapting the release rate of drugs such as insulin in response to changes in glucose concentration. Such closed feedback loops are highly attractive for diabetes therapy. Further, sulfonamide-based hydrogels with decreased swelling capacity at high glucose concentration, were fabricated [230].

Conventionally GOx based biosensors have been used in monitoring blood glucose levels in diabetic patients. Detection of blood glucose levels is achieved via the electrochemical detection of blood glucose levels using a “finger-stick” apparatus. This method is based on the indirect electrochemical detection of hydrogen peroxide generated by the oxidation of glucose with GOx [231]. The use of chemical ligands, however, makes the detection system more robust and affords longer term stability. Derivatives of boronic acids have been used as ligands to “sense” glucose in aqueous media. Specifically, boronic acids bind to *cis* diols in aqueous media, with the tetrahedral form of boronic acid having much higher affinity for *cis* diols than the trigonal form. Since the tetrahedral form predominates when the pH is higher than the  $pK_a$  value of boronic acid, for physiologically responsive glucose sensors syntheses of boronic acid derivatives with lower  $pK_a$  values is required. One of the most commonly researched derivatives of boronic acids for binding glucose is phenylboronic acid (PBA) or its derivatives, with the  $pK_a$  value of PBA being 8.9. Lowe *et al.* constructed a holographic sensor for monitoring glucose using a PBA derivative, namely 4-vinylphenylboronic acid, co-polymerized with acrylamide using *N,N'*-methylenebisacrylamide as crosslinker [232]. Stable hydrogel films with pendant PBA groups were obtained. Holograms were recorded with these films and the resultant diffraction wavelength was used to monitor the swelling behavior of the film in the presence of glucose. The increase in the holographic replay wavelength on the addition of glucose to the media was mediated by the formation of charged boronate moieties creating a Donnan potential and inducing hydrogel swelling. Importantly, the hologram returned to its original diffraction wavelength on replacing glucose containing media with buffer solutions without glucose indicating the reversible property of the holographic sensor. However, the rather high  $pK_a$  value of PBA necessitates the synthesis of alternate glucose

ligands (with lower  $pK_a$  values). To reduce the  $pK_a$  value of PBAs to physiologically relevant values, two basic methods have been proposed. First, the aromatic ring of PBA can be modified by incorporating electron donors in them. As an example, 3-acrylamido phenylboronic acid, with an amide moiety on the aromatic ring has been shown to bind glucose at physiological pH values [233,234]. Second, electron donors can be polymerized as co-monomers with PBA (or its derivatives) and acrylamide to form a physiologically effective and “smart” film. In line with the second method, Okano *et al.* demonstrated the enhanced stability of boronic acid-polyol complexes when PBA was co-polymerized with tertiary amines, demonstrating greater promise in sensing glucose [235].

Glucose-sensitive phase-reversible gels have also been prepared based on the specific interaction between polymer-bound glucose and the lectin, concanavalin A (Con-A). Con-A can hold up to four glucose units per molecule. Obaidat *et al.* have fabricated porous poly (hydroxyethyl methacrylate) (PHEMA) membranes to sandwich the mixture of glucose-containing polymers and Con-A in between the donor and receptor chambers. The porous PHEMA membranes allowed diffusion of glucose, and the model proteins tested, namely, insulin and lysozyme, while preventing loss of glucose-containing polymers and Con-A in the sol state. The release rate of model proteins through the glucose-sensitive hydrogel membrane was found to be well modulated by the concentration of free glucose. The release rate of the proteins did not remain constant, however, due to the change in free glucose concentration resulting from diffusion of glucose from the receptor chamber to the donor chamber [236-238]. For any glucose-sensitive insulin delivery system to be practically useful, fast removal of glucose after activating the glucose-sensitive hydrogel system is essential.

**3.3.2 Glutathione-sensitive gels**—Glutathione ( $\gamma$ -ECG; i.e.,  $\gamma$ -Glutamate-Cysteine-Glycine), a gamma-glutamyl tripeptide, is a highly distinctive amino acid derivative with several important roles. For example, glutathione, present at high levels (5 mM) in animal cells, protects red blood cells from oxidative damage precipitating from reactive oxygen species. Glutathione (G) also facilitates maintenance of overall cellular redox homeostasis by transitioning between a reduced thiol form (GSH with a free sulfhydryl group) and an oxidized disulfide form (GSSG with a disulfide linkage). GSSG is reduced to GSH by glutathione reductase, a flavoprotein that uses NADPH as the electron source. The ratio of GSH to GSSG in most cells is greater than 500 [5].

With the above discussion of the importance of GSH in cells as a powerful metabolite and a sulfhydryl buffer, it is logical to infer that a delivery system sensitive to levels of glutathione can be beneficial in delivering therapeutics or drugs to intracellular compartments of cells. This rationale has prompted several researchers to develop innovative glutathione sensitive forms of delivery systems. For example, Kataoka *et al.* developed a novel cytoplasmic delivery system for delivering antisense oligodeoxynucleotides (asODN). This delivery system was engineered by assembling a PEG-asODN conjugate with a disulfide-based smart linkage, PEG-SS-asODN. This conjugate was complexed with branched polyethylenimine (B-PEI) to form polyion complex (PIC) micelles. Results indicated that the fabricated smart micelles demonstrated significant antisense effect via disulfide bond cleavage in the cellular interior. This was because the delivery system crosslinked using disulfide linkages “sensed” high glutathione concentrations in the cellular cytoplasmic compartment [239].

Along similar lines, exploiting the reversibility of disulfide bond-sulfhydryl chemistry, Kakizawa *et al.* used disulfide crosslinked, thiolated PIC micelles, fabricated using block copolymers of PEG and thiolated poly(L-lysine) (PEG-thioPLL). The thiolated micelles demonstrated sufficient colloidal stability, mediated by the PEGylation of the PIC core composed of PLL and ODN. Again, in the presence of GSH at a concentration comparable to the intracellular environment, the PIC micelles dissociated to release ODN [240]. Similarly, a

block polycationic complex, demonstrating high stability in the extracellular medium efficiently released plasmid DNA (pDNA) in the intracellular compartment. Obviously, engineering an optimum balance between the densities of the cationic charge and those of the disulfide linkages played a crucial role in the delivery and controlled release of entrapped pDNA into the intracellular compartment, enhancing transfection efficiency [241].

El-Sayed *et al.* recently proposed a dual stimuli responsive delivery system, using both pH and glutathione responsive polymeric modules, to therapeutically deliver ODNs [242]. This dual stimuli-sensitive system afforded the additional advantage of tuning release kinetics by systematically varying the composition of the pH-sensitive hydrophobic moiety, butyl acrylate, or by modifying the glutathione responsive moiety, pyridyl disulfide acrylate, or by modifying both.

A novel class of biochemically degradable ABA triblock copolymer where A is 2-(methacryloyloxy)ethyl phosphorylcholine (MPC) and B is N-isopropylacrylamide (NIPAM) was fabricated to form “flower micelles” under physiologically relevant conditions at a copolymer concentration above approximately 8% w/v [243]. Glutathione mediated degradation of these flower micelles resulted in alterations of the rheological properties of the gel due to the breakdown of the “flower structure”. Changing the block polymer architecture from triblock disulfide-linked “flower” micelles to diblock sulfhydryl-terminated conventional micelles resulted in “degelation” of the system [Figure 9]. The resulting sulfhydryl-terminated micelles still exhibited temperature sensitive micellar self-assembly. This strategy illustrates a promising paradigm for altering the rheology of polymeric delivery systems using biochemical stimuli that are known to be ubiquitous in intracellular compartments. Further, important design parameters in engineering dissolvable, glutathione sensitive hydrogels include the disulfide crosslinking density, the dimensions of the hydrogel, and the distribution of the disulfide linkages.

Aluru *et al.* modeled the transduction of biochemical signals in dissolvable hydrogels to optimize the design parameters in hydrogels with disulfide chemistries [244]. Once the design parameters of such hydrogels are optimized, precisely engineered microfluidic devices using such biochemically modulated hydrogels can be devised.

**3.3.3 Antigen-sensitive gels**—To induce reversible antigen-responsiveness, Miyata *et al.* synthesized an antigen-antibody semi-interpenetrating (SIPN) hydrogel network [245, 246]. The hydrogel was fabricated by first polymerizing the vinyl conjugated form of Goat Anti-Rabbit (GAR) IgG (i.e., GAR IgG coupled to N-succinimidylacrylate) and then copolymerizing GAR IgG with vinyl-modified rabbit IgG, in the presence of the crosslinker, N,N'-methylenebisacrylamide. Non-covalent crosslinking between grafted antigens and antibodies resulted in de-swelling of the hydrogel network in the absence of free antigens in the system. However, when free antigens were present in the system, the hydrogel network swelled due to the rupture of the antigen-antibody crosslinks [Figure 10]. This was due to competitive binding (to the immobilized antibodies) exhibited by the immobilized and free antigens in the solution. Further, the free antigens can be thought to be more inclined to supersede the grafted antigens in this race due to the greater degree of freedom of the free antigens with respect to the immobilized antigens. In addition, using the model protein hemoglobin, it was shown that reversible changes in the swelling profile and consequently protein permeation occurred. In fact stepwise changes in antigen concentrations induced pulsatile permeation of the model drug.

The semi-IPN structure was found to be critical for the reversibility of the gel structure, modulated by the presence and absence of the stimulus, namely, the antigenic stimulus. Thus, the hydrogel shrinks in the absence of free rabbit IgG exhibiting a “shape-memory-like effect”.

This spontaneous transition in the on–off state of the hydrogel structure and consequent alterations in model drug permeation, in response to antigenic stimuli, makes this approach an attractive one for novel stimuli–sensing drug delivery platforms. Interestingly, this concept of competitive binding, underlying the mechanism of action of the antigen–responsive hydrogels, is very reminiscent of competitive binding of inhibitors to receptors in the body. In classical competitive inhibition, the inhibitor binds to the same active site as the normal enzyme substrate, without undergoing a reaction. Strictly speaking, therefore, the antigen–responsive hydrogels described above do not necessarily mimic competitive inhibitors in the true sense of the term. The idea in elucidating the analogy with competitive inhibition in biochemical reactions, however, is to appreciate how interdisciplinary marvels are pointing toward the already existing feats of evolution.

**3.3.4 Gels sensitive to other analytes**—As evident from the discussion of biomolecule–sensitive gels so far, the responsiveness of hydrogels to signal biomolecules can translate to potential applications in smart devices. A hydrogel membrane sensitive to the metabolite nicotinamide adenine dinucleotide (NAD) and containing immobilized ligands and receptors was investigated for the controlled diffusion of model proteins [247]. Both cibacron blue (ligand) and lysozyme (receptor) were covalently linked to dextran. NAD serves as a competing ligand and competes with cibacron blue in its interaction with lysozyme. Using cytochrome C and hemoglobin as model proteins to examine diffusion across the hydrogel membrane in response to differential concentrations of NAD, saturation kinetics was observed. The diffusion rate saturated with a maximum rate of  $0.23 \mu\text{g}/\text{cm}^2/\text{min}$  and a half saturation constant of 26.5 mM for cytochrome C. This approach of sensing ambient levels of NAD can be generalized to diagnose the levels of different analytes by a suitable selection of a competing ligand–receptor interaction, thereby affecting the permeability of the polymer membrane. Further, in this kind of ligand–modulated release, it is important to maximize selective transport and minimize intrinsic diffusion [247]. This can be achieved by optimizing the affinity kinetics between the analyte and the receptors as well as engineering the crosslinking density to attain a desired distribution and geometry of pores in the network. Effective modeling of the transport kinetics of the analyte of interest with differentially engineered crosslinking parameters can facilitate selective transport through the polymer matrix. Another point of concern raised by the authors is the hysteresis associated with the transition of the gel–matrix properties with the waxing and waning of the stimuli strength (i.e., antigen concentration); this hysteresis has been found to be an artifact of the polymer chain relaxation time. The volume transition rate in fast responsive hydrogels has attracted great attention, especially because of the greater demands associated with the applications of fast–responsive gels. In general, the volume transition rate of hydrogels is dependent on both hydrogel molecular design and processing conditions. Thermodynamic models, transport models, multiphasic mixture theory and molecular simulation have been proposed as tools to engineer fast–responsive hydrogel networks with greater precision [248].

**3.3.5 Analyte sensitivity of molecularly imprinted gels**—Molecular imprinting is a versatile method for creating macromolecular matrices (hosts) that display selective molecular recognition behavior. This is achieved by enabling the synthetic hosts to “memorize” the outfits of targeted guests [Figure 11]. As Klaus Mosbach aptly puts it, molecular imprints are “tiny plastic imprints and mimics of biological molecules” and are “poised to speed drug discovery, warn of bioterror attacks and remove toxins from the environment, among other applications” [249].

These molecularly imprinted matrices or polymers, MIPs for short, tend to be simple and inexpensive to prepare and generally robust. Four main areas of application for MIPs have evolved: affinity separation; antibody binding mimics; enzyme mimics; and biomimetic sensors [250].



Miyata *et al.* in a recently reported article on stimuli-sensitive gels reported dynamic glycoprotein (GP) recognition by gels prepared by biomolecular imprinting [251]. The GP-imprinted gels had lectin and antibodies as ligands for tumor-specific marker GPs and were prepared with minute amounts of crosslinkers. This was in contrary to the common belief in the MIP community of the requirement of large amounts of crosslinkers to depress the mobile polymer chains, creating robust recognition sites. In fact, lower crosslinking density can be potentially effective in achieving fast response rates due to the larger mesh size ( $\zeta$ ) between the polymer chains in the hydrogel network, facilitating faster solvent and solute diffusion [252]. The imprinting approach described by the authors was a smart one; engineered to increase the specificity of molecular recognition by using a dual ligand system. Specifically, a lectin molecule (Con-A) and an antibody molecule (polyclonal anti-AFP antibody; anti-AFP) were grafted with vinyl groups and then the vinyl-conjugated ligands were copolymerized with acrylamide. Next, the ligand grafted acrylamide monomers were crosslinked with *N,N'*-methylenebisacrylamide in the presence of the template molecules. The template molecules aligned the ligands in proper orientations to maximize ligand-template interactions. The tumor responsive template used here was  $\alpha$ -fetoprotein (AFP); a glycoprotein widely used for the serum diagnosis of primary hepatoma. Notably, the AFP gene is normally expressed in fetal liver and is transcriptionally silent in the adult liver under normal conditions. In human hepatocellular carcinoma (HCC), however, the AFP gene is overexpressed [253]. The ligands grafted to the AFP-imprinted gels, Con-A and anti-AFP, were designed to recognize the saccharide and peptide chains of AFP, respectively. This led to AFP-responsive syneresis (shrinking) of the imprinted gel in the presence of both ligands. Specifically, GP-responsive syneresis of the imprinted gel resulted from the formation of Con A-AFP-anti AFP complexes. These complexes acted as dynamic (reversible) crosslinking points in the gel. Notably, ovalbumin with a saccharide chain similar to AFP but with a peptide chain different from AFP, resulted in only slight swelling of AFP-imprinted gels [251]. Since volume transition in AFP-imprinted gels specifically enabled the recognition of the tumor-specific marker, AFP, the application of such gels can be further explored in the realm of molecular diagnostics and cancer therapeutics.

Park *et al.* used a smart synthetic strategy to fabricate molecularly imprinted glucose sensors by copolymerizing mixtures of amino acid-mimicking functional monomers, as molecular recognition agents, and glucose as template molecules, using excess crosslinker amounts. Specifically, amino acid-mimicking monomers, vinyl acetic acid (VAA); acrylamide (AM); allyl benzene (AB); and 4-pentenoic acid (PA) were used [Table 1]; rather than using lectins (e.g., Con-A) or enzymes (e.g., GOx) as molecular recognition agents for glucose [254]. Notably, the use of proteins in biosensors is limited by the poor stability of proteins over the long-term *in vivo*. Further early studies have documented the immunotoxicity of Con-A [255-257]. Therefore this synthetic strategy of molecular recognition of glucose can afford greater immunogenic compliance, in addition to structural versatility in mimicking glucose binding motifs. A comparative stereochemical analysis by the authors of the interaction of glucose with five glucose-binding proteins indicated that the most commonly involved amino acids in hydrogen bonding interactions with glucose were Asp, Glu, and Asn. Further, Phe and Trp played an important role in hydrophobic interactions with the pyranose ring of glucose. Importantly, the optimal spatial orientation of these amino acid residues or their derivatives via molecular imprinting conferred glucose-binding ability to the resulting MIPs consisting of VAA, AM, AB, and PA with glucose interaction strengths in the order: VAA > AM > AB > PA.

## 4 SMART HYDROGELS IN FLOW CONTROL AND BIOFABRICATION: MICROFLUIDICS AND BEYOND

In this section, microfluidics has been selected and described in detail as a sample application, but there are numerous other biomedical applications of smart hydrogels. Some of the potential biomedical applications of smart hydrogels, described earlier in the text, include: temporally and spatially controlling delivery of therapeutics (e.g., glucose sensitive phase reversible gels for insulin delivery, pH sensitive block copolymers for targeted gene delivery); engineering scaffolds for cell culture and tissue reconstruction (e.g., thermo-responsive surfaces for cell detachment, MMP-sensitive biodegradable polymers for ECM-mimicry); engineering fast swelling superporous hydrogel hybrids for applications ranging from drug delivery to biomimetic actuators; developing matrices for chromatographic separations using antigen specific matrices (via the use of immobilized antibodies); and developing advanced stenting applications using shape-memory hydrogels. Description of the techniques without their applications would have made the techniques difficult to appreciate in isolation. Considering the enormity of applications of smart hydrogels and the existence of prior reviews dealing with applications such as drug and gene delivery [156,258-260], and chromatographic separations [261]; microfluidics was selected for a detailed discussion in this section. Notably, microfluidics is a relatively young field, especially in its current incarnation, considering the sophistication of electronic sensors and actuators. Also, it is a dynamically evolving field which has the promise of exploiting the versatile properties of smart hydrogels to the fullest extent.

As pointed out earlier, the swelling kinetics of hydrogels is controlled by diffusion through the porous gel networks. Since hydrogels are conventionally macroscopic, the slow diffusion kinetics would result in swelling equilibria over times that can range from hours to weeks. In many novel applications, however, especially in the context of sensors and actuators, fast response times are essential. The response rate of hydrogels can be improved in two ways. First, as discussed in Section 2.1, one can introduce porosity within the gel network, as in the interconnected porous networks of superporous hydrogels. Also, Moore *et al.* have created porous hydrogel networks sensitive to ionic strength and pH alterations from lyotropic surfactant phase templates, mediated by phase separation [252]. The second way of achieving fast response rates is by downscaling the size of hydrogels. This is because the swelling rate of hydrogels has been found to be inversely proportional to the square of the hydrogel's major dimension. Empirically, it has been found that the swelling process is well described by a second order rate expression given by:

$$dv/dt = k(v_{\infty} - v)^2 \quad (1)$$

where the dimensionless volume  $\infty = (V_{gel,eq} - V_0)/V_{gel,eq}$ ,  $V_{gel,eq}$  is the gel volume corresponding to maximum or equilibrium swelling,  $V_0$  is the gel volume in the collapsed state; and the dimensionless volume  $u = (V_{gel} - V_0)/V_{gel}$ ,  $V_{gel}$  is the gel volume at any given time; and  $k$  is the rate constant. A linear relation obtained by integrating Equation 1 can be used to analyze the swelling and de-swelling kinetics of differentially swelling hydrogels [252,262], and is given as:

$$t/v = \left(1/kv_{\infty}^2\right) + (1/v_{\infty})t \quad (2)$$

The rationale for downscaling the size of hydrogels has been vastly exploited by microfluidic (and, nanofluidic) applications of smart hydrogels. Interestingly, this section may well be replaced by a section titled nanofluidics in a couple years, given the fast explosion in nanoapplications! This can be visualized in light of the evolution of microgels and nanogels [263,264] from conventional hydrogels and, on a wider scale, the evolution of nanofabrication strategies from conventional scales of fabrication. Even in nanofabrication strategies, there has in fact been a diversification in the conceptual basis of such fabrication methods. For example,

latest research trends are exploring the intricacies of supramolecular chemistry [265-269], a bottom-up strategy for fabricating supramolecular structures.

The development of the semiconductor industry has been driven by the famous “Moore's law” over the past several decades. With the innovation of semiconductor microelectronics, however, the gate length of a metal-oxide-semiconductor field-effect transistor (MOSFET) device has reached the scale of 90 nm. If this trend of miniaturization is to continue, semiconductor devices are projected to face fundamental and technological limitations in the future. In fact, with the advent of research in the areas of molecular quantum wires [270-272] and viral nanoelectronics [273,274], it is generally believed that molecular electronics will replace conventional miniaturization strategies. This will pave the way for the more commonplace cousin of bottom-up strategies, namely, top-down strategies that involve miniaturized fabrication strategies, to wane off [272]. In fact, judging from the endless possibilities of iterating supramolecular structures and combinatorial libraries, it may not be too early to say that the next generation of smart nanostructures will be conceived in the womb of supramolecularly assembling frameworks.

It is here that the demand for smart materials to evolve into such supramolecular structures translates into huge dimensions. To keep pace with such demands and perceiving the attractive potentials of polymeric gels, it is important to develop precisely engineered polymeric microstructures. Microfluidics, along with the rapidly advancing field of bio-microelectromechanical systems (MEMS), has shown tremendous promise in setting forth new paradigms for biomedical innovations. Specifically, in the context of microfluidics, responsive hydrogels have been engineered as microscale components including valves, jackets, and flow sorters. Kuhn *et al.* first identified hydrogels as “chemical muscles” in 1950 [275]; from then until now, there has been significant progress in the field with the conceptualization of artificial muscle-like actuators [276-280]. On a slightly sour note, however, no artificial muscle model based on MEMS or even otherwise, appropriately emulating the coordination and power of natural muscles, has been conceptualized. Optimistically, nevertheless, the inter-related fields of microfluidics and bioMEMS seem to be in the right track for prototyping artificial muscle actuators. Beebe *et al.*, in a very well organized review, elucidated the potentials of hydrogels in the fabrication of flow control devices in the format of smart channels and valves [Figure 12] [281]. The hydrogels used in the fabrication of these flow modulators typically respond to pH or temperature alterations in the environment and (ideally) reversibly actuate flow through the microfluidic device. Flow actuation is achieved by coupling the volume expansion of hydrogels to the channel width or orifice radius. Effectively, by modeling the swelling ratio of hydrogels the smart channels can either be completely occluded or the rate of flow can be controlled by varying the flow resistance, either mechanically or more precisely by the integration of digital electronic devices.

Beebe *et al.* have fabricated an organic self-regulating microfluidic device consisting of acrylic acid and 2-hydroxyethyl methacrylate (HEMA) as the polymeric components. Here the feedback controlled volume transitions of the *in situ* photopolymerized pH sensitive polymeric network were transduced to oscillatory changes in a star-shaped orifice valve [282]. Further, hydrogel based microfluidic systems can be engineered to respond to a range of relevant stimuli by selecting appropriate monomer compositions, in addition to variable crosslinking chemistries. West and colleagues have developed nanocomposite hydrogels demonstrating dramatic changes in size and shape when exposed to specific wavelengths of light [283]. The use of light as a stimulus is particularly attractive since it affords accurate spatial tuning of exposure to photochemical stimuli [66,284]. Further, microfluidic systems can be engineered that are responsive to ambient glucose levels [57,228,281,285] by engineering network chemistries that can directly respond to glucose by recognition of glucose as an antigen. Alternately, as described in Section 3.3.1, glucose can be recognized by enzymes immobilized

to hydrogel membranes which can actuate other stimuli mediated changes (e.g., pH in the case of GOx mediated glucose degradation). Again, these reversible transitions of hydrogels modulated by variable stimuli can induce partial or complete occlusion of orifices or valves of microfluidic devices.

Another very innovative stimulus responsive system has been engineered by Daunert *et al.* [286]. Genetically engineered calmodulin (CaM), a calcium binding protein with a ligand binding site and an allosteric site, was used as the recognition module in the devised microfluidic system. CaM can exist in three different conformations, namely, native conformation in the absence of  $\text{Ca}^{2+}$ , dumbbell-shaped  $\text{Ca}^{2+}$  bound conformation, and phenothiazine bound conformation (in the presence of  $\text{Ca}^{2+}$ ). Further, the swelling rate of CaM-based hydrogels non-covalently crosslinked by  $\text{Ca}^{2+}$  and phenothiazine can be increased by adding a  $\text{Ca}^{2+}$  chelator such as ethylene glycol-bis-( $\beta$ -aminoethyl ether)  $-N,N,N',N'$ -tetraacetic acid (EGTA) to the system. The release of  $\text{Ca}^{2+}$  by the incorporation of the chelator also releases phenothiazine from CaM due to allosteric modulation. This smart hydrogel was also found to be responsive to phenothiazines such as chlorpromazine (CPZ) because the immobilized phenothiazine was replaced by the free CPZ, increasing hydrogel mesh size ( $\xi$ ), resulting in the relaxation of polymer chains. Also, this smart hydrogel was integrated in a “plunger” microactuator configuration to modulate “gated” flow from a reservoir. The resultant system demonstrated pulsatile swelling cycles under the influence of calcium-CPZ stimuli. Therefore integration of such modular hydrogels, based on allosteric and ligand binding sites of integrated proteins, afford enhanced control over hydrogel swelling properties and consequently facilitate hydrogel-based flow sorting and actuation.

Fabrication of microscale features for patterning various templates is yet another challenge in the evolution of sophisticated microfluidic devices. More traditionally employed techniques to impart microscale and nanoscale features to materials have included photolithography, microcontact printing, and dip-pen printing. As stated by Yi *et al.*, a broad generalization of such fabrication methods is that they pattern templates by coupling localized external stimuli (optical or mechanical) with desired functionalities [287]. Interest in biofabrication has been fueled by the broader range of fabrication options made available by emulating biologically assembled structures. These options include directed assembly, enzymatic assembly, and self-assembly [287,288]. For a detailed understanding of such techniques, the reader is directed to a descriptive review by Yi *et al.* [287].

Chitosan is a polycationic aminopolysaccharide and is widely researched for biofabrication strategies for microfluidic applications as well as for modulating drug release by fabricating innovative delivery systems. The attractive range of chitosan's  $pK_a$  values is in contrast to that of the polyelectrolyte form of lysine, with a considerably higher  $pK_a$  value ( $\sim 10$ ). Thus polylysine exists only in the polycationic state in physiological systems while chitosan can exist in both cationic (with protonated amine groups) and neutral forms, resulting in electrostatically driven interactions *in vivo*. Structurally, chitosan is a linear  $\beta$ -1,4-linked aminopolysaccharide, obtained by the partial deacetylation of chitin. Consequently, this incomplete deacetylation results in the formation of a copolymer composed of glucosamine and *N*-acetylglucosamine. Importantly, “chitosan” refers to such deacetylated structures with varying molecular weights, degrees of deacetylation, and differential distribution of these deacetylated residues in the polymer network. Three-dimensional scaffolds of chitosan, in addition to chitosan films and membranes, have been fabricated by employing rapid prototyping (RP) technology [289]. Prototype modeling and visualization based on computer-aided design and computer-aided manufacturing (CAD and CAM) have been instrumental in applications of the RP technology in tissue engineering [290].

Chitosan's ability to conjugate with nanoparticles (e.g., carbon nanotubes and quantum dots) [291-293] and biologically active motifs (e.g., peptides [294] and proteins [295,296]), offers additional versatility in generating hybrid structures for biofabrication. Also, chitosan itself has been ionotropically crosslinked with sodium tripolyphosphate (TPP), via simple complexation and ionic gelation techniques, to form nanoparticles. Chitosan-TPP nanoparticles with entrapped small interfering RNA (siRNA) have been shown to be better gene delivery vehicles than chitosan-siRNA complexes, possibly due to their high binding capacity and better loading efficiency [297]. Hydrophobically modified glycol chitosan, in the form of self-assembling nanoparticles, have been devised as promising carriers for the hydrophobic drug, paclitaxel (PTX). These nanoparticles showed sustained release of the incorporated PTX and were found to be less cytotoxic in tumor-bearing mice than the currently used PTX formulation with Cremophor EL. The use of Cremophor EL, a formulation vehicle used for various hydrophobic drugs, has been associated with side effects, including severe anaphylactoid hypersensitivity reactions, aggregation of erythrocytes, and peripheral neuropathy [298]. Further, PEGylation of chitosan has resulted in the formulation of novel nanocarriers with good stability, low cytotoxicity, and greater bioavailability [299].

In addition to pH-mediated modulation of release kinetics of drugs and therapeutics, chitosan's potential toward directed assembly, specifically via electrodeposition, on standard microfabrication templates, makes it additionally attractive in biofabrication [287,300-302]. Electrodeposition can be defined as the process resulting in the production of a coating on a substrate surface by the action of electric current, specifically resulting in the precipitation of the coating material on the surface via charge neutralization. Chitosan is known to be electrodeposited on the cathodic surface in response to localized elevation in pH. Electrodeposition of chitosan stems from its transition from a polycationic, soluble form to a network-forming, insoluble form at high (localized) pH values in the vicinity of the cathode [303] [Figure 13]. This transition in the properties of chitosan has been exploited as a novel mechanism for converting chitosan from its sol form to its gel form. Mandler *et al.* have aptly identified three major advantages of this electrochemical technique [304]. First, the pH varies only close to the electrode surface leaving the bulk solution unchanged, i.e., there is a localized pH change in the vicinity of the cathode. Second, the thickness and other properties of the electrodeposit can be reproducibly controlled by varying electrochemical parameters. Third, the electrodeposition of films is restricted to the conducting part of the surface, affording the additional benefit of spatially selective cathode patterning—electropatterning, and the process is largely controlled by the kinetics of the electrochemical process [304]. The reader is directed to an excellent review on biofabrication strategies using chitosan by Yi *et al.* for a detailed understanding of chitosan's versatility in biofabrication [287].

Interestingly, Chen and colleagues have used chitosan modulated directed assembly to fabricate a smart glucose biosensor. This was done by dispersing gold nanoparticles (AuNP, 17 nm) to form nanoparticle-glucose oxidase (GOx) hybrids in the chitosan matrix [228]. Along similar lines, they used chitosan's one step electrodeposition potential to form a composite with carbon nanotubes and GOx as another variant of a glucose biosensor [212]. Other polyelectrolytes, such as poly(dimethyldiallyl ammonium chloride) (PDDA), in the form of PDDA/AuNP/PDDA/GOx multilayer films, have also been used by Chen *et al.* to fabricate extended-range glucose biosensors [305]. Notably, by amalgamating the ability of chitosan to selectively electrodeposit (at the device surface) and functionalize biological components (electrostatically or via covalent tethers), it can be visualized as a versatile “device-biology-interface”. For example, electrodeposited chitosan tethered with probe DNA has been used for hybridization (or, self-assembly) of complementary oligonucleotides [228]. This method enables better orientation of oligonucleotides on the chitosan modified wafer. Further, electrodeposited chitosan has been tagged to fluorescein labeled tobacco mosaic virus (TMV) nanotubes. In addition, the virion surface can be further manipulated to form dimensionally



assembled nanotemplates for nanoscale electronic circuits [306]. Intriguingly, viruses have been shown to actually improve the electron transport properties of semiconductor nanotubes assembled on them. Along these lines, engineering hybrids of viral and inorganic assemblies have resulted in promising trends toward viral nanoelectronics [307].

## 5 INSIGHTS AND PERSPECTIVES: LEARNING FROM THE BODY

Bionic engineers are making rapid progress in their endeavor to model artificial biomimetic circuitry, namely, the brain circuits and the meshwork of tissues in the rest of the body. Literally, the brain and the rest of the sensorimotor system is a complex network of neurons and blood vessels, among other components. The “microwires” in the brain can decode volitional signals and transform the signals to a range of motions. The minimum number of individual neurons to transform such volitions into actions probably exceeds 1,000 [308]. This kind of decoding cannot yet be done by artificial circuitry that can be fitted into the cranium; wireless signals of cognitive thoughts would have to be relayed to and from between the body and a remotely placed versatile analog electronic device [309]. In fact, the human brain can be envisioned as the best example of a bioMEMS device that can decode complex volitional signals in real time with intricately engineered neural microwires.

Nanotechnology and supramolecular chemistry are powerful tools in the arms race to develop bionic systems. However, for the final integration of any device with the body, the crucial prerequisite is to engineer a smart biological interface. Simply put, a biological interface is fabricated by engineering a biomaterial template to act in unison with the body. “Acting in unison” is the main challenge here. Not only does the science of engineering the biomaterial template have to be smart, but also, the actual interfacing of the device with the body has to be perfect. So much so, that every imperfection in the interface will be recognized by the body with high fidelity (many times higher than the fidelity achieved by molecular imprinting technologies) and will lead to cascaded immune responses. Polymeric gels have demonstrated the potential to generate “smart responses” to environmental stimuli. This again is very reminiscent of the body machine, responding appropriately to various stimuli. Yet, the response of the body machine is so accurate, especially in the context of “bionic parts”, that the process of eluding the immune system with current technology is fraught with uncertainty.

Researchers are gradually unraveling the self-assembling facets of supramolecular processes, commonplace in the body, to finally integrate into bionic parts. Supramolecular materials are by nature dynamic materials, i.e., materials whose constituents are linked together by reversible connections that can undergo assembling or de-assembling processes in response to environmental stimuli. Supramolecular materials are thus constitutionally dynamic materials adapting to stimuli by functionally driven optimization [268]. It is these intriguing dynamics of supramolecular chemistry that have inspired cutting edge trends in nanofabrication. Further, researchers are now simulating the self-propelling ability of biomolecular motors, particularly motor proteins such as F<sub>1</sub>-ATPase [310] and microtubule-depolymerizing kinesins [311]. In fact, the first prototypes of synthetic motors have already been crafted [312-318]. For example, F<sub>1</sub>-ATPase powered nanodevices, with histidine-tagged F<sub>1</sub>-ATP nanomotors attached to Ni-nitrilotriacetic acid (NTA) arrayed surfaces, have been fabricated as basic proof-of-principle devices [319,320]. The integration of such nano-powered motors with smart polymeric gels using supramolecular principles in order to engineer devices such as sensors, actuators, and self-regulating nanomotors, can truly unleash the power of interdisciplinary toolkits.

## 6 CONCLUSION

In this article, smart polymeric gels were classified on the basis of structural properties. Next, they were classified on the basis of the types of stimuli the gels respond to. Then, a sample

application domain, namely, microfluidic applications of hydrogels, was described. Current modalities and concepts employing bottom-up strategies, taking lessons from the elegant structures of the body, have also been discussed. These novel strategies are unraveling exciting new tools of supramolecular chemistry to fabricate smart nanostructures.

This review began by acknowledging the gap between the responsiveness of a simple cell in the body and the “smartness” of reconstructive implants and devices. At the end of this review, it is clear that further research will serve to narrow the gap, deftly reverse engineering “cellular” powerhouses of energy and life with smarter and a broader array of toolkits.

#### Acknowledgements

This study was supported in part by grants from NIH through 511–1336–1761 and from Purdue Cancer Center.

#### REFERENCES

1. Putnam AJ, Mooney DJ. Tissue engineering using synthetic extracellular matrices. *Nat Med* 1996;2:824–826. [PubMed: 8673932]
2. Lutolf MP, Hubbell JA. Synthetic biomaterials as instructive extracellular microenvironments for morphogenesis in tissue engineering. *Nat Biotechnol* 2005;23:47–55. [PubMed: 15637621]
3. Pratt AB, Weber FE, Schmoekel HG, Muller R, Hubbell JA. Synthetic extracellular matrices for in situ tissue engineering. *Biotechnol Bioeng* 2004;86:27–36. [PubMed: 15007838]
4. Nuttelman CR, Tripodi MC, Anseth KS. Synthetic hydrogel niches that promote hMSC viability. *Matrix Biol* 2005;24:208–218. [PubMed: 15896949]
5. Alberts B., JA.; Lewis, J.; Raff, M.; Roberts, K.; Walter, P. *Molecular Biology of the Cell*. Garland Science, a member of the Taylor and Francis Group; 2002.
6. Wichterle O, LÍM D. Hydrophilic Gels for Biological Use. *Nature* 1960;185:117–118.
7. Kopecek J. Polymer chemistry: swell gels. *Nature* 2002;417:424–428. [PubMed: 12024209]
8. Canal T, Peppas NA. Correlation between mesh size and equilibrium degree of swelling of polymeric networks. *J Biomed Mater Res* 1989;23:1183–1193. [PubMed: 2808463]
9. Peppas NA, Wright SL. Drug diffusion and binding in ionizable interpenetrating networks from poly (vinyl alcohol) and poly (acrylic acid). *Eur J Pharm Biopharm* 1998;46:15–29. [PubMed: 9700019]
10. Stevens MM, George JH. Exploring and Engineering the Cell Surface Interface. *Science* 2005;310:1135–1138. [PubMed: 16293749]
11. Webster TJ, Waid MC, McKenzie JL, Price RL, Ejirofor JU. Nano-biotechnology: carbon nanofibres as improved neural and orthopaedic implants. *Nanotechnology* 2004;15:48–54.
12. Chun AL, Moralez JG, Fenniri H, Webster TJ. Helical rosette nanotubes: a more effective orthopaedic implant material. *Nanotechnology* 2004;15:S234–S239.
13. Palin E, Liu H, Webster TJ. Mimicking the nanofeatures of bone increases bone-forming cell adhesion and proliferation. *Nanotechnology* 2005;16:1828–1835.
14. Liu H, Slamovich EB, Webster TJ. Increased osteoblast functions among nanophase titania/poly (lactide-co-glycolide) composites of the highest nanometer surface roughness. *J Biomed Mater Res* 2006;78:798–807.
15. Balasundaram G, Webster TJ. Nanotechnology and biomaterials for orthopedic medical applications. *Nanomedicine* 2006;1:169–176. [PubMed: 17716106]
16. Santoso SS, Vauthey S, Zhang S. Structures, function and applications of amphiphilic peptides. *Curr Opin Colloid Interface Sci* 2002;7:262–266.
17. Werb Z. ECM and cell surface proteolysis: Regulating cellular ecology. *Cell* 1997;91:439–442. [PubMed: 9390552]
18. Seliktar D, Zisch AH, Lutolf MP, Wrana JL, Hubbell JA. MMP-2 sensitive, VEGF-bearing bioactive hydrogels for promotion of vascular healing. *J Biomed Mater Res* 2004;68A:704–716.
19. Stemlicht MD, Werb Z. How matrix metalloproteinases regulate cell behavior. *Annu Rev Cell Dev Biol* 2001;17:463–516. [PubMed: 11687497]

20. Park KI, Teng YD, Snyder EY. The injured brain interacts reciprocally with neural stem cells supported by scaffolds to reconstitute lost tissue. *Nat Biotechnol* 2002;20:1111–1117. [PubMed: 12379868]
21. Nur-E-Kamal A, Ahmed I, Kamal JM, Schindler M, Meiners S. Three-Dimensional Nanofibrillar Surfaces Promote Self-Renewal in Mouse Embryonic Stem Cells. *Stem Cells*. 2005
22. Lutolf MP, Weber FE, Schmoekel HG, Schense JC, Kohler T, Muller R, Hubbell JA. Repair of bone defects using synthetic mimetics of collagenous extracellular matrices. *Nat Biotechnol* 2003;21:513–518. [PubMed: 12704396]
23. Liu Y, Ahmad S, Shu XZ, Sanders RK, Kopesec SA, Prestwich GD. Accelerated repair of cortical bone defects using a synthetic extracellular matrix to deliver human demineralized bone matrix. *J Orthop Res*. 2006
24. D'Andrea LD, Del Gatto A, Pedone C, Benedetti E. Peptide-based Molecules in Angiogenesis. *Chem Biol Drug Des* 2006;67:115–126. [PubMed: 16492159]
25. Rouet V, Hama-Kourbali Y, Petit E, Panagopoulou P, Katsoris P, Barritault D, Caruelle JP, Courty J. A Synthetic Glycosaminoglycan Mimetic Binds Vascular Endothelial Growth Factor and Modulates Angiogenesis. *J Biol Chem* 2005;280:32792. [PubMed: 16014624]
26. Russell TP. Surface-Responsive Materials. *Science* 2002;297:964. [PubMed: 12169722]
27. van Esch JH, Feringa BL. New Functional Materials Based on Self-Assembling Organogels: From Serendipity towards Design. *Angew Chem Int Ed Engl* 2000;39:2263–2266. [PubMed: 10941059]
28. Chen J, Blevins WE, Park H, Park K. Gastric retention properties of superporous hydrogel composites. *J Controlled Release* 2000;64:39–51.
29. Hwang SJ, Park H, Park K. Gastric retentive drug-delivery systems. *Crit Rev Ther Drug Carrier Syst* 1998;15:243–284. [PubMed: 9699081]
30. Chen J, Park H, Park K. Synthesis of superporous hydrogels: Hydrogels with fast swelling and superabsorbent properties. *J Biomed Mater Res* 1999;44:53–62. [PubMed: 10397904]
31. Chen J, Park K. Superporous hydrogels: Fast responsive hydrogel systems. *J Macromol Sci, Chem* 1999;A36:917–930.
32. Chen J, Park K. Synthesis and characterization of superporous hydrogel composites. *J Controlled Release* 2000;65:73–82.
33. Gemeinhart RA, Chen J, Park H, Park K. pH-sensitivity of fast responsive superporous hydrogels. *J Biomater Sci Polym Ed* 2000;11:1371–1380. [PubMed: 11261878]
34. Gemeinhart RA, Park H, Park K. Pore structure of superporous hydrogels. *Polymers for Advanced Technologies* 2000;11:617–625.
35. Omidian H, Rocca JG, Park K. Advances in superporous hydrogels. *J Control Release* 2005;102:3–12. [PubMed: 15653129]
36. Omidian H, Rocca JG, Park K. Elastic, Superporous Hydrogel Hybrids of Polyacrylamide and Sodium Alginate. *Macromol Biosci* 2006;703:710.
37. Park H, Park K, Kim D. Preparation and swelling behavior of chitosan-based superporous hydrogels for gastric retention application. *J Biomed Mater Res* 2006;76A:144–150.
38. Baek N, Park K, Park JH, Bae YH. Control of the swelling rate of superporous hydrogels. *J Bioact Compat Polym* 2001;16:47–57.
39. van der Wey LP, Gabreels-Festen AA, Merks MH, Polder TW, Stegeman DF, Spauwen PH, Gabreels FJ. Peripheral nerve elongation by laser Doppler flowmetry controlled expansion: morphological aspects. *Acta Neuropathol (Berl)* 1995;89:166–171. [PubMed: 7732788]
40. Wiese KG. Osmotically induced tissue expansion with hydrogels: a new dimension in tissue expansion? A preliminary report. *J Craniomaxillofac Surg* 1993;21:309–313. [PubMed: 8263217]
41. Kauffman GB, Mayo I. The Story of Nitinol: The Serendipitous Discovery of the Memory Metal and Its Applications. *The Chemical Educator* 1996;2:1–21.
42. Yahia L, Manceur A, Chaffraix P. Bioperformance of shape memory alloy single crystals. *Biomed Mater Eng* 2006;16:101–118. [PubMed: 16477119]
43. Lendlein A, Kelch S. Shape-memory polymers as stimuli-sensitive implant materials. *Clin Hemorheol Microcirc* 2005;32:105–116. [PubMed: 15764819]

44. Lendlein A, Langer R. Biodegradable, Elastic Shape-Memory Polymers for Potential Biomedical Applications. *Science* 2002;296:1673–1676. [PubMed: 11976407]
45. Lendlein A, Schmidt AM, Langer R. AB-polymer networks based on oligo(epsilon-caprolactone) segments showing shape-memory properties. *Proc Natl Acad Sci U S A* 2001;98:842–847. [PubMed: 11158558]
46. Koerner H, Price G, Pearce NA, Alexander M, Vaia RA. Remotely actuated polymer nanocomposites--stress-recovery of carbon-nanotube-filled thermoplastic elastomers. *Nat Mater* 2004;3:115–120. [PubMed: 14743213]
47. Lendlein A, Kratz K, Kelch S. Smart Implant Materials. *Med Device Technol* 2005;16:12–14. [PubMed: 15871417]
48. Osada Y, Matsuda A. Shape memory in hydrogels. *Nature* 1995;376:219–219. [PubMed: 7617029]
49. Zheng X, Zhou S, Li X, Weng J. Shape memory properties of poly(D,L-lactide)/hydroxyapatite composites. *Biomaterials* 2006;27:4288–4295. [PubMed: 16675009]
50. Alteheld A, Feng Y, Kelch S, Lendlein A. Biodegradable, amorphous copolyester-urethane networks having shape-memory properties. *Angew Chem, Int Ed Engl* 2005;44:1188–1192. [PubMed: 15654685]
51. Ping P, Wang W, Chen X, Jing X. Poly(epsilon-caprolactone) polyurethane and its shape-memory property. *Biomacromolecules* 2005;6:587–592. [PubMed: 15762617]
52. Liu Y, Gall K, Dunn ML, Greenberg AR, Diani J. Thermomechanics of shape memory polymers: Uniaxial experiments and constitutive modeling. *Int J Plast* 2006;22:279–313.
53. Liu Y, Gall K, Dunn ML, McCluskey P. Thermomechanics of shape memory polymer nanocomposites. *Mechanics of Materials* 2004;36:929–940.
54. Kymakis E, Alexandou I, Amaratunga GAJ. Single-walled carbon nanotube-polymer composites: electrical, optical and structural investigation. *Synth Met* 2002;127:59–62.
55. Kornbluh, R.; Pelrine, R.; Eckerle, J.; Joseph, J. Robotics and Automation. 3. IEEE; Leuven, Belgium: 1998. Electrostrictive polymer artificial muscle actuators; p. 2147-2154.
56. Liu RH, Yu Q, Beebe DJ. Fabrication and characterization of hydrogel-based microvalves. *JMEMS* 2002;11:45–53.
57. Eddington DT, Beebe DJ. A Valved Responsive Hydrogel Microdispensing Device With Integrated Pressure Source. *JMEMS* 2004;13
58. Richter AK, Howitz D, Arndt STG. Electronically controllable microvalves based on smart hydrogels: magnitudes and potential applications. *JMEMS* 2003;12:748–753.
59. Lee S, Eddington DT, Kim Y, Kim W, Beebe DJ. Control mechanism of an organic self-regulating microfluidic system. *JMEMS* 2003;12:848–854.
60. Albuérne J, Marquez L, Müller AJ, Raquez JM, Degée P, Dubois P. Hydrolytic Degradation of Double Crystalline PPDX-b-PCL Diblock Copolymers. *Macromol Chem Phys* 2005;206:903–914.
61. Jiang HY, Kelch S, Lendlein A. Polymers Move in Response to Light. *Advanced Materials* 2006;18:1471–1475.
62. Jiang HY, Kelch S, Lendlein A. Polymers Move in Response to Light. *Adv Mater (Weinheim, Fed Repub Ger)* 2006;18:1471–1475.
63. Ahir SV, Terentjev EM. Photomechanical actuation in polymer-nanotube composites. *Nat Mater* 2005;4:491–495. [PubMed: 15880115]
64. Gall K, Dunn ML, Liu Y, Stefanic G, Balzar D. Internal stress storage in shape memory polymer nanocomposites. *Appl Phys Lett* 2004;85:290.
65. Lendlein A, Jiang H, Junger O, Langer R. Light-induced shape-memory polymers. *Nature* 2005;434:879–882. [PubMed: 15829960]
66. Lu S, Panchapakesan B. Optically driven nanotube actuators. *Nanotechnology* 2005;16:2548–2554.
67. van Hest JC, Tirrell DA. Protein-based materials, toward a new level of structural control. *Chem Commun (Camb)* 2001;19:1897–1904. [PubMed: 12240211]
68. Cornish VW, Benson DR, Altenbach CA, Hideg K, Hubbell WL, Schultz PG. Site-specific incorporation of biophysical probes into proteins. *Proc Natl Acad Sci U S A* 1994;91:2910. [PubMed: 8159678]

69. De Filippis V, Frasson R, Fontana A. 3-Nitrotyrosine as a spectroscopic probe for investigating protein protein interactions. *Protein Sci* 2006;15:976–986. [PubMed: 16641485]
70. Forster AC, Tan Z, Nalam MNL, Lin H, Qu H, Cornish VW, Blacklow SC. Programming peptidomimetic syntheses by translating genetic codes designed de novo. *Proc Natl Acad Sci U S A* 2003;100:6353–6357. [PubMed: 12754376]
71. Chin JW, Martin AB, King DS, Wang L, Schultz PG. Addition of a photocrosslinking amino acid to the genetic code of *Escherichia coli*. *Proc Natl Acad Sci U S A* 2002;99:11020–11024. [PubMed: 12154230]
72. Cohen BE, McAnaney TB, Park ES, Jan YN, Boxer SG, Jan LY. Probing protein electrostatics with a synthetic fluorescent amino acid. *Science* 2002;296:1700–1703. [PubMed: 12040199]
73. Weiss S. Fluorescence spectroscopy of single biomolecules. *Science* 1999;283:1676–1683. [PubMed: 10073925]
74. Budisa N, Minks C, Alefelder S, Wenger W, Dong F, Moroder L, Huber R. Toward the experimental codon reassignment in vivo: protein building with an expanded amino acid repertoire. *FASEB J* 1999;13:41–51. [PubMed: 9872928]
75. Nowak MW, Kearney PC, Sampson JR, Saks ME, Labarca CG, Silverman SK, Zhong W, Thorson J, Abelson JN, Davidson N. Nicotinic receptor binding site probed with unnatural amino acid incorporation in intact cells. *Science* 1995;268:439–442. [PubMed: 7716551]
76. Dawson PE, Muir TW, Clark-Lewis I, Kent SB. Synthesis of proteins by native chemical ligation. *Science* 1994;266:776–779. [PubMed: 7973629]
77. Lodish, H.; Berk, A.; Zipursky, L.S.; Matsudaira, P.; Baltimore, D.; Darnell, J. *Molecular Cell Biology*. W. H. Freeman and Company; 2000.
78. Pakstis LM, Ozbas B, Hales KD, Nowak AP, Deming TJ, Pochan D. Effect of Chemistry and Morphology on the Biofunctionality of Self-Assembling Diblock Copolypeptide Hydrogels. *Biomacromolecules* 2004;5:312–318. [PubMed: 15002989]
79. Nowak AP, Breedveld V, Pakstis L, Ozbas B, Pine DJ, Pochan D, Deming TJ. Rapidly recovering hydrogel scaffolds from self-assembling diblock copolypeptide amphiphiles. *Nature* 2002;417:424–428. [PubMed: 12024209]
80. Deming TJ. Facile synthesis of block copolypeptides of defined architecture. *Nature* 1997;390:386–389. [PubMed: 9389476]
81. Yang J, Xu C, Kopeckova P, Kopecek J. Hybrid Hydrogels Self-Assembled from HPMA Copolymers Containing Peptide Grafts. *Macromol Biosci* 2006;6:201–209. [PubMed: 16514591]
82. Tang A, Wang C, Stewart RJ, Kopecek J. The coiled coils in the design of protein-based constructs: hybrid hydrogels and epitope displays. *J Controlled Release* 2001;72:57–70.
83. Yang J, Xu C, Wang C, Kopecek J. Refolding Hydrogels Self-Assembled from N-(2-Hydroxypropyl) methacrylamide Graft Copolymers by Antiparallel Coiled-Coil Formation. *Biomacromolecules* 2006;7:1187–1195. [PubMed: 16602737]
84. Lupas A. Coiled coils: new structures and new functions. *Trends Biochem Sci* 1996;21:375–382. [PubMed: 8918191]
85. Crick FHC. The packing of alpha-helices: simple coiled-coils. *Acta Crystallogr* 1953;6:689–697.
86. Pauling L, Corey RB. Compound helical configurations of polypeptide chains: structure of proteins of the alpha-keratin type. *Nature* 1953;171:59–61. [PubMed: 13025480]
87. Gruber M, Lupas AN. Historical review: Another 50th anniversary-new periodicities in coiled coils. *Trends Biochem Sci* 2003;28:679–685. [PubMed: 14659700]
88. Lupas A, Van Dyke M, Stock J. Predicting coiled coils from protein sequences. *Science* 1991;252:1162–1164.
89. Mason JM, Arndt KM. Coiled Coil Domains: Stability, Specificity, and Biological Implications. *ChemBioChem* 2004;5:170–176. [PubMed: 14760737]
90. Wolf E, Kim PS, Berger B. MultiCoil: A program for predicting two-and three-stranded coiled coils. *Protein Sci* 1997;6:1179–1189. [PubMed: 9194178]
91. Zhu BY, Zhou NE, Kay CM, Hodges RS. Packing and hydrophobicity effects on protein folding and stability: effects of beta-branched amino acids, valine and isoleucine, on the formation and stability



- of two-stranded alpha-helical coiled coils/leucine zippers. *Protein Sci* 1993;2:383–394. [PubMed: 8453376]
92. Wang C, Stewart RJ, Kopecek J. Hybrid hydrogels assembled from synthetic polymers and coiled-coil protein domains. *Nature* 1999;397:417–420. [PubMed: 9989405]
  93. Petka WA, Harden JL, McGrath KP, Wirtz D, Tirrell DA. Reversible Hydrogels from Self-Assembling Artificial Proteins. *Science* 1998;281:389–392. [PubMed: 9665877]
  94. Mi L, Fischer S, Chung B, Sundelacruz S, Harden JL. Self-assembling protein hydrogels with modular integrin binding domains. *Biomacromolecules* 2006;7:38–47. [PubMed: 16398496]
  95. Pasqualini R, Koivunen E, Ruoslahti E. Peptides in cell adhesion: powerful tools for the study of integrin-ligand interactions. *Braz J Med Biol Res* 1996;29:1151–1158. [PubMed: 9181058]
  96. Hubbell JA. Biomaterials in tissue engineering. *Nat Biotechnol* 1995;13:565–576.
  97. Ruoslahti E. RGD and other recognition sequences for integrins. *Annu Rev Cell Dev Biol* 1996;12:697–715. [PubMed: 8970741]
  98. Deng C, Tian H, Zhang P, Sun J, Chen X, Jing X. Synthesis and Characterization of RGD Peptide Grafted Poly(ethylene glycol)-*b*-Poly(L-lactide)-*b*-Poly(L-glutamic acid) Triblock Copolymer. *Biomacromolecules* 2006;7:590–596. [PubMed: 16471935]
  99. Hu Y, Winn SR, Krajchich I, Hollinger JO. Porous polymer scaffolds surface-modified with arginine-glycine-aspartic acid enhance bone cell attachment and differentiation in vitro. *J Biomed Mater Res* 2003;64A:583–590.
  100. Lin HB, Sun W, Mosher DF, Garcia-Echeverria C, Schaufelberger K, Lelkes PI, Cooper SL. Synthesis, surface, and cell-adhesion properties of polyurethanes containing covalently grafted RGD-peptides. *J Biomed Mater Res* 1994;28:329–342. [PubMed: 8077248]
  101. Kao WJ, Lee D, Schense JC, Hubbell JA. Fibronectin modulates macrophage adhesion and FBGC formation: The role of RGD, PHSRN, and PRRARV domains. *J Biomed Mater Res* 2001;55
  102. Garcia AJ, Schwarzbauer JE, Boettiger D. Distinct activation states of alpha5beta1 integrin show differential binding to RGD and synergy domains of fibronectin. *Biochemistry* 2002;41:9063–9069. [PubMed: 12119020]
  103. Lin X, Takahashi K, Liu Y, Zamora PO. Enhancement of cell attachment and tissue integration by a IKVAV containing multi-domain peptide. *Biochim Biophys Acta* 2006;1760:1403–1410. [PubMed: 16860485]
  104. Adams DN, Kao EY, Hypolite CL, Distefano MD, Hu WS, Letourneau PC. Growth cones turn and migrate up an immobilized gradient of the laminin IKVAV peptide. *J Neurobiol* 2005;62:134–147. [PubMed: 15452851]
  105. Yamada M, Kadoya Y, Kasai S, Kato K, Mochizuki M, Nishi N, Watanabe N, Kleinman HK, Yamada Y, Nomizu M. Ile-Lys-Val-Ala-Val (IKVAV)-containing laminin alpha1 chain peptides form amyloid-like fibrils. *FEBS Lett* 2002;530:48–52. [PubMed: 12387864]
  106. Jun HW, West JL. Endothelialization of Microporous YIGSR/PEG-Modified Polyurethaneurea. *Tissue Eng* 2005;11:1133–1140. [PubMed: 16144449]
  107. Jun HW, West JL. Modification of polyurethaneurea with PEG and YIGSR peptide to enhance endothelialization without platelet adhesion. *J Biomed Mater Res* 2005;72B:131–139.
  108. Aggeli A, Bell M, Boden N, Keen JN, Knowles PF, McLeish TC, Pitkeathly M, Radford SE. Responsive gels formed by the spontaneous self-assembly of peptides into polymeric beta-sheet tapes. *Nature* 1997;386:259–262. [PubMed: 9069283]
  109. Collier JH, Messersmith PB. Enzymatic modification of self-assembled peptide structures with tissue transglutaminase. *Bioconjug Chem* 2003;14:748–755. [PubMed: 12862427]
  110. Shen CL, Murphy RM. Solvent effects on self-assembly of beta-amyloid peptide. *Biophys J* 1995;69:640–651. [PubMed: 8527678]
  111. Scheibel T, Parthasarathy R, Sawicki G, Lin XM, Jaeger H, Lindquist SL. Conducting nanowires built by controlled self-assembly of amyloid fibers and selective metal deposition. *Proc Natl Acad Sci U S A* 2003;100:4527–4532. [PubMed: 12672964]
  112. Ricka J, Tanaka T. Swelling of ionic gels: quantitative performance of the Donnan theory. *Macromolecules* 1984;17:2916–2921.

113. Lee JW, Kim SY, Kim SS, Lee YM, Lee KH, Kim SJ. Synthesis and Characteristics of Interpenetrating Polymer Network Hydrogel Composed of Chitosan and Poly (acrylic acid). *J Appl Polym Sci* 1999;73:113–120.
114. Babu VR, Rao K, Sairam M, Naidu BVK, Hosamani KM, Aminabhavi TM. pH Sensitive Interpenetrating Network Microgels of Sodium Alginate-Acrylic Acid for the Controlled Release of Ibuprofen. *J Appl Polym Sci* 2006;99:2671.
115. Zhang J, Peppas NA. Synthesis and characterization of pH-and temperature-sensitive poly (methacrylic acid)/poly (N-isopropylacrylamide) interpenetrating polymeric networks. *Macromolecules* 2000;33:102–107.
116. Bell CL, Peppas NA. Water, solute and protein diffusion in physiologically responsive hydrogels of poly (methacrylic acid-g-ethylene glycol). *Biomaterials* 1996;17:1203–1218. [PubMed: 8799505]
117. Nakamura K, Murray RJ, Joseph JJ, Peppas NA, Morishita M, Lowman AM. Oral insulin delivery using P (MAA-g-EG) hydrogels: effects of network morphology on insulin delivery characteristics. *J Controlled Release* 2004;95:589–599.
118. Sethuraman VA, Na K, Bae YH. pH-Responsive Sulfonamide/PEI System for Tumor Specific Gene Delivery: An in Vitro Study. *Biomacromolecules* 2006;7:64–70. [PubMed: 16398499]
119. Sideratou Z, Tsiourvas D, Paleos CM. Quaternized Poly (propylene imine) Dendrimers as Novel pH-Sensitive Controlled-Release Systems. *Langmuir* 2000;16:1766–1769.
120. Goycoolea FM, Heras A, Aranaz I, Galed G, Fernandez-Valle ME, Argueelles-Monal W. Effect of Chemical Crosslinking on the Swelling and Shrinking Properties of Thermal and pH-Responsive Chitosan Hydrogels. *Macromol Biosci* 2003;3:612–619.
121. Chen SC, Wu YC, Mi FL, Lin YH, Yu LC, Sung HW. A novel pH-sensitive hydrogel composed of N, O-carboxymethyl chitosan and alginate cross-linked by genipin for protein drug delivery. *J Control Release* 2004;96:285–300. [PubMed: 15081219]
122. Risbud MV, Hardikar AA, Bhat SV, Bhande RR. pH-sensitive freeze-dried chitosan-polyvinyl pyrrolidone hydrogels as controlled release system for antibiotic delivery. *J Controlled Release* 2000;68:23–30.
123. Qu X, Wirsén A, Albertsson AC. Structural change and swelling mechanism of pH-sensitive hydrogels based on chitosan and D,L-lactic acid. *J Appl Polym Sci* 1999;74:3186–3192.
124. Burke SE, Barrett CJ. pH-responsive properties of multilayered poly (L-lysine)/hyaluronic acid surfaces. *Biomacromolecules* 2003;4:1773–1783. [PubMed: 14606908]
125. Toncheva V, Wolfert MA, Dash PR, Oupicky D, Ulbrich K, Seymour LW, Schacht EH. Novel vectors for gene delivery formed by self-assembly of DNA with poly (L-lysine) grafted with hydrophilic polymers. *Biochim Biophys Acta* 1998;1380:354–368. [PubMed: 9555094]
126. Bennis JM, Choi JS, Mahato RI, Park JS, Kim SW. pH-sensitive cationic polymer gene delivery vehicle: N-Ac-poly (L-histidine)-graft-poly (L-lysine) comb shaped polymer. *Bioconjug Chem* 2000;11:637–645. [PubMed: 10995206]
127. Park JS, Han TH, Lee KY, Han SS, Hwang JJ, Moon DH, Kim SY, Cho YW. N-acetyl histidine-conjugated glycol chitosan self-assembled nanoparticles for intracytoplasmic delivery of drugs: Endocytosis, exocytosis and drug release. *J Controlled Release* 2006;115:37–45.
128. Casolaro M, Bottari S, Cappelli A, Mendichi R, Ito Y. Vinyl polymers based on L-histidine residues. Part 1. The thermodynamics of poly(ampholyte)s in the free and in the cross-linked gel form. *Biomacromolecules* 2004;5:1325–1332. [PubMed: 15244447]
129. Casolaro M, Bottari S, Ito Y. Vinyl Polymers Based on l-Histidine Residues. Part 2. Swelling and Electric Behavior of Smart Poly (ampholyte) Hydrogels for Biomedical Applications. *Biomacromolecules* 2006;7:1439–1448. [PubMed: 16677025]
130. Odijk T. Electrostatic persistence length and its relation to a unified theory of polyelectrolytes. *Polymer* 1978;19:989–990.
131. Duyndam A, Odijk T. Viscosity of Wormlike Micelles: Determination of the End Cap Energy and Persistence Length. *Langmuir* 1996;12:4718–4722.
132. Odijk T. Physics of tightly curved semiflexible polymer chains. *Macromolecules* 1993;26:6897–6902.

133. Konak C, Bansil R. Swelling equilibria of ionized poly (methacrylic acid) gels in the absence of salt. *Polymer* 1989;30:677–680.
134. Luo L, Kato M, Tsuruta T, Kataoka K, Nagasaki Y. Stimuli-sensitive polymer gels that stiffen upon swelling. *Macromolecules* 2000;33:4992–4994.
135. Jeong B, Gutowska A. Lessons from nature: stimuli-responsive polymers and their biomedical applications. *Trends Biotechnol* 2002;20:305–311. [PubMed: 12062976]
136. Philippova OE, Hourdet D, Audebert R, Khokhlov AR. pH-responsive gels of hydrophobically modified poly (acrylic acid). *Macromolecules* 1997;30:8278–8285.
137. Thomas JL, You H, Tirrell DA. Tuning the response of a pH-sensitive membrane switch. *J Am Chem Soc* 1995;117:2949–2950.
138. Glynn SA, Albanes D. Folate and cancer: a review of the literature. *Nutr Cancer* 1994;22:101–119. [PubMed: 14502840]
139. Tannock IF, Rotin D. Acid pH in tumors and its potential for therapeutic exploitation. *Cancer Res* 1989;49:4373–4384. [PubMed: 2545340]
140. Gottesman MM, Fojo T, Bates SE. Multidrug resistance in cancer: role of ATP-dependent transporters. *Nat Rev Cancer* 2002;2:48–58. [PubMed: 11902585]
141. Helmlinger G, Yuan F, Dellian M, Jain RK. Interstitial pH and pO<sub>2</sub> gradients in solid tumors in vivo: High-resolution measurements reveal a lack of correlation. *Nat Med* 1997;3:177–182. [PubMed: 9018236]
142. Vaupel P, Kallinowski F, Okunieff P. Blood flow, oxygen and nutrient supply, and metabolic microenvironment of human tumors: a review. *Cancer Res* 1989;49:6449–6465. [PubMed: 2684393]
143. Xu S, Kramer M, Haag R. pH-Responsive dendritic core-shell architectures as amphiphilic nanocarriers for polar drugs. *J Drug Target* 2006;14:367–374. [PubMed: 17092837]
144. Tanaka T, Shiramoto S, Miyashita M, Fujishima Y, Kaneo Y. Tumor targeting based on the effect of enhanced permeability and retention (EPR) and the mechanism of receptor-mediated endocytosis (RME). *Int J Pharm* 2004;277:39–61. [PubMed: 15158968]
145. De Smedt SC, Demeester J, Hennink WE. Cationic polymer based gene delivery systems. *Pharm Res* 2000;17:113–126. [PubMed: 10751024]
146. Mi FL, Sung HW, Shyu SS. Drug release from chitosan-alginate complex beads reinforced by a naturally occurring cross-linking agent. *Carbohydr Polym* 2002;48:61–72.
147. Chen SC, Wu YC, Mi FL, Lin YH, Yu LC, Sung HW. A novel pH-sensitive hydrogel composed of N, O-carboxymethyl chitosan and alginate cross-linked by genipin for protein drug delivery. *J Controlled Release* 2004;96:285–300.
148. Chen H, Ouyang W, Lawuyi B, Prakash S. Genipin cross-linked alginate-chitosan microcapsules: membrane characterization and optimization of cross-linking reaction. *Biomacromolecules* 2006;7:2091–2098. [PubMed: 16827575]
149. Takeuchi H, Yasuji T, Yamamoto H, Kawashima Y. Spray-dried lactose composite particles containing an ion complex of alginate-chitosan for designing a dry-coated tablet having a time-controlled releasing function. *Pharm Res* 2000;17:94–99. [PubMed: 10714615]
150. Yu SH, Mi FL, Wu YB, Peng CK, Shyu SS, Huang RN. Antibacterial Activity of Chitosan–Alginate Sponges Incorporating Silver Sulfadiazine: Effect of Ladder-Loop Transition of Interpolyelectrolyte Complex and Ionic Crosslinking on the Antibiotic Release. *J Appl Polym Sci* 2005;98:538–549.
151. Shu XZ, Zhu KJ, Song W. Novel pH-sensitive citrate cross-linked chitosan film for drug controlled release. *Int J Pharm* 2001;212:19–28. [PubMed: 11165817]
152. Giacomelli C, Le Men L, Borsali R, Lai-Kee-Him J, Brisson A, Armes SP, Lewis AL. Phosphorylcholine-Based pH-Responsive Diblock Copolymer Micelles as Drug Delivery Vehicles: Light Scattering, Electron Microscopy, and Fluorescence Experiments. *Biomacromolecules* 2006;7:817–828. [PubMed: 16529419]
153. Garrett Q, Laycock B, Garrett RW. Hydrogel Lens Monomer Constituents Modulate Protein Sorption. *Invest Ophthalmol Vis Sci* 2000;41:1687–1695. [PubMed: 10845587]
154. Tanaka T. Dynamics of critical concentration fluctuations in gels. *Physical Review A: Atomic, Molecular, and Optical Physics* 1978;17:763–766.

155. Bae YH. Smart Polymers in Drug Delivery. *Pharmaceutical News* 2002;9:417–424.
156. Qiu Y, Park K. Environment-sensitive hydrogels for drug delivery. *Advanced Drug Delivery Reviews* 2001;53:321–339. [PubMed: 11744175]
157. Aronoff DM, Neilson EG. Antipyretics: mechanisms of action and clinical use in fever suppression. *Am J Med* 2001;111:304–315. [PubMed: 11566461]
158. Zareie HM, Volga Bulmus E, Gunning AP, Hoffman AS, Piskin E, Morris VJ. Investigation of a stimuli-responsive copolymer by atomic force microscopy. *Polymer* 2000;41:6723–6727.
159. Hirokawa Y, Jinnai H, Nishikawa Y, Okamoto T, Hashimoto T. Direct Observation of Internal Structures in Poly (N-isopropylacrylamide) Chemical Gels. *Macromolecules* 1999;32:7093–7099.
160. Qiu Y, Park K. Environment-sensitive hydrogels for drug delivery. *Adv Drug Deliv Rev* 2001;53:321–339. [PubMed: 11744175]
161. Bae YH, Okano T, Kim SW. Temperature dependence of swelling of crosslinked poly (N, N'-alkyl substituted acrylamides) in water. *J Polym Sci, Part B: Polym Phys* 1990;28:923–936.
162. Song SC, Lee SB, Jin JI, Sohn YS. A new class of biodegradable thermosensitive polymers. I. Synthesis and characterization of poly (organophosphazenes) with methoxy-poly (ethylene glycol) and amino acid esters as side groups. *Macromolecules* 1999;32:2188–2193.
163. Sershen S, West J. Implantable, polymeric systems for modulated drug delivery. *Adv Drug Deliv Rev* 2002;54:1225–1235. [PubMed: 12393303]
164. Schild HG. Poly(N-isopropylacrylamide): experiment, theory and application. *Prog Polym Sci* 1992;17:163–249.
165. Tsuda Y, Kikuchi A, Yamato M, Sakurai Y, Umezu M, Okano T. Control of cell adhesion and detachment using temperature and thermoresponsive copolymer grafted culture surfaces. *J Biomed Mater Res* 2004;69:70–78.
166. Takei YG, Aoki T, Sanui K, Ogata N, Okano T, Sakurai Y. Temperature-responsive bioconjugates. 2. Molecular design for temperature-modulated bioseparations. *Bioconjug Chem* 1993;4:341–346. [PubMed: 8274517]
167. Iwata H, Oodate M, Uyama Y, Amemimya H, Ikada Y. Preparation of temperature-sensitive membranes by graft polymerization onto a porous membrane. *J Membr Sci* 1991;55:119–130.
168. Feil H, Bae YH, Feijen J, Kim SW. Effect of comonomer hydrophilicity and ionization on the lower critical solution temperature of N-isopropylacrylamide copolymers. *Macromolecules* 1993;26:2496–2500.
169. Feil H, Bae YH, Feijen J, Kim SW. Mutual influence of pH and temperature on the swelling of ionizable and thermosensitive hydrogels. *Macromolecules* 1992;25:5528–5530.
170. Hirotsu S. Coexistence of phases and the nature of first-order phase transition in poly(N-isopropylacrylamide) gels. *Adv Polym Sci* 1993;110:1–26.
171. Irie M. Stimuli-responsive poly(N-isopropylacrylamide). Photo- and chemical-induced phase transitions. *Adv Polym Sci* 1993;110:49–65.
172. Bae YH, Okano T, Kim SW. “On-off” thermocontrol of solute transport. I. Temperature dependence of swelling of N-isopropylacrylamide networks modified with hydrophobic components in water. *Pharm Res* 1991;8:531–537. [PubMed: 1871053]
173. Bae YH, Okano T, Kim SW. “On-off” thermocontrol of solute transport. II. Solute release from thermosensitive hydrogels. *Pharm Res* 1991;8:624–628. [PubMed: 1866377]
174. Yoshida R, Sakai K, Okano T, Sakurai Y. Modulating the phase transition temperature and thermosensitivity in N-isopropylacrylamide copolymer gels. *J Biomater Sci Polym Ed* 1994;6:585–598. [PubMed: 7873510]
175. Brazel CS, Peppas NA. Pulsatile local delivery of thrombolytic and antithrombotic agents using poly(N-isopropylacrylamide-co-methacrylic acid) hydrogels. *J Controlled Release* 1996;39:57–64.
176. Katono H, Maruyama A, Sanui K, Ogata N, Okano T, Sakurai Y. Thermoresponsive swelling and drug release switching of interpenetrating polymer networks composed of poly(acrylamide-co-butyl methacrylate) and poly(acrylic acid). *J Controlled Release* 1991;16:215–227.
177. Aoki T, Kawashima M, Katono H, Sanui K, Ogata N, Okano T, Sakurai Y. Temperature-Responsive Interpenetrating Polymer Networks Constructed with Poly(acrylic acid) and Poly (N,Ndimethylacrylamide). *Macromolecules* 1994;27:947–952.

178. Kavanagh CA, Rochev YA, Gallagher WM, Dawson KA, Keenan AK. Local drug delivery in restenosis injury: thermoresponsive co-polymers as potential drug delivery systems. *Pharmacol Ther* 2004;102:1–15. [PubMed: 15056495]
179. Stayton PS, Shimoboji T, Long C, Chilkoti A, Ghen G, Harris JM, Hoffman AS. Control of protein–ligand recognition using a stimuli-responsive polymer. *Nature* 1995;378:472–474. [PubMed: 7477401]
180. Morikawa N, Matsuda T. Thermoresponsive artificial extracellular matrix: N-isopropylacrylamide-graft-copolymerized gelatin. *J Biomater Sci Polym Ed* 2002;13:167–183. [PubMed: 12022748]
181. Vogel KG. Effects of hyaluronidase, trypsin, and EDTA on surface composition and topography during detachment of cells in culture. *Exp Cell Res* 1978;113:345–357. [PubMed: 122554]
182. Canavan HE, Cheng X, Graham DJ, Ratner BD, Castner DG. Cell sheet detachment affects the extracellular matrix: a surface science study comparing thermal liftoff, enzymatic, and mechanical methods. *J Biomed Mater Res* 2005;75 A:1–13.
183. Shimizu T, Yamato M, Kikuchi A, Okano T. Two-dimensional manipulation of cardiac myocyte sheets utilizing temperature-responsive culture dishes augments the pulsatile amplitude. *Tissue Eng* 2001;7:141–151. [PubMed: 11304450]
184. Shimizu T, Yamato M, Isoi Y, Akutsu T, Setomaru T, Abe K, Kikuchi A, Umezu M, Okano T. Fabrication of pulsatile cardiac tissue grafts using a novel 3-dimensional cell sheet manipulation technique and temperature-responsive cell culture surfaces. *Circ Res* 2002;90:e40. [PubMed: 11861428]
185. Ohya S, Matsuda T. Poly(N-isopropylacrylamide) (PNIPAM)-grafted gelatin as thermoresponsive three-dimensional artificial extracellular matrix: molecular and formulation parameters vs. cell proliferation potential. *J Biomater Sci Polym Ed* 2005;16:809–827. [PubMed: 16128290]
186. Matsuda T. Poly (N-isopropylacrylamide)-grafted gelatin as a thermoresponsive cell-adhesive, mold-releasable material for shape-engineered tissues. *J Biomater Sci Polym Ed* 2004;15:947–955. [PubMed: 15318803]
187. Ohya S, Nakayama Y, Matsuda T. Thermoresponsive artificial extracellular matrix for tissue engineering: hyaluronic acid bioconjugated with poly (N-isopropylacrylamide) grafts. *Biomacromolecules* 2001;2:856–863. [PubMed: 11710042]
188. Ohya S, Kidoaki S, Matsuda T. Poly (N-isopropylacrylamide)(PNIPAM)-grafted gelatin hydrogel surfaces: interrelationship between microscopic structure and mechanical property of surface regions and cell adhesiveness. *Biomaterials* 2005;26:3105–3111. [PubMed: 15603805]
189. Ohya S, Sonoda H, Nakayama Y, Matsuda T. The potential of poly (N-isopropylacrylamide) (PNIPAM)-grafted hyaluronan and PNIPAM-grafted gelatin in the control of post-surgical tissue adhesions. *Biomaterials* 2005;26:655–659. [PubMed: 15282143]
190. Okano T, Yamada N, Okuhara M, Sakai H, Sakurai Y. Mechanism of cell detachment from temperature-modulated, hydrophilic-hydrophobic polymer surfaces. *Biomaterials* 1995;16:297–303. [PubMed: 7772669]
191. Takamizawa K, Shoda K, Matsuda T. Pull-out mechanical measurement of tissue-substrate adhesive strength: endothelial cell monolayer sheet formed on a thermoresponsive gelatin layer. *J Biomater Sci Polym Ed* 2002;13:81–94. [PubMed: 12003077]
192. Kim S, Chung EH, Gilbert M, Healy KE. Synthetic MMP-13 degradable ECMs based on poly (N-isopropylacrylamide-co-acrylic acid) semi-interpenetrating polymer networks. I. Degradation and cell migration. *J Biomed Mater Res* 2005;75 A:73–88.
193. Meyer DE, Shin BC, Kong GA, Dewhirst MW, Chilkoti A. Drug targeting using thermally responsive polymers and local hyperthermia. *J Controlled Release* 2001;74:213–224.
194. Chilkoti A, Dreher MR, Meyer DE. Design of thermally responsive, recombinant polypeptide carriers for targeted drug delivery. *Adv Drug Deliv Rev* 2002;54:1093–1111. [PubMed: 12384309]
195. Chilkoti A, Dreher MR, Meyer DE, Raucher D. Targeted drug delivery by thermally responsive polymers. *Adv Drug Deliv Rev* 2002;54:613–630. [PubMed: 12204595]
196. Dreher MR, Liu W, Zalutsky MR, Dewhirst MW, Chilkoti A. Targeted drug delivery to solid tumors using thermally responsive elastin-like polypeptide macromolecular drug carriers. *Proc Amer Assoc Cancer Res* 2006;47



197. McPherson DT, Xu J, Urry DW. Product purification by reversible phase transition following *Escherichia coli* expression of genes encoding up to 251 repeats of the elastomeric pentapeptide GVGVP. *Protein Expr Purif* 1996;7:51–57. [PubMed: 9172783]
198. Meyer DE, Kong GA, Dewhirst MW, Zalutsky MR, Chilkoti A. Targeting a genetically engineered elastin-like polypeptide to solid tumors by local hyperthermia. *Cancer Res* 2001;61:1548–1554. [PubMed: 11245464]
199. Betre H, Liu W, Zalutsky MR, Chilkoti A, Kraus VB, Setton LA. A thermally responsive biopolymer for intra-articular drug delivery. *J Controlled Release* 2006;115:175–182.
200. Valiaev A, Clark RL, Chilkoti A, Zauscher S. Conformational mechanics of stimulus-responsive polypeptides. *Proc SPIE-Int Soc Opt Eng* 2003;5053:31–40.
201. Bromberg LE, Ron ES. Temperature-responsive gels and thermogelling polymer matrixes for protein and peptide delivery. *Advanced Drug Delivery Reviews* 1998;31:197–221. [PubMed: 10837626]
202. Auguste DT, Armes SP, Brzezinska KR, Deming TJ, Kohn J, Prud'homme RK. pH triggered release of protective poly(ethylene glycol)-*b*-polycation copolymers from liposomes. *Biomaterials* 2006;27:2599–2608. [PubMed: 16380161]
203. Li H, Yu G-E, Price C, Booth C, Hecht E, Hoffmann H. Concentrated Aqueous Micellar Solutions of Diblock Copoly(oxyethylene/oxybutylene) E41B8: A Study of Phase Behavior. *Macromolecules* 1997;30:1347–1354.
204. Yu G-E, Yang Y-W, Yang Z, Attwood D, Booth C, Nace VM. Association of Diblock and Triblock Copolymers of Ethylene Oxide and Butylene Oxide in Aqueous Solution. *Langmuir* 1996;12:3404–3412.
205. Jeong B, Bae YH, Kim SW. Thermoreversible Gelation of PEG-PLGA-PEG Triblock Copolymer Aqueous Solutions. *Macromolecules* 1999;32:7064–7069.
206. Jeong B, Bae YH, Lee DS, Kim SW. Biodegradable block copolymers as injectable drug-delivery systems. *Nature (London)* 1997;388:860–862. [PubMed: 9278046]
207. Jeong B, Lee DS, Shon J-I, Bae YH, Kim SW. Thermoreversible gelation of poly(ethylene oxide) biodegradable polyester block copolymers. *J Polym Sci, Part A: Polym Chem* 1999;37:751–760.
208. Cohn D, Sosnik A. Novel reverse thermoresponsive injectable poly (ether carbonate)s. *J Mater Sci - Mater Med* 2003;14:175–180. [PubMed: 15348490]
209. Kim HD, Valentini RF. Retention and activity of BMP-2 in hyaluronic acid-based scaffolds in vitro. *J Biomed Mater Res* 2002;59:573–584. [PubMed: 11774316]
210. Anderson BC, Cox SM, Bloom PD, Sheares VV, Mallapragada SK. Synthesis and characterization of diblock and gel-forming pentablock copolymers of tertiary amine methacrylates, poly (ethylene glycol), and poly (propylene glycol). *Macromolecules* 2003;36:1670–1676.
211. Determan MD, Guo L, Thiyagarajan P, Mallapragada SK. Supramolecular Self-Assembly of Multiblock Copolymers in Aqueous Solution. *Langmuir* 2006;22:1469–1473. [PubMed: 16460063]
212. Agarwal A, Unfer R, Mallapragada SK. Novel cationic pentablock copolymers as non-viral vectors for gene therapy. *J Controlled Release* 2005;103:245–258.
213. Kuijpers AJ, Engbers GHM, Feijen J, De Smedt SC, Meyvis TKL, Demeester J, Krijgsveld J, Zaat SAI, Dankert J. Characterization of the Network Structure of Carbodiimide Crosslinked Gelatin Gels. *Macromolecules* 1999;32:3325–3333.
214. Dentini M, Desideri P, Crescenzi V, Yuguchi Y, Urakawa H, Kajiwaru K. Solution and gelling properties of gellan benzyl esters. *Macromolecules* 1999;32:7109–7115.
215. Ramzi M, Rochas C, Guenet J-M. Structure-properties relation for agarose thermoreversible gels in binary solvents. *Macromolecules* 1998;31:6106–6111.
216. Chen T, Embree Heather D, Wu L-Q, Payne Gregory F. In vitro protein-polysaccharide conjugation: tyrosinase-catalyzed conjugation of gelatin and chitosan. *Biopolymers* 2002;64:292–302. [PubMed: 12124847]
217. Chenite A, Chaput C, Wang D, Combes C, Buschmann MD, Hoemann CD, Leroux JC, Atkinson BL, Binette F, Selmani A. Novel injectable neutral solutions of chitosan form biodegradable gels in situ. *Biomaterials* 2000;21:2155–2161. [PubMed: 10985488]
218. Nordby Marianne H, Kjoniksen A-L, Nystrom B, Roots J. Thermoreversible gelation of aqueous mixtures of pectin and chitosan. *Rheology. Biomacromolecules* 2003;4:337–343.

219. Ruel-Gariepy E, Leroux J-C. In situ-forming hydrogels-review of temperature-sensitive systems. *Eur J Pharm Biopharm* 2004;58:409–426. [PubMed: 15296964]
220. Kawasaki N, Ohkura R, Miyazaki S, Uno Y, Sugimoto S, Attwood D. Thermally reversible xyloglucan gels as vehicles for oral drug delivery. *Int J Pharm* 1999;181:227–234. [PubMed: 10370218]
221. Alvarez-Lorenzo C, Concheiro A, Dubovik AS, Grinberg NV, Burova TV, Grinberg VY. Temperature-sensitive chitosan-poly (N-isopropylacrylamide) interpenetrated networks with enhanced loading capacity and controlled release properties. *J Controlled Release* 2005;102:629–641.
222. Lutolf MP, Lauer-Fields JL, Schmoekel HG, Metters AT, Weber FE, Fields GB, Hubbell JA. Synthetic matrix metalloproteinase-sensitive hydrogels for the conduction of tissue regeneration: Engineering cell-invasion characteristics. *Proc Natl Acad Sci U S A* 2003;100:5413–5418. [PubMed: 12686696]
223. Miyata T, Uragami T, Nakamae K. Biomolecule-sensitive hydrogels. *Adv Drug Deliv Rev* 2002;54:79–98. [PubMed: 11755707]
224. Kabilan S, Blyth J, Lee MC, Marshall AJ, Hussain A, Yang XP, Lowe CR. Glucose-sensitive holographic sensors. *J Mol Recognit* 2004;17:162–166. [PubMed: 15137024]
225. Ghanem A, Ghaly A. Immobilization of glucose oxidase in chitosan gel beads. *J Appl Polym Sci* 2004;91:861–866.
226. Srivastava R, Brown JQ, Zhu H, McShane MJ. Stabilization of glucose oxidase in alginate microspheres with photoreactive diazoresin nanofilm coatings. *Biotechnol Bioeng* 2005;91:124–131. [PubMed: 15849694]
227. Kang SI, Bae YH. A sulfonamide based glucose-responsive hydrogel with covalently immobilized glucose oxidase and catalase. *J Controlled Release* 2003;86:115–121.
228. Chu LY, Li Y, Zhu JH, Wang HD, Liang YJ. Control of pore size and permeability of a glucose-responsive gating membrane for insulin delivery. *J Control Release* 2004;97:43–53. [PubMed: 15147803]
229. Chu LY, Liang YJ, Chen WM, Ju XJ, Wang HD. Preparation of glucose-sensitive microcapsules with a porous membrane and functional gates. *Colloids Surf B Biointerfaces* 2004;37:9–14. [PubMed: 15450302]
230. Kang SI, Bae YH. A sulfonamide based glucose-responsive hydrogel with covalently immobilized glucose oxidase and catalase. *J Control Release* 2003;86:115–121. [PubMed: 12490377]
231. Shafer-Peltier KE, Haynes CL, Glucksberg MR, Van Duyne RP. Toward a glucose biosensor based on surface-enhanced Raman scattering. *J Am Chem Soc* 2003;125:588–593. [PubMed: 12517176]
232. Kabilan S, Marshall AJ, Sartain FK, Lee MC, Hussain A, Yang X, Blyth J, Karangu N, James K, Zeng J. Holographic glucose sensors. *Biosens Bioelectron* 2005;20:1602–1610. [PubMed: 15626615]
233. Hisamitsu I, Kataoka K, Okano T, Sakurai Y. Glucose-Responsive Gel from Phenylborate Polymer and Poly (Vinyl Alcohol): Prompt Response at Physiological pH Through the Interaction of Borate with Amino Group in the Gel. *Pharm Res* 1997;14:289–293. [PubMed: 9098868]
234. Kanekiyo Y, Sano M, Iguchi R, Shinkai S. Novel nucleotide-responsive hydrogels designed from copolymers of boronic acid and cationic units and their applications as a QCM resonator system to nucleotide sensing. *J Polym Sci, Part A: Polym Chem* 2000;38:1302–1310.
235. Shiino D, Murata Y, Kubo A, Kim YJ, Kataoka K, Koyama Y, Kikuchi A, Yokoyama M, Sakurai Y, Okano T. Amine containing phenylboronic acid gel for glucose-responsive insulin release under physiological pH. *J Controlled Release* 1995;37:269–276.
236. Obaidat AA, Park K. Characterization of protein release through glucose-sensitive hydrogel membranes. *Biomaterials* 1997;18:801–806. [PubMed: 9177859]
237. Sato K, Kodama D, Anzai J. Sugar-sensitive thin films composed of concanavalin A and sugar-bearing polymers. *Anal Sci* 2005;21:1375–1378. [PubMed: 16317909]
238. Tanna S, Sahota TS, Sawicka K, Taylor MJ. The effect of degree of acrylic derivatisation on dextran and concanavalin A glucose-responsive materials for closed-loop insulin delivery. *Biomaterials* 2006;27:4498–4507. [PubMed: 16678254]

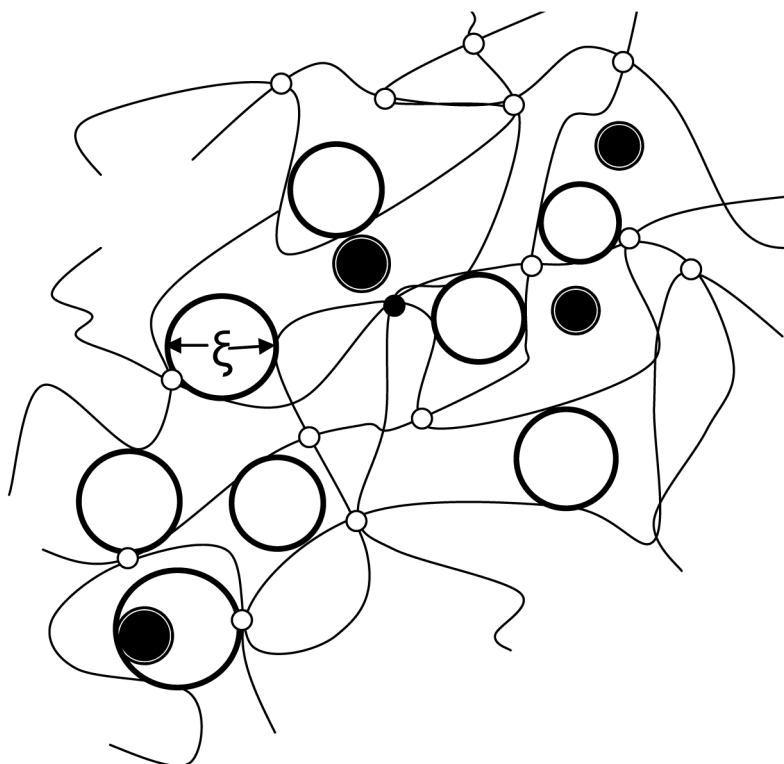
239. Oishi M, Hayama T, Akiyama Y, Takae S, Harada A, Yamasaki Y, Nagatsugi F, Sasaki S, Nagasaki Y, Kataoka K. Supramolecular assemblies for the cytoplasmic delivery of antisense oligodeoxynucleotide: polyion complex (PIC) micelles based on poly(ethylene glycol)-SSoligodeoxynucleotide conjugate. *Biomacromolecules* 2005;6:2449–2454. [PubMed: 16153078]
240. Kakizawa Y, Harada A, Kataoka K. Glutathione-sensitive stabilization of block copolymer micelles composed of antisense DNA and thiolated poly(ethylene glycol)-block-poly(L-lysine): a potential carrier for systemic delivery of antisense DNA. *Biomacromolecules* 2001;2:491–497. [PubMed: 11749211]
241. Miyata K, Kakizawa Y, Nishiyama N, Harada A, Yamasaki Y, Koyama H, Kataoka K. Block cationomer polyplexes with regulated densities of charge and disulfide cross-linking directed to enhance gene expression. *J Am Chem Soc* 2004;126:2355–2361. [PubMed: 14982439]
242. El-Sayed ME, Hoffman AS, Stayton PS. Rational design of composition and activity correlations for pH-responsive and glutathione-reactive polymer therapeutics. *J Control Release* 2005;104:417–427. [PubMed: 15984055]
243. Li C, Madsen J, Armes SP, Lewis AL. A New Class of Biochemically Degradable, Stimulus-responsive Triblock Copolymer Gelators. *Angew Chem Int Ed Engl* 2006;45:3510–3513. [PubMed: 16634101]
244. Chatterjee, AN.; Moore, JS.; Beebe, DJ.; Aluru, NR. International Conference on Transducers, Solid State Sensors, Actuators, and Microsystems. 1. IEEE; 2003. Dissolvable hydrogels as transducers of biochemical signals: models and simulations; p. 734-737.
245. Miyata T, Asami N, Uragami T. Preparation of an antigen-sensitive hydrogel using antigen-antibody bindings. *Macromolecules* 1999;32:2082–2084.
246. Miyata T, Asami N, Uragami T. A reversibly antigen-responsive hydrogel. *Nature* 1999;399:766–769. [PubMed: 10391240]
247. Tang M, Zhang R, Bowyer A, Eisenthal R, Hubble J. NAD-sensitive hydrogel for the release of macromolecules. *Biotechnol Bioeng* 2004;87:791–796. [PubMed: 15329937]
248. Deng Y, Wang C, Shen X, Yang W, Jin L, Gao H, Fu S. Preparation, Characterization, and Application of Multistimuli-Responsive Microspheres with Fluorescence-Labeled Magnetic Cores and Thermoresponsive Shells. *Chem Eur J* 2005;11:6006–6013.
249. Mosbach K. The promise of molecular imprinting. *Sci Am* 2006;295:86–91. [PubMed: 16989485]
250. Cormack PAG, Mosbach K. Molecular imprinting: recent developments and the road ahead. *React Funct Polym* 1999;41:115–124.
251. Miyata T, Jige M, Nakaminami T, Uragami T. Tumor marker-responsive behavior of gels prepared by biomolecular imprinting. *Proc Natl Acad Sci U S A* 2006;103:1190–1193. [PubMed: 16432230]
252. Zhao B, Moore JS. Fast pH-and ionic strength-responsive hydrogels in microchannels. *Langmuir* 2001;17:4758–4763.
253. Kanai F, Lan KH, Shiratori Y, Tanaka T, Ohashi M, Okudaira T, Yoshida Y, Wakimoto H, Hamada H, Nakabayashi H. In vivo gene therapy for alpha-fetoprotein-producing hepatocellular carcinoma by adenovirus-mediated transfer of cytosine deaminase gene. *Cancer Res* 1997;57:461–465. [PubMed: 9012474]
254. Seong H, Lee HB, Park K. Glucose binding to molecularly imprinted polymers. *J Biomater Sci Polym Ed* 2002;13:637–649. [PubMed: 12182549]
255. Powell AE, Leon MA. Reversible interaction of human lymphocytes with the mitogen concanavalin A. *Exp Cell Res* 1970;62:315–325. [PubMed: 5495449]
256. Reichert CF, Pan PM, Mathews KP, Goldstein IJ. Lectin-induced blast transformation of human lymphocytes. *Nat New Biol* 1973;242:146–148. [PubMed: 4512653]
257. Trowbridge IS. Mitogenic Properties of Pea Lectin and Its Chemical Derivatives. *Proc Natl Acad Sci U S A* 1973;70:3650–3654. [PubMed: 4519653]
258. Soppimath KS, Aminabhavi TM, Dave AM, Kumbar SG, Rudzinski WE. Stimulus-Responsive “Smart” Hydrogels as Novel Drug Delivery Systems. *Drug Dev Ind Pharm* 2002;28:957–974. [PubMed: 12378965]
259. Robert Langer NAP. Advances in biomaterials, drug delivery, and bionanotechnology. *AIChE J* 2003;49:2990–3006.

260. Gil ES, Hudson SM. Stimuli-responsive polymers and their bioconjugates. *Prog Polym Sci* 2004;29:1173–1222.
261. Hoffman AS. Bioconjugates of Intelligent Polymers and Recognition Proteins for Use in Diagnostics and Affinity Separations. *Clin Chem* 2000;46:1478–1486. [PubMed: 10973893]
262. Quintana JR, Valderruten NE, Katime I. Synthesis and Swelling Kinetics of Poly (Dimethylaminoethyl acrylate methyl chloride quaternary-co-itaconic acid) Hydrogels. *Langmuir* 1999;15:4728–4730.
263. Das M, Zhang H, Kumacheva E. Microgels: Old Materials with New Applications. *Annu Rev Mater Res* 2006;36:117–142.
264. Sahiner N, Godbey WT, McPherson GL, John VT. Microgel, nanogel and hydrogel–hydrogel semi-IPN composites for biomedical applications: synthesis and characterization. *Colloid Polym Sci* 2006;284:1121–1129.
265. Jeong KS, Park EJ. Self-assembly of interlocked supramolecular dendrimers. *J Org Chem* 2004;69:2618–2621. [PubMed: 15049674]
266. Franz A, Bauer W, Hirsch A. Complete Self-Assembly of Discrete Supramolecular Dendrimers. *Angew Chem, Int Ed Engl* 2005;44:1564–1567. [PubMed: 15678436]
267. Diederich F, Felber B. Supramolecular chemistry of dendrimers with functional cores. *Proc Natl Acad Sci U S A* 2002;99:4778–4781. [PubMed: 11891306]
268. Lehn JM. Toward complex matter: supramolecular chemistry and self-organization. *Proc Natl Acad Sci US A* 2002;99:4763–4768.
269. Lehn JM. Toward Self-Organization and Complex Matter. *Science* 2002;295:2400–2403. [PubMed: 11923524]
270. Tans SJ, Devoret MH, Dai H, Thess A, Smalley RE, Geerligs LJ, Dekker C. Individual single-wall carbon nanotubes as quantum wires. *Nature* 1997;386:474–477.
271. Joachim C, Gimzewski JK, Aviram A. Electronics using hybrid-molecular and mono-molecular devices. *Nature* 2000;408:541–548. [PubMed: 11117734]
272. Wu, CY.; Sue, CH.; Chiang, PC. Third IEEE Conference on Nanotechnology. 2. IEEE-NANO. IEEE; 2003. p. 510–511.
273. Nam KT, Peelle BR, Lee SW, Belcher AM. Genetically Driven Assembly of Nanorings Based on the M13 Virus. *Nano Lett* 2005;4:23–27.
274. Ross PE. Viral nano electronics. *Sci Am* 2006;295:52–55. [PubMed: 16989480]
275. Kuhn W, Hargitay B, Katchalsky A, Eisenberg H. Reversible dilation and contraction by changing the state of ionization of high-polymer acid networks. *Nature* 1950;165:514–516.
276. Liu Z, Calvert P. Multilayer Hydrogels as Muscle-Like Actuators. *Adv Mater (Weinheim, Fed Repub Ger)* 2000;12:288–291.
277. Kolosov O, Suzuki M, Yamanaka K. Microscale evaluation of the viscoelastic properties of polymer gel for artificial muscles using transmission acoustic microscopy. *J Appl Phys* 2006;74:6407–6412.
278. Moschou EA, Peteu SF, Bachas LG, Madou MJ, Daunert S. Artificial Muscle Material with Fast Electroactuation under Neutral pH Conditions. *Chem Mater* 2004;16:2499–2502.
279. He KQ, Peteu SF, Madou MJ. Microfabricated artificial-muscle-based microvalve array. *Proc SPIE-Int Soc Opt Eng* 2001;4560:8–18.
280. Kim SJ, Kim HI, Park SJ, Kim IY, Lee SH, Lee TS. Behavior in electric fields of smart hydrogels with potential application as bio-inspired actuators. *Smart Mater Struct* 2005;14:511–514.
281. Eddington DT, Beebe DJ. Flow control with hydrogels. *Adv Drug Deliv Rev* 2004;56:199–210. [PubMed: 14741116]
282. Eddington DT, Liu RH, Moore JS, Beebe DJ. An organic self-regulating microfluidic system. *Lab Chip* 2001;1:96–99. [PubMed: 15100866]
283. Serksen SR, Mensing GA, Ng M, Halas NJ, Beebe DJ, West JL. Independent Optical Control of Microfluidic Valves Formed from Optomechanically Responsive Nanocomposite Hydrogels. *Advanced Materials* 2005;17:1366–1368.
284. Serksen SR, Ng M, Halas NJ, West JL. Optically controllable materials: potential valves and actuators in microfluidics and MEMS. 2002;3:1822–1823.vol.1823

285. Chu LY, Li Y, Zhu JH, Wang HD, Liang YJ. Control of pore size and permeability of a glucose-responsive gating membrane for insulin delivery. *J Controlled Release* 2004;97:43–53.
286. Ehrick JD, Deo SK, Browning TW, Bachas LG, Madou MJ, Daunert S. Genetically engineered protein in hydrogels tailors stimuli-responsive characteristics. *Nat. Mat* 2005;4:298–302.
287. Yi H, Wu LQ, Bentley WE, Ghodssi R, Rubloff GW, Culver JN, Payne GF. Biofabrication with Chitosan. *Biomacromolecules* 2005;6:2881–2894. [PubMed: 16283704]
288. Wu LQ, Payne GF. Biofabrication: using biological materials and biocatalysts to construct nanostructured assemblies. *Trends Biotechnol* 2004;22:593–599. [PubMed: 15491804]
289. Amyl Ghanem DS. Effect of preparation method on the capture and release of biologically active molecules in chitosan gel beads. *J Appl Polym Sci* 2002;84:405–413.
290. Marin A, Sun H, Hussein GA, Pitt WG, Christensen DA, Rapoport NY. Drug delivery in pluronic micelles: effect of high-frequency ultrasound on drug release from micelles and intracellular uptake. *J Control Release* 2002;84:39–47. [PubMed: 12399166]
291. Tan WB, Zhang Y. Surface modification of gold and quantum dot nanoparticles with chitosan for bioapplications. *J Biomed Mater Res A* 2005;75:56–62. [PubMed: 16086419]
292. Xie M, Liu HH, Chen P, Zhang ZL, Wang XH, Xie ZX, Du YM, Pan BQ, Pang DW. CdSe/ZnS-labeled carboxymethyl chitosan as a bioprobe for live cell imaging. *Chem Commun (Camb)* 2005;44:5518–5520. [PubMed: 16358048]
293. Wang F, Zhang Y, Fan X, Wang M. One-pot synthesis of chitosan/LaF<sub>3</sub>:Eu<sup>3+</sup> nanocrystals for bio-applications. *Nanotechnology* 2006;17:1527–1532.
294. Bernkop-Schnurch A. Chitosan and its derivatives: potential excipients for peroral peptide delivery systems. *Int J Pharm* 2000;194:1–13. [PubMed: 10601680]
295. Darias R, Villalonga R. Functional stabilization of cellulase by covalent modification with chitosan. *J Chem Technol Biotechnol* 2001;76:489–493.
296. Chen T, Vazquez-Duhalt R, Wu CF, Bentley WE, Payne GF. Combinatorial screening for enzyme-mediated coupling. Tyrosinase-catalyzed coupling to create protein--chitosan conjugates. *Biomacromolecules* 2001;2:456–462. [PubMed: 11749206]
297. Katas H, Alpar HO. Development and characterisation of chitosan nanoparticles for siRNA delivery. *J Controlled Release* 2006;115:216–225.
298. Gelderblom H, Verweij J, Nooter K, Sparreboom A. Cremophor EL: the drawbacks and advantages of vehicle selection for drug formulation. *Eur J Cancer* 2001;37:1590–1598. [PubMed: 11527683]
299. Prego C, Torres D, Fernandez-Megia E, Novoa-Carballal R, Quinoa E, Alonso MJ. Chitosan-PEG nanocapsules as new carriers for oral peptide delivery Effect of chitosan pegylation degree. *J Controlled Release* 2006;111:299–308.
300. Sashiwa H, Aiba S. Chemically modified chitin and chitosan as biomaterials. *Prog Polym Sci* 2004;29:887–908.
301. Chang YC, Chen DH. Adsorption kinetics and thermodynamics of acid dyes on a carboxymethylated chitosan-conjugated magnetic nano-adsorbent. *Macromol Biosci* 2005;5:254–261. [PubMed: 15768445]
302. Guibal E. Heterogeneous catalysis on chitosan-based materials: a review. *Prog Polym Sci* 2005;30:71–109.
303. Peng CK, Yu SH, Mi FL, Shyu SS. Polysaccharide-Based Artificial Extracellular Matrix: Preparation and Characterization of Three-Dimensional, Macroporous Chitosan and Chondroitin Sulfate Composite Scaffolds. *J Appl Polym Sci* 2006;99:2091.
304. Shacham R, Avnir D, Mandler D. Electrodeposition of Methylated Sol-Gel Films on Conducting Surfaces. *Adv Mater (Weinheim, Fed Repub Ger)* 1999;11:384–388.
305. Liu G, Zhao X. Electromechanochemical Behavior of Gelatin Hydrogel Under Electric Field. *Journal of Macromolecular Science, Part A: Pure and Applied Chemistry* 2005;42:51–59.
306. Fwu-Long, Mi. Fabrication of chondroitin sulfate-chitosan composite artificial extracellular matrix for stabilization of fibroblast growth factor. *Journal of Biomedical Materials Research* 2006;76A (Part A):1–15.S-SSC-KPY-BWH-WSP-SWC-CH
307. Fonoberov VA, Balandin AA. Phonon confinement effects in hybrid virus-inorganic nanotubes for nanoelectronic applications. *Nano Lett* 2005;5:1920–1923. [PubMed: 16218710]

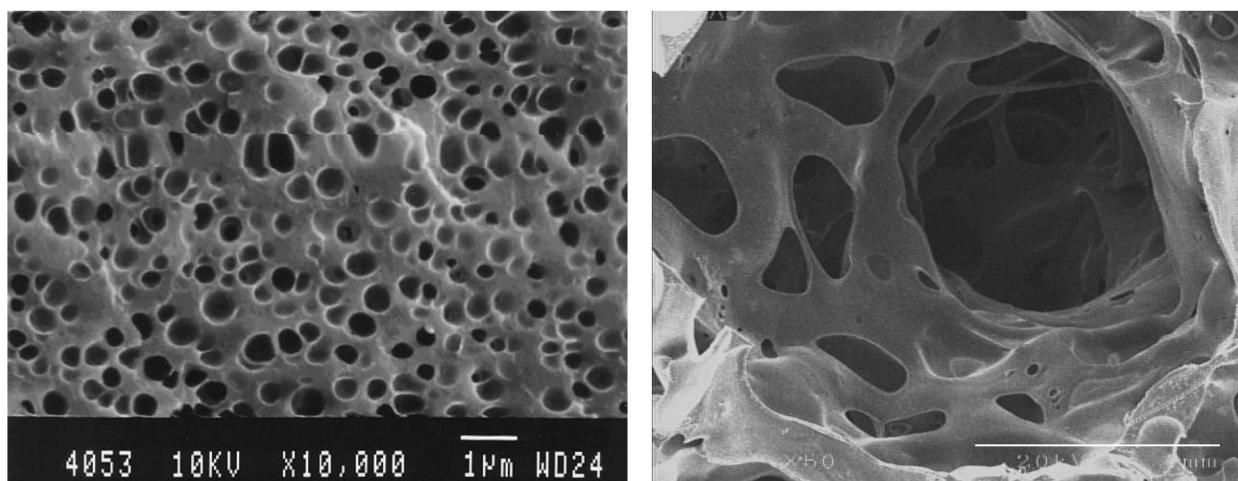


308. Chapin JK, Moxon KA, Markowitz RS, Nicolelis MA. Real-time control of a robot arm using simultaneously recorded neurons in the motor cortex. *Nat Neurosci* 1999;2:664–670. [PubMed: 10404201]
309. Craelius W. The Bionic Man: Restoring Mobility. *Science* (Washington, D C, 1883-) 2002;295:1018–1021.
310. Koga N, Takada S. Folding-based molecular simulations reveal mechanisms of the rotary motor F1-ATPase. *Proc Natl Acad Sci U S A* 2006;103:5367–5372. [PubMed: 16567655]
311. Wordeman L. Microtubule-depolymerizing kinesins. *Curr Opin Cell Biol* 2005;17:82–88. [PubMed: 15661523]
312. Hess H, Bachand GD, Vogel V. Powering nanodevices with biomolecular motors. *Chemistry* 2004;10:2110–2116. [PubMed: 15112199]
313. Soong RK, Bachand GD, Neves HP, Olkhovets AG, Craighead HG, Montemagno CD. Powering an inorganic nanodevice with a biomolecular motor. *Science* 2000;290:1555–1558. [PubMed: 11090349]
314. Jia L, Moorjani SG, Jackson TN, Hancock WO. Microscale transport and sorting by kinesin molecular motors. *Biomed Microdevices* 2004;6:67–74. [PubMed: 15307447]
315. Clemmens J, Hess H, Doot R, Matzke CM, Bachand GD, Vogel V. Motor-protein “roundabouts”: microtubules moving on kinesin-coated tracks through engineered networks. *Lab Chip* 2004;4:83–86. [PubMed: 15052344]
316. Hess H. Materials science. Toward devices powered by biomolecular motors. *Science* 2006;312:860–861. [PubMed: 16690850]
317. Liu H, Schmidt JJ, Bachand GD, Rizk SS, Looger LL, Hellinga HW, Montemagno CD. Control of a biomolecular motor-powered nanodevice with an engineered chemical switch. *Nat Mater* 2002;1:173–177. [PubMed: 12618806]
318. Karplus M, Gao YQ. Biomolecular motors: the F1-ATPase paradigm. *Curr Opin Struct Biol* 2004;14:250–259. [PubMed: 15093841]
319. Soong R, Montemagno CD. Engineering hybrid nano-devices powered by the F1-ATPase biomolecular motor. *IJNT* 2005;2:371–396.
320. Soong RK, Bachand GD, Neves HP, Olkhovets AG, Craighead HG, Montemagno CD. Powering an Inorganic Nanodevice with a Biomolecular Motor. *Science* (Washington, D C, 1883-) 2000;290:1555–1558.
321. van Hest JC, Tirrell DA. Protein-based materials, toward a new level of structural control. *Chem Commun (Camb)* 2001;19:1897–1904. [PubMed: 12240211]

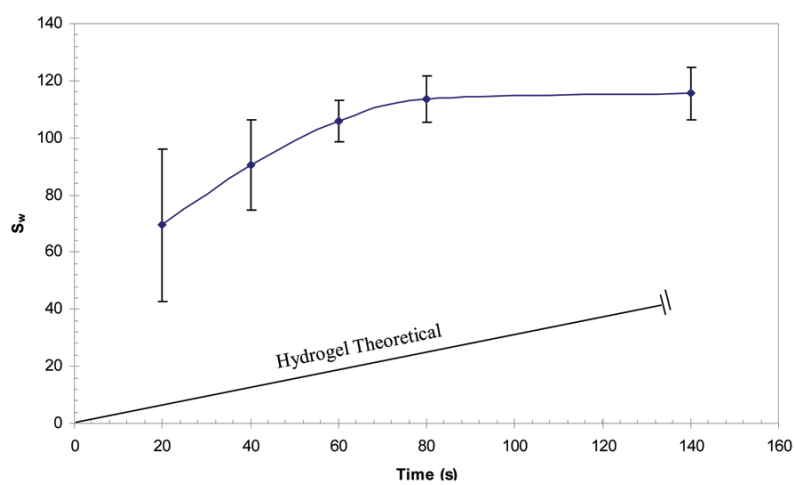


**Figure 1.**

A crosslinked structure of a polymeric hydrogel. The effective area of diffusion for solutes is characterized by the average mesh size ( $\zeta$ ) of the hydrogels. The solutes with diameters smaller than  $\zeta$  (indicated by dark circles) easily diffuse through the hydrogel network (Modified from Reference [9]).

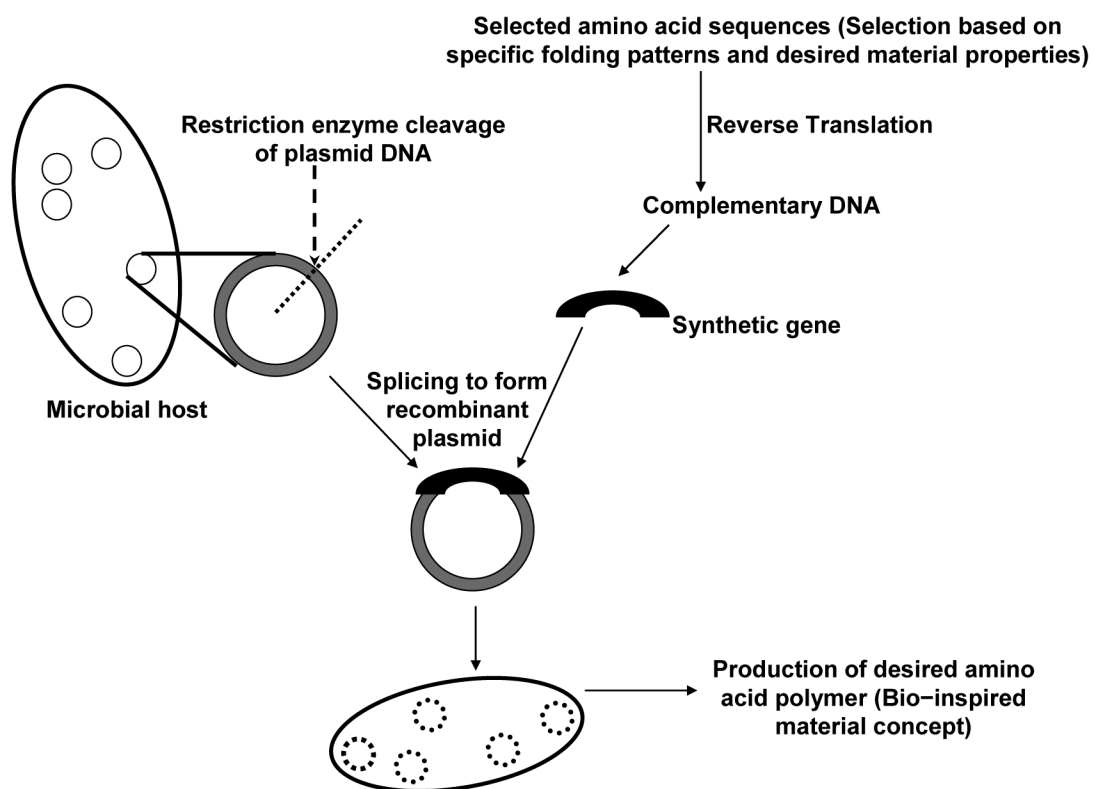


**Figure 2.** Scanning electron micrographs of SPHs with pore sizes less than 1  $\mu\text{m}$  (left) and larger than 1 mm (right). The scale bars are 1  $\mu\text{m}$  and 1 mm for the pictures on the left and right, respectively.



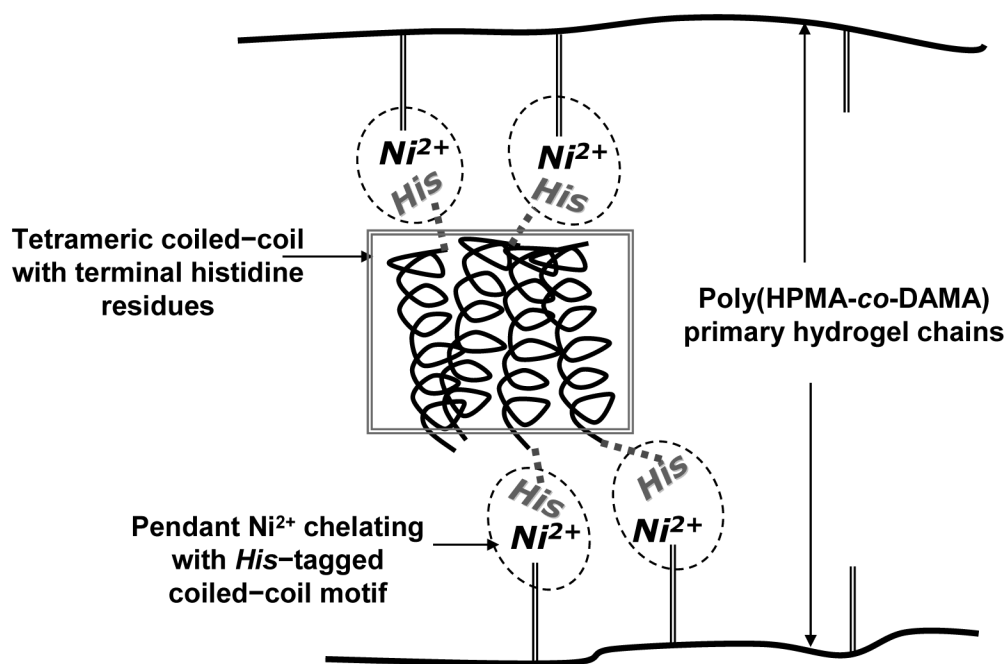
**Figure 3.**

An example of swelling ratio ( $S_w$ ) as a function of time for SPHs made of acrylic acid (AA) and acrylamide (AM). The straight line representing “hydrogel theoretical” describes a typical example of the increase in  $S_w$  with time for a hypothetical non-porous hydrogel.



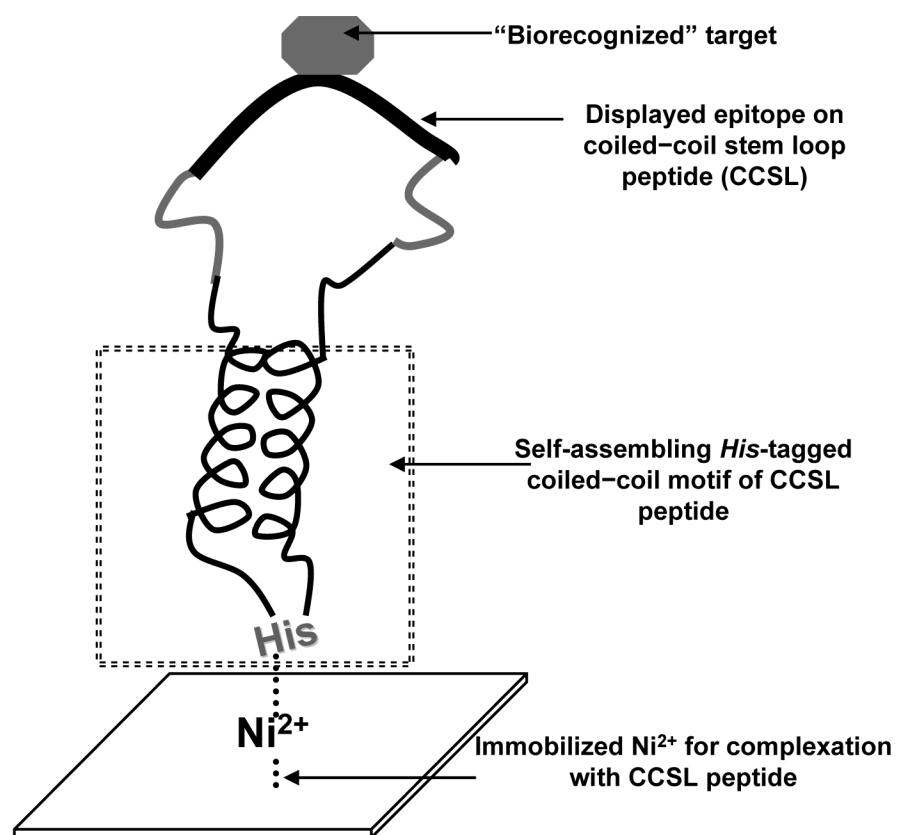
**Figure 4.** Overview of the protein engineering methodology (Modified from Reference [321]).



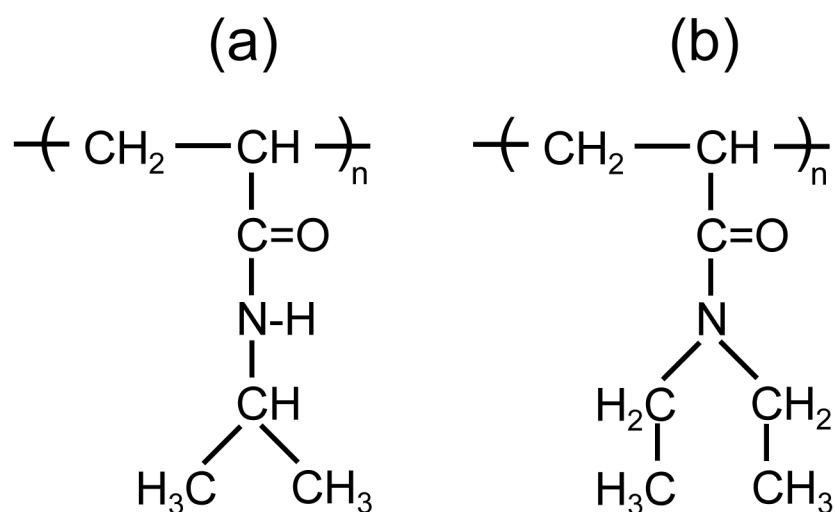


**Figure 5.**

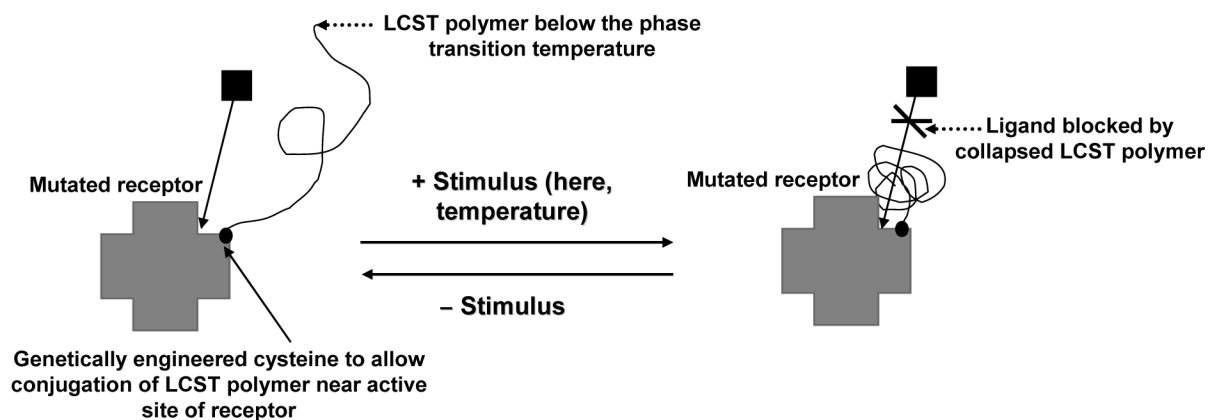
Schematic of a hybrid hydrogel assembled from histidine-tagged coiled-coil proteins and the synthetic polymer, poly(HPMA-co-DAMA). The pendant iminodiacetate groups from DAMA complex with  $\text{Ni}^{2+}$ , to which the terminal histidines of the coiled-coil tetramer (not drawn to scale) are attached. The tetrameric, self-assembling coiled-coil motif, crosslinking the primary hydrogel chains, consist of two parallel dimers associating in an antiparallel fashion, and constitute only one of the several possible conformations of coiled-coil proteins (Modified from Reference [92]).



**Figure 6.** Biorecognition of target via the displayed epitope on a coiled-coil stem loop (CCSL) peptide (Modified from Reference [82]).

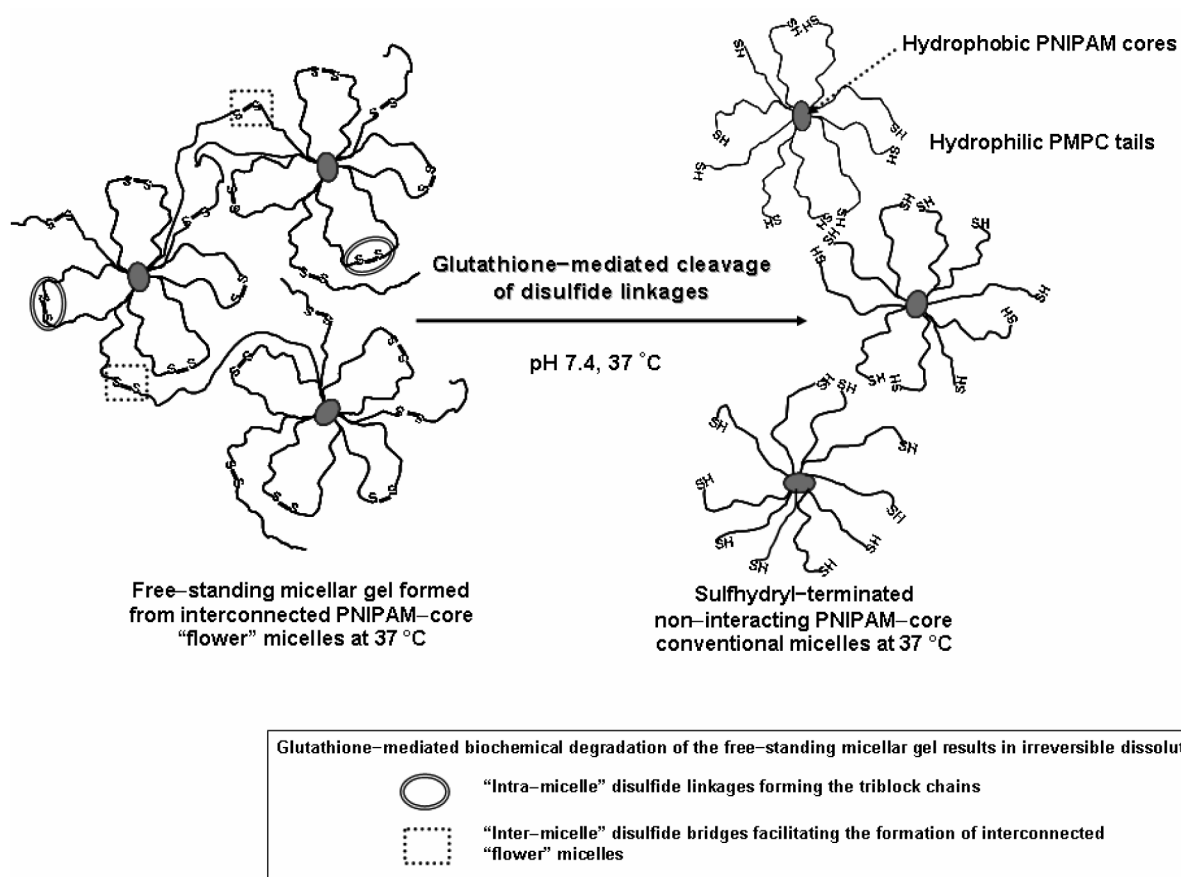
**Figure 7.**

Chemical structures of thermally responsive poly(*N*-substituted acrylamides). (a) poly(*N*-isopropylacrylamide); (b) poly(*N,N'*-diethylacrylamide). These polymers exhibit LCST phase transition. Notably, a common characteristic of most LCST polymers is the presence of hydrophobic alkyl groups.



**Figure 8.**

Schematic of molecular gating using an LCST polymer. The polymer switches from its hydrated, random coil state to its collapsed state on increasing the temperature above LCST and blocks ligand binding to the substrate. This specific example describes the blocking of the interaction between a mutant streptavidin–poly(NIPAM) conjugate and biotin (ligand molecule), induced by the phase transition of poly(NIPAM). For poly(NIPAM), this phase transition induced molecular gating occurs around 37 °C (Modified from Reference [179]).

**Figure 9.**

Strategy for the fabrication of glutathione-responsive and thermally-responsive "doubly smart gels". Irreversible biochemical degradation of novel PNIPAM-PMPC-S-S-PMPC-PNIPAM "flower micelles" to free-flowing sulfhydryl-terminating micelles by the cleavage of inter-micellar bridges is mediated by the tripeptide, glutathione. The reductive degradation of the interacting micelles to free-flowing micelles results in approximate halving of the original copolymer molecular weight (Modified from Reference [243]).



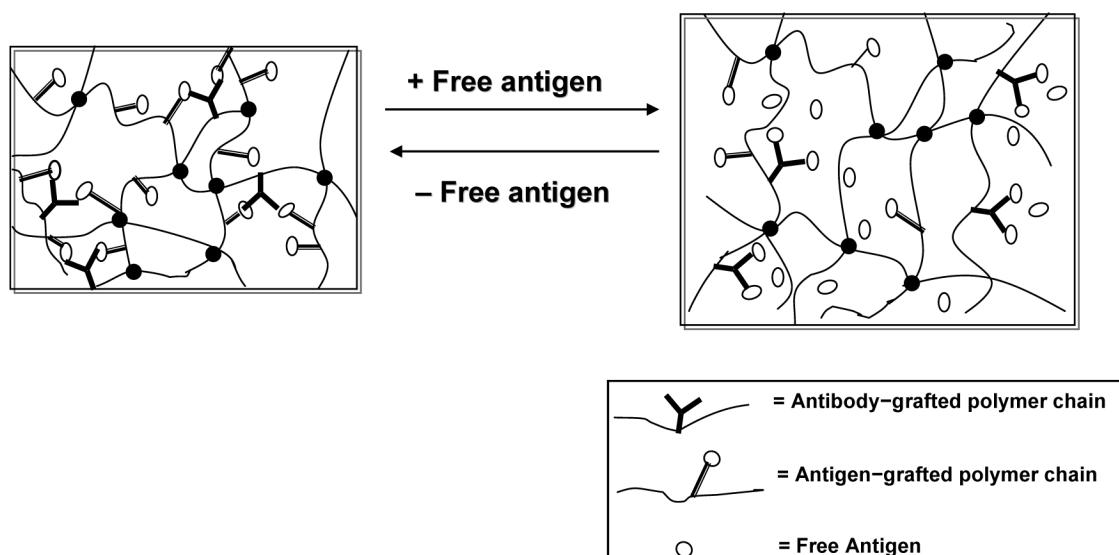


**Figure 10.**

Strategy for the fabrication of a reversibly antigen responsive gel. *Left:* The gel is in its collapsed state due to crosslinking via grafted antigens and antibodies. *Right:* The addition of free antigen to the system results in competitive binding interaction between the grafted antigen and the free antigen resulting in gel swelling due to decreased extent of non-covalent crosslinking. Here, the antigen is rabbit IgG and the antibody is GAR IgG (Modified from Reference [245]).

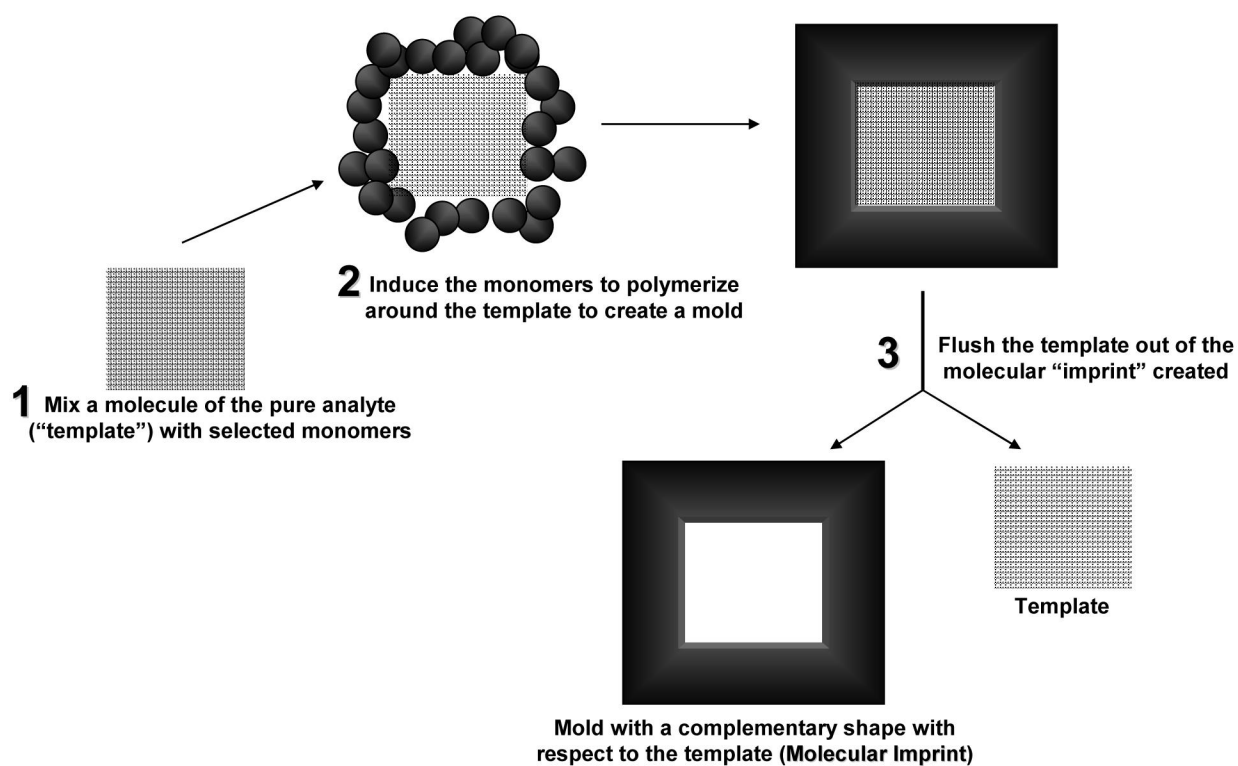


**Figure 11.** Schematic for the fabrication of molecularly imprinted polymers (MIPs) (Modified from Reference [249]).

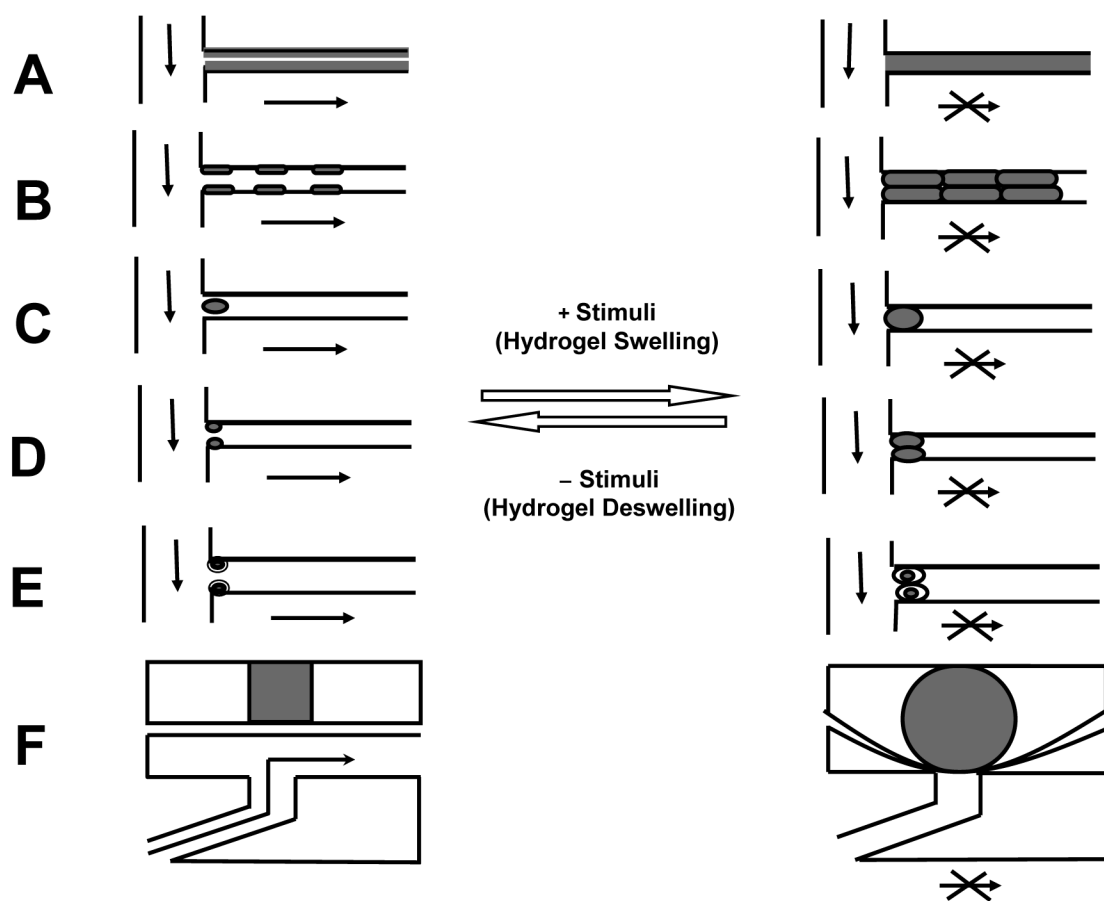


**Figure 12.**

Schematic for hydrogel swelling–modulated flow control via smart channels and valves: (A) and (B) represent smart channel designs—with a hydrogel strip (A), with a patterned array of hydrogel posts (B); (C)—(E) represent smart valve designs—with a single post (C), multiple posts (D), and multiple jacketed posts (E); (F) represents a hybrid hydrogel–flexible diaphragm (e.g., PDMS) valve where the expansion of the hydrogel deforms the diaphragm, reminiscent of the deformation of a bimetallic strip on heating (Modified from [281]).

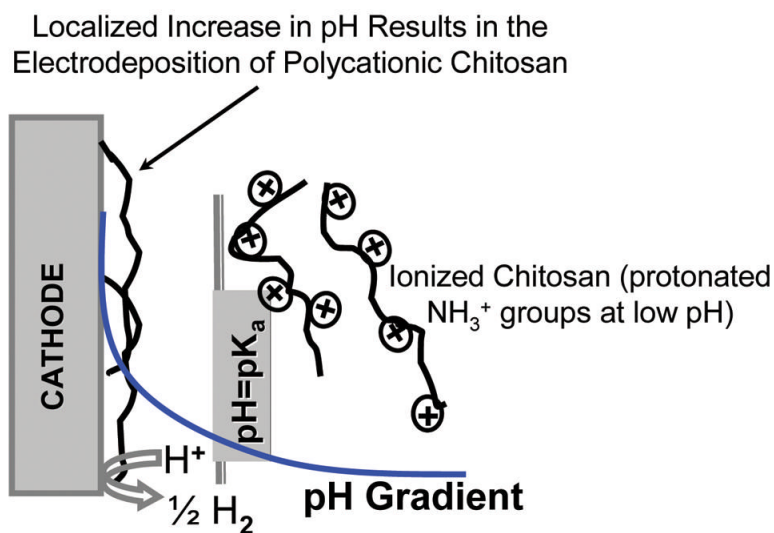


**Figure 13.**

Directed assembly of chitosan in response to locally applied electrical stimuli, i.e., electrodeposition of chitosan; the thickness and other properties of the electrodeposit can be controlled by varying electrochemical parameters (Modified from [287]).

**Table 1**

Structural analogy of the amino acid-mimicking synthetic monomers used to fabricate glucose imprinted polymers with the corresponding amino acid residues. (Modified from reference [254]).

Amino acid residues postulated to be interacting with glucose	Structures	Synthetic monomers mimicking amino acid side chains	Structures	Postulated type of interaction
Aspartic Acid (Asp, D)	$\begin{array}{c} \text{NH}_2-\text{CH}-\text{COOH} \\   \\ \text{CH}_2 \\   \\ \text{COOH} \end{array}$	Vinyl Acetic Acid (VAA)	$\begin{array}{c} \text{CH}_2=\text{CH} \\   \\ \text{CH}_2 \\   \\ \text{COOH} \end{array}$	Hydrogen bonding with glucose hydroxyls facilitated by water molecules
Glutamic Acid (Glu, E)	$\begin{array}{c} \text{NH}_2-\text{CH}-\text{COOH} \\   \\ (\text{CH}_2)_2 \\   \\ \text{COOH} \end{array}$	4-Pentenoic Acid (PA)	$\begin{array}{c} \text{CH}_2=\text{CH} \\   \\ (\text{CH}_2)_2 \\   \\ \text{COOH} \end{array}$	Hydrogen bonding with glucose hydroxyls facilitated by water molecules
Asparagine (Asn, N)	$\begin{array}{c} \text{NH}_2-\text{CH}-\text{COOH} \\   \\ \text{CO} \\   \\ \text{NH}_2 \end{array}$	Acrylamide (AM)	$\begin{array}{c} \text{CH}_2=\text{CH} \\   \\ \text{CO} \\   \\ \text{NH}_2 \end{array}$	Hydrogen bonding with glucose hydroxyls via side chain amino groups and with water molecules
Phenylalanine (Phe, F)	$\begin{array}{c} \text{NH}_2-\text{CH}-\text{COOH} \\   \\ \text{CH}_2 \\   \\ \text{C}_6\text{H}_5 \end{array}$	Allyl Benzene (AB)	$\begin{array}{c} \text{CH}_2=\text{CH} \\   \\ \text{CH}_2 \\   \\ \text{C}_6\text{H}_5 \end{array}$	Hydrophobic interaction of the benzene ring with the pyranose ring of glucose